2008

Adenovirus as a Platform for Assembly and Targeted Delivery of Gold Nanoparticles to Tumor Cells

Vaibhav Saini
University Of Alabama At Birmingham

ADENOVIRUS AS A PLATFORM FOR ASSEMBLY AND TARGETED DELIVERY OF GOLD NANOPARTICLES TO TUMOR CELLS

by

VAIBHAV SAINI

DAVID T. CURIEL, COMMITTEE CHAIR
SUSAN BELLIS
MAAIKE EVERTS
LISA SCHWIEBERT
YOGESH VOHRA

A DISSERTATION

Submitted to the graduate faculty of The University of Alabama at Birmingham,
in partial fulfillment of the requirements for the degree of
Doctor of Philosophy

BIRMINGHAM, ALABAMA

2008

ADENOVIRUS AS A PLATFORM FOR ASSEMBLY AND TARGETED DELIVERY OF GOLD NANOPARTICLES TO TUMOR CELLS

VAIBHAV SAINI

CELLULAR AND MOLECULAR PHYSIOLOGY GRADUATE PROGRAM

ABSTRACT

Novel combinatorial strategies need to be explored to achieve tumor eradication. In this regard, viral vector based gene therapy and nanotechnology offer unique possibilities for cancer therapy. As an example, multifunctional adenoviral (Ad) vectors capable of targeting, imaging, and successful cancer gene therapy have been advanced into multiple clinical trials. Similarly, novel multifunctional gold nanoparticles (AuNPs) have been utilized for drug delivery, targeting, imaging, and hyperthermia tumor therapy. Therefore, to accrue the benefits of both gene therapy and nanotechnology for cancer therapy, we proposed to combine Ad vectors and AuNPs in a single multifunctional nanodevice. Towards this goal, herein, we have developed two methods with universal applications for coupling NPs non-specifically or specifically to Ad vectors. Upon obtaining a specifically AuNP-labeled Ad vector, we analyzed its ability for hyperthermic tumor cell ablation. Due to the technical limits imposed on the amount of AuNPs that can be delivered by Ad vectors, at this time we were unable to utilize AuNP-labeled Ad vectors for hyperthermic tumor cell ablation. However, future efforts to overcome this coupling limitation may achieve the potential of the NP-labeled Ad vector for simultaneous targeting, imaging, and combined gene therapy and nanotechnology for the treatment of tumors.

ACKNOWLEDGMENTS

I want to acknowledge my committee members: Drs. David T. Curiel, Susan Bellis, Maaike Everts, Lisa Schwiebert, and Yogesh Vohra for their invaluable suggestions and for taking time out of their busy schedules to be on my committee. I want to thank my mentor Dr. David T. Curiel and my supervisor Dr. Maaike Everts for their constant support. They encouraged me to try new things and made every effort to help me in every possible way. This thesis would not have been possible without them. Dr. Curiel is a great person to work with. He is the kind of mentor I always wanted to have. He is very open-minded and helped with things both inside and outside the lab. Most importantly, he helped me in selecting the place for my post-doctoral training. Dr. Maaike Everts is the best supervisor anyone could have had. She is practical, modest, honest, loving, fashionable, broad-minded, and friendly (I can go on and on… I guess the word I am looking for is *cool.*). She is very active in all the areas of her life and is a big inspiration for me. I would really like to be like both Dr. Curiel and Maaike. Dr. Susan Bellis was extremely helpful with picking out details of my experiments. She has always been friendly and approachable with me. Dr. Lisa Schwiebert has helped me many, many times; initially as our graduate program director (she interviewed me and got me here), and subsequently as an enthusiastic member of my committee. She always suggested great ways to test my hypothesis and made sure that I progressed through graduate school in a timely manner. Dr. Yogesh Vohra is the only member of my committee who is knowledgeable about physics stuff. He helped with the physics part of my project. I want

to thank Dr. Peter Smith for helping with the official issues and the administrative staff in the Department of Physiology and Biophysics and the Gene Therapy Center for helping with miscellaneous issues. I also want to acknowledge all the members of our lab, especially my dearest, first, undergraduate student Victoria D. Towner, for making our lab a fun place to work in. I want to thank my friends and family.

TABLE OF CONTENTS

Page

LIST OF TABLES

Table *Page*

LIST OF FIGURES

Figures *Page*

INTRODUCTION

PART ONE

IMPORTANCE OF VIRUSES AND CELLS IN CANCER GENE THERAPY

by

VAIBHAV SAINI[1,2], JUSTIN C. ROTH [1], LARISA PEREBOEVA[1,3], MAAIKE EVERTS[1,3]

[1]Division of Human Gene Therapy, Departments of Medicine, Obstetrics and Gynecology, Pathology, Surgery, and the Gene Therapy Center, [2]Department of Physiology and Biophysics, [3]Division of Molecular and Cellular Pathology, Pathology, University of Alabama at Birmingham (UAB), Birmingham, Alabama, USA

Advances in Gene, Molecular and Cell Therapy 1(1), 30-43

Abstract

Viruses have a documented history for being used in treatment and prevention of diseases for centuries, with their application in vaccination strategies as a prime early example. In more recent history, viral vectors have been employed for gene and cell therapy of tumors. In this regard, the increased understanding of the aberrant molecular pathways underlying the process of tumorigenesis has rationalized genetic correction of these pathophysiological processes using viral vector based gene and cell therapy approaches. For example, viruses have been genetically engineered to develop oncolytic potency or mediate long-term gene expression. Also, viral vectors carrying therapeutic genes or targeting molecules have been loaded into cells, which can be exploited as delivery vehicles for these therapeutic payloads to the desired target site. However, issues pertaining to viral and cell targeting as well as host immune response elicited upon viral or cell administration remain to be addressed. In summary, the plasticity of the viral structure has rendered them amenable for the development of unique gene and cell therapy approaches, for the treatment of tumors.

Keywords: cell vehicles, immune evasion, tumor-targeting, viral vectors

Abbreviations: Δ24, delta-24; AAV, adeno-associated virus; Ad, adenovirus; Ad5/H3, Ad3 hexon protein; Ad5/H5, Ad5 hexon protein; APC, antigen presenting cells; AuNPs, gold nanoparticles; CAR, coxsackie adenovirus receptor; CEA, carcino-embryonic antigen; Cox-2, cyclooxygenase-2; CTL, cytotoxic T lymphocytes; E, early; EGF, epidermal growth factor; EGFR, epidermal growth factor receptor; flt-1, vascular endothelial growth factor receptor Type-1; GCV, gancyclovir; HSV, herpes simplex virus; HSV-1, herpes simplex virus Type-1; HVS, herpesvirus Samiri; IFN, interferons;

IgG, immunoglobulin G; IL-12, interleukin-12; MHC, major histocompatibility complex; MV, measles virus; PEG, poly(ethylene glycol); PKR, RNA-activated protein kinase; RCA, replication competent adenoviruses; RGD, arginine-glycine-aspartate; SCC, squamous cell carcinoma; scDb, single chain diabody; scFv, single chain antibody; TAM, tumor-associated macrophages; TCR, T cell receptor; TIL, tumor-infiltrating lymphocytes; TK, thymidine kinase; Tregs, regulatory T cells; VEGF, vascular endothelial growth factor; VSV, vesicular stomatitis virus

Introduction

Viruses have been utilized for therapeutic purposes for many centuries. They are interesting biological entities harboring on the borderline between non-living things and living organisms. Upon infection of the host cells, viruses manipulate the cellular machinery to their own advantage. This ability of viruses to induce changes in the target cells presented them as one of the most suitable candidates for serving as gene therapy vectors. A variety of viral vectors have been developed for gene therapy, such as herpes simplex virus (HSV), adenovirus (Ad), adeno-associated virus (AAV) and measles virus (MV), just to name a few. Although viral vector-based gene therapy has demonstrated great potential for treatment of diseases like cancer, many hurdles still need to be overcome before the full potential of viral vectors can be realized.

Cell therapy describes the implantation of cells to achieve a therapeutic purpose. This definition includes routine medical procedures, such as bone marrow transplants and blood transfusions, but it also encompasses the use of genetically manipulated cells for therapeutic purposes. Gene transfer, in general, can be used to replace a mutated gene in

order to restore a natural cellular function, or to confer novel therapeutic modalities to a cell. Although viral vectors are efficient gene transfer agents, as described above, systemically administered virions can be nonspecifically sequestered or inactivated via innate or acquired immune mechanisms prior to reaching the intended target cell population. However, cells can be genetically loaded using viral vectors *ex vivo* and these transduced cells can then serve as vehicles to deliver the therapeutic payload to target sites *in vivo*. The combined use of gene and cell-based medicines allows for multifaceted approaches that may be required to treat complex diseases such as cancer.

The use of viruses for gene therapy is marred with problems such as targeted delivery of the viral vector to specific cells, the immune response against the vector and the resulting toxicity issues. Attempts to resolve these issues have resulted in the development of viral vectors with improved characteristics. In this review, we discuss the strategies that have been employed for the construction of viral vectors with enhanced potential for efficacious gene therapy. We outline the construction of 'gutless' and oncolytic viral vectors, which have improvements in terms of increased transgene carrying capacity and expression, improved therapy and enhanced safety. Following this, we discuss the various approaches that have been developed for targeting of viral vectors to desired cell types, as well as strategies for host immune system evasion. We end with future considerations for the utilization of viral vectors for gene therapy.

Viral Vectors and their Modifications for Gene therapy

Many viruses have been used for gene therapy. However, multiple factors limit the effective utilization of viruses for gene therapy. For instance, it has been observed

that upon transgene delivery to the target cells the transgene expression diminishes with time, warranting re-administration of the viral vectors. In this regard, viral vectors utilized for gene therapy can be either integrating or non-integrating. Integrating viruses, such as retroviruses (Chang et al., 2001) and AAV (McCarty et al., 2004), integrate their genome within the genome of the host organism. Non-integrating viruses, such as adenoviruses (Marini et al., 2002), do not integrate into the host genome, and therefore the viral genome is lost in proliferating cells. Historically it was therefore believed that integrating viral vectors would provide long-term expression of the therapeutic gene in the host and thus would not require repeated administration, unlike the non-integrating viruses. However, pre-clinical experience with the utilization of integrating vectors such as AAV for gene therapy has demonstrated that repeated administration might be necessary for integrating viruses as well. For example, when AAV was used for genetic correction of a cystic fibrosis defect in the lungs, the limited viral transduction efficiency resulted in low therapeutic gene delivery to the lung cells. Moreover, an antibody response generated against the viral vector reduced the amount of gene transfer that could be achieved and also prevented re-administration of the virus (Halbert et al., 2000). Modification of viral vectors to circumvent or mitigate an immune response against the infected cell and the vector itself is thus warranted, even if integrating vectors are used.

Gutless vectors

As noted above, administration of viral vectors results in an immune response. Upon first vector administration, the body responds by mounting an immune response against the virus itself, viral proteins that are expressed in the infected cells and the therapeutic

gene if it is foreign to the host. This immune response severely limits the efficacy of the therapeutic vector since infected cells that express the transgene will be cleared from the body. In addition, the development of immunological memory restricts the efficacy of subsequent administrations, and limits the dosage and the number of times the viral vector can be administered to the patient. To circumvent the immune response generated against the viral vector and the viral proteins, one of the strategies employed is the deletion of the unnecessary viral genome sequences. The removal of the unnecessary viral genome sequences drastically reduces the immunogenicity of the viral vector, and increases the efficacy of the viral gene therapy. Another benefit of the deletion of viral genome sequences is the increase in carrying capacity for foreign therapeutic genes. This is especially important when large genomic sequences need to be delivered, such as the dystrophin gene for the treatment of duchenne muscular dystrophy (Bogdanovich et al., 2004).

As a representative example of viral vectors with deleted genome sequences, the construction of adenoviral (Ad) vectors carrying progressively less amounts of the viral genome can be studied, which is described below.

First generation Ad vectors

One of the considerations in deciding which viral genes can be deleted from the genome is the role played by these various genes in the viral reproduction cycle. As an example, for Ads it was discovered that early (E) expression gene products could be provided *in trans* in order to achieve mature adenoviral progeny production during the production process. In particular, E1, E2, E3 and E4 regions have been deleted or

inactivated. Initially, it was the E1 region that was deleted from the Ad genome considering its essential role in transcriptional activation of other early genes, inhibition of apoptosis of the infected cell and modification of the intracellular environment to make it more conducive for Ad protein production (Akusjarvi, 1993; Dyson, 1998; Flint et al., 1997; Young et al., 1997). Deletion of E1 resulted in replication deficient viral vectors that were propagated in helper cell lines that provided E1 gene product *in trans* (Trapnell et al., 1994).

Subsequently, the E3 region was deleted, which encodes proteins that inhibit various death pathways elicited by the host immune system against the cells infected with Ad vectors (Wold et al., 1999; Wold et al., 1995). The Ad vectors with deleted E1, with or without deletion of E3, are referred to as 'first generation' Ad vectors (Figure 1). The first generation Ad vectors have a carrying capacity of ~8 kb for foreign genes (Bett et al., 1993). However, unfortunately, even after deletion of E1 and E3, these viral vectors still suffer from immune resistance due to leaky viral protein expression in the host. This results in clearance of the viral vectors as well as host cells infected with the virus (Yang et al., 1994). In addition, propagation of these vectors in complementing cell lines may result in replication competent adenoviruses (RCA) due to recombination with the viral DNA sequences present in the complementing cell line (Amalfitano et al., 1998). The RCA contaminates the replication incompetent viral vector preparations. The possibility of uncontrolled replication of this RCA contaminant in the patient increases the safety considerations.

Second generation Ad vectors

The problems with the first generation Ads mentioned above sparked the further minimalization of the viral genome, and thus the viral protein expression in the host. For this, in addition to E1 and E3, the E2 region was also deleted (Amalfitano et al., 1998). The E2 region encodes proteins needed for Ad DNA replication (Van der Vliet, 1995). Following the E2 deletion, the E4 region was also deleted. The E4 region encodes multiple proteins that are utilized for Ad DNA replication, mRNA transport and splicing, inhibition of host cell protein synthesis, and regulation of apoptosis (Bridge et al., 1989; Huang et al., 1989). With regards to E4, viral vectors with modification other than deletion, such as removal of the E4 promoter, have also been generated. The vectors with deletion in E2 and E4, along with E1 and E3 in different combinations, are referred to as 'second generation' Ad vectors (Figure 1). This second generation has a transgene carrying capacity of ~14 kb (Alba et al., 2005).

In addition to reducing the host immune response and increasing the transgene carrying capacity of Ad vectors, these deletions also resulted in more severely crippled replication deficient vectors than the first generation vectors, thereby increasing their safety profile (Parks et al., 1996). For example, an Ad vector carrying the tumor suppressor p53 in the deleted E1 region, deleted for E3 and having an inactivated E4 region was compared to a vector with a wild type E4 region, to analyze whether deleting multiple viral genes can enhance the safety profile of the Ad vector. The Ad vector with the inactivated E4 region demonstrated a reduced host immune response compared to the control vector, resulting in reduced toxicity and prolonged duration of p53 expression *in vivo* in immunocompetent mice (Ji et al., 1999).

However, despite these encouraging results, the residual gene expression from the remaining viral genes still resulted in immunogenicity and toxicity for these second generation Ad vectors. In this regard, it was soon realized that for the Ad vectors, in addition to the early region genes, many more genes could be deleted and their functions provided *in trans*. Thus, true "gutless" vectors came into being.

Third generation 'gutless' Ad vectors

Gutless vectors are the most advanced form of Ad vectors currently available. These vectors are devoid of all the viral genes except those that are required *in cis* for packaging and replication. These vectors are also known as gutted, amplicon, high-capacity, helper-dependent and fully-deleted adenoviral vectors (Figure 1). The transgene carrying capacity of gutless vectors is ~36 kb (Alba et al., 2005). These vectors have demonstrated a better safety profile than the first and second generation of Ad vectors. However, there are still some problems with gutless Ad, especially in regard to problematic production of high titers that are required for clinical use. Also, contamination with RCA remains as concern that requires further investigation (Alba et al., 2005). These problems are currently being countered utilizing various approaches, such as episomally maintained Ad vectors (Kreppel et al., 2004) and improved packaging cell lines (Alba et al., 2005; Sakhuja et al., 2003).

In addition to the above mentioned 'gutless' Ad vectors, other viral vectors with deleted viral genomes have been constructed. For example, lentiviral (Naldini et al., 2000) and retroviral vectors devoid of viral genome sequences in the transfer vector have been constructed, such that no viral proteins are produced in the infected cells.

In conclusion, even though many issues pertaining to efficient production of the gutless vectors still need to be resolved, it is anticipated that gutless vectors will be increasingly used for gene therapy in coming years due to their improved efficacy and safety profile.

Oncolytic viral vectors

The proposed use of viruses for gene therapy applications has always caused concern because of the inherent pathogenic nature of these agents. In this regard, viral vectors were modified to limit their replication potential in the host organism (Figure 2). Therefore, initially only the gene delivery capacity of viral vectors was utilized for gene therapy. Although this addressed the concerns related to safety issues in a cancer therapy context, this also prevented the use of a very efficient cell killing method, i.e., viral vector mediated lysis of infected tumor cells. For example, replication deficient Ad vectors were utilized to deliver a bacterial cytosine deaminase gene into glioma cells, which chemosensitizes glioma cells for otherwise non-toxic 5-fluorocytosine (Dong et al., 1996). This strategy kills those tumor cells which are infected with the viral vectors, but not the remaining tumor cells. However, if the viral vector could replicate selectively in the tumor cells thereby resulting in oncolysis, then the viral progeny could potentially infect the adjoining tumor mass which escaped the primary infection. Moreover, replicative virus can kill tumors in combination with the chemosensitizing approach.

Thus, in order to utilize the inherent cell killing potential of viruses with a lytic replication cycle but avoid side-effects in healthy cells, viral vectors capable of selective replication in tumor cells were constructed. These viral vectors are replication competent

and thus oncolytic, but only in target cells by using a variety of mechanisms, as described below. The use of oncolytic viruses for killing target tumor cells has been defined as virotherapy (Nettelbeck et al., 2003).

Advantages of oncolytic viral vectors

There are multiple advantages that mandate the use of conditionally replicative oncolytic viruses for tumor treatment. Being replicative, after the initial infection, viral progeny can spread through the tumor mass and effectively remove all of the tumor cells. In addition to their oncolytic properties, these viruses can also introduce therapeutic genes, such as suicide genes and cytokines. In addition, expression of viral proteins can be utilized to elicit an anti-tumor immune response, increasing the effectiveness of tumor treatment.

A variety of oncolytic viruses have been used as potential candidates for oncolytic therapy, including HSV, reovirus, vesicular stomatitis virus (VSV), and Ad, to name a few.

The viruses currently under investigation for oncolytic therapy are either inherently selective or are genetically modified to be selective for replication competence in tumor cells. In this regard, herpesvirus samiri (HVS) was demonstrated to be naturally selectively oncolytic for pancreatic cancer line PANC-1 (Stevenson et al., 2000). Similarly, human reovirus (Hashiro et al., 1977) and VSV (Stojdl et al., 2000) were shown to replicate more efficiently in transformed cell lines as compared to non-transformed cells lines (Ring, 2002). Reovirus is an example of a naturally oncolytic virus with replication limited to tumor cells with activated Ras-signaling pathway. Upon

infection of normal cells by reovirus, the early viral transcripts activate double-stranded RNA-activated protein kinase (PKR), which inhibits viral protein translation and viral replication. However, in tumor cells, the activated Ras as well as upstream and downstream elements of the Ras-pathway, inhibit (or reverse) PKR activation, thereby allowing reoviral replication resulting in oncolysis (Wilcox et al., 2001). The activating mutations in *Ras* have been reported for >30% of tumors. In addition, the mutations in upstream and downstream arms leading to constitutive Ras pathway signaling have been reported for an even greater proportion of tumors (Norman et al., 2004). Based on these facts, reovirus has been shown to be effective as an oncolytic agent for a variety of tumors, including malignant glioma (Wilcox et al., 2001), breast cancer (Norman et al., 2002) and pancreatic cancer (Etoh et al., 2003) in animal models.

VSV provides an example of an oncolytic virus where a tumor cell advantage over normal cells has been exploited for selective viral oncolytic activity. All cells exposed to viral infection produce antiviral interferons (IFNs). However, cancer-specific mutations of gene products in the IFN pathway have been reported in tumors (Stojdl et al., 2000). This defect in IFN response against viral infection has been utilized for selective VSV replication and oncolysis of tumors, such as melanoma (Stojdl et al., 2000) and colorectal carcinoma metastatic to liver (Shinozaki et al., 2005) in mouse models.

In some cases, natural oncolytic activity has been artificially restricted to a particular type of cell, thereby rending the virus useful for selective treatment of tumors. For example, oncolytic herpes simples virus type 1 (HSV-1) has been exploited for tumor therapy because it can be modified for restricted viral replication in proliferating glioma cells. Of note, one of the advantages of HSV-based oncolytic vectors is the potential use

of the antiviral drug acyclovir, should replication become out of control. HSV-1 based vectors have been tested in various phases of clinical trials for glioma with promising results. In addition, oncolytic viral activity of HSV-1 has been combined with the elicitation of an anti-tumor immune response, in order to improve tumor treatment. For example, Wong *et al.* used an oncolytic HSV-1 expressing the pro-inflammatory cytokine IL-12 for treatment of distantly metastatic squamous cell carcinoma (SCC), and observed significantly improved survival in mice with this combination of oncolytic and immune therapy (Wong et al., 2004) as compared to oncolytic therapy alone for treating disseminated disease.

A similar strategy based upon a combination of oncolysis and immunomodulation was used with an oncolytic recombinant VSV expressing murine IL-12 (rVSV-IL12). This virus demonstrated a significant reduction in murine squamous cell carcinoma volume as compared to the control virus without IL-12 (Shin et al., 2007).

In addition to above listed viruses, conditionally replicative oncolytic adenoviruses (CRAds) have been used for tumor treatment. These vectors have been developed based upon the understanding of aberrant molecular pathways in tumor cells in conjunction with the understanding of Ad biology. For example, the Rb and p53 oncogenes have mutations in many tumors. This fact has been exploited for the generation of an oncolytic Ad vector, delta-24 (Δ24). In this vector, the E1A region that interacts with Rb has been deleted. This virus therefore replicated more efficiently in tumor cells with mutations in Rb as compared to healthy cells (Fueyo et al., 2000). Similarly, another Ad genome sequence, E1B 55kDa, which interacts with p53, was deleted to construct a CRAd named *dl*1520 (Onyx-015) (Bischoff et al., 1996). This virus replicates in tumors with mutations

in p53. However, it is now assumed that in addition to p53, other factors like infectivity and cell permissiveness also contribute to the differential replication of Onyx-015 (Ring, 2002). It was determined that the use of Onyx-015 along with chemotherapy might have synergistic effects for tumor treatment (Khuri et al., 2000). However, Onyx-015 is not suitable by itself due to limited replication potency. One of the reasons for the limited efficacy of Onyx-015 might be the loss of functions of E1B that are critical for the Ad life cycle, such as mRNA transport and shut-off of host cell protein synthesis (Ring, 2002).

Another type of CRAds are those with tissue specific promoters to impose transcriptional limitations for oncolytic replication in specific target cells. For example, cyclooxygenase-2 (Cox-2) has been shown to be highly expressed in a number of epithelial tumors (Lam et al., 2007). Based on this consideration, an infectivity enhanced CRAd with the E1 region under transcriptional control of the Cox-2 promoter was constructed. This vector demonstrated potent anti-tumor effects as compared to the wild type vector for pancreatic (Yamamoto et al., 2003) and ovarian tumors (Kanerva et al., 2004) both *in vitro* and *in vivo*. Another example of transcriptional control of CRAd replication exploits the fact that tumor cell growth is dependent upon neovasularization. For this purpose, vascular endothelial growth factor (VEGF) is produced by tumor cells to drive the angiogenesis. Takayama *et al.* utilized a tropism-modified CRAd in which expression of E1 region, necessary for viral replication, was put under transcriptional control of VEGF promoter. This vector replicated efficiently in lung tumors *in vitro* and *in vivo* (Takayama et al., 2007).

Issues pertaining to oncolytic viral therapy

Despite all these developments, many problems have hampered successful utilization of oncolytic viruses for tumor treatment. Upon intra-tumoral or peripheral administration of the oncolytic virus, it was expected that viral progeny would spread to the entire tumor mass and eliminate the tumors efficiently. However, when the first pre-clinical analyses were performed, it was apparent that oncolytic viruses did not spread through the tumor mass as expected. This might be due to the large size of the virus (90 nm for Ad), and physical barriers such as cell-to-cell barriers, basement membranes, necrotic regions and intermixed normal cells (Vile et al., 2002).

Another issue that needs to be addressed is the targeting of the virus to specific cells. For example, Ad vectors bind to coxsackie adenovirus receptor (CAR), which is expressed at high levels in normal tissues of the body such as liver, but at low or negligible level in certain tumors. This results in low viral vector infection efficiency for the tumor cells. In order to achieve the needed infectivity enhancement, viral vectors have been genetically modified. For instance, Krasnykh *et al.* constructed chimeric Ad5/3 vectors, in which the knob domain of Ad5 was replaced by the knob domain of Ad3. This chimeric virus was shown to bind to cells by utilizing receptors other than CAR (Krasnykh et al., 1996), resulting in its ability to infect cell lines deficient in CAR-expression. Another example for the Ad vector infectivity enhancement is provided by Wu *et al.*, who constructed Ad vectors with RGD and pK7 motifs in the fiber. It is known that the amino acid sequence arginine-glycine-aspartate (RGD) binds to integrins. Furthermore, it has been demonstrated that poly-lysine sequences (pK7) bind to heparin sulfate-containing receptors. Integrins and heparin sulfate-containing receptors are

overexpressed in many tumors. The double modified Ad vector containing RGD and pK7 motifs in the fiber was shown to be capable of infection in both CAR-positive as well as CAR-negative cell lines. The observed infectivity enhancement was a result of the utilization of additional receptors for cell entry by the double modified Ad vectors (Wu et al., 2002b).

In addition to the above issues, it has been realized that oncolytic potency of the viral vectors must be determined before these vectors are employed in clinical trials. The oncolytic vectors are usually evaluated in immunodeficient mouse models containing xenografts of human tumors. However, being immunodeficient, these mouse models do not represent the actual scenario in the body of an immunocompetent human patient. In addition, mouse tissues are not very permissive for the replication of human viral vectors such as Ad vectors. In order to overcome these issues, Thomas *et al.* have developed a Syrian hamster model for study of the oncolytic Ad vectors. This model is immunocompetent and permissive to infection by the Ad vectors, thereby mimicking the human physiological system more closely than the mouse models (Thomas et al., 2006). However, this model still needs better characterization before its potential can be fully exploited.

In addition to the use of animal models, liver and tumor tissue slices from patients have also been used to evaluate the toxicity characteristics of oncolytic viruses. Since tissue slices can be directly derived from cancer patients, they provide a more physiologically relevant platform for analysis of toxicity of oncolytic viruses (Stoff-Khalili et al., 2007b). However, there are practical considerations regarding the availability of fresh tissue slices that are currently limiting their widespread application.

Another method to analyze the characteristics of oncolytic viruses is the use of *in vitro* human cell cultures. However, adherent cell culture is a two-dimensional system as opposed to the three-dimensional tumor environment. Thus, novel assay systems are being developed to aid in pre-clinical analysis of the oncolytic potency of the viruses. For example, Lam *et al.* have developed a tumor-spheroid three-dimensional system as compared to two-dimensional cell culture mono-layers to measure the viral penetration and oncolytic potency (Lam et al., 2007).

Thus, selectively replicative oncolytic viruses are a potent tool for treatment of diseases like cancer. These viruses will be used more widely for treatment once issues related to their oncolytic potency and safety are resolved.

Targeting of Viral Vectors

In gene therapy, it is imperative that the therapeutic gene is delivered specifically to the intended target cells. Similarly, the viral vectors that are used for oncolytic therapy must infect and replicate only in the particular cell type that needs to be killed. However, the native tropism of viruses utilized for gene therapy does not necessarily correspond with the desired cell type that needs to be infected. For example, Ads bind to coxsackie and adenovirus receptor (CAR), which is expressed at high levels in normal tissues of the body, such as liver, and not in the intended targets like tumor cells. Therefore, upon Ad vector administration, liver related toxicity can be observed. Similarly, retroviruses are known to infect proliferating cells. Although tumor cells proliferate rapidly, there are other body cells that also undergo proliferation. Thus, retroviral replication must be restricted to tumor cells only and not to normal body cells. Another example is AAV-2,

which infects liver cells. This interaction is mediated by heparin sulfate proteoglycan molecules that are present on liver cells. Thus, to use AAV-2 for gene therapy of extra-hepatic tissues, its binding to hepatic cells must be perturbed. Therefore, for the development of effective gene therapy viral vectors, the native viral tropism needs to be ablated and viral vectors need to be retargeted to tumor cells.

The targeting of viral vectors can be either transductional or transcriptional. Transductional targeting involves modification of viral tropism whereas transcriptional targeting involves modulation of the viral gene expression such that viral genes are expressed only in desired cell types.

Transductional targeting

Transductional targeting has been achieved through a variety of approaches, including bifunctional adapters and genetic modifications of the viral vector.

Bifunctional adapters for transductional targeting

Bifunctional adapters, as the name indicates, are a combination of two different subunits, one of which binds to the viral vector and the other binds to the target cell. The two different subunits can be attached to each other by either chemical or genetic methods. There are a variety of subunits, some of which will be discussed in more detail below.

Chemically conjugated bifunctional adapters

Due to the technical ease of coupling two subunits by chemical methods, the

initial bifunctional adapters contained subunits that were chemically linked. For example, a chemically coupled bispecific antibody conjugate was generated, in which an antibody against Ad was chemically liked to an antibody against epidermal growth factor receptor (anti-EGFR). This bispecific antibody was successfully utilized for targeting Ad vectors to EGFR expressing human glioma cells (Miller et al., 1998). However, due to the chemical coupling strategy employed for linking the two subunits, there was variability in the resulting bispecific antibody product, leading to batch to batch variations. Thus, a more consistent production strategy was desired.

Genetically conjugated bifunctional adapters

To circumvent the problems observed with chemical coupling of the subunits, genetic coupling of the subunits constituting the bifunctional adapters was endeavored. For example, an adenobody is a genetic fusion of a single chain antibody (scFv) directed against the Ad fiber knob to a ligand that binds to a target cell. For example, Watkins *et al.* fused a scFv against Ad knob with epidermal growth factor (EGF), which can bind to EGFR on human cells (Watkins et al., 1997). Haisma *et al.* further extended the adenobody approach by constructing a bispecific scFv, called a single chain diabody (scDb). For this purpose, a scFv against Ad was genetically fused with a scFV against the EGFR (Haisma et al., 2000). Another example of a scDb is the melanoma retargeted Ad vectors, where a scFv against Ad was genetically fused with a scFv against the high molecular weight melanoma antigen (Nettelbeck et al., 2004).

In addition to the use of scFc against the Ad knob, other types of subunits with an affinity for Ad knob have been utilized for construction of bifunctional adapters. For

example, the ectodomain of the native adenoviral receptor CAR fused to scFvs that target tumor associated antigens has also been exploited for retargeting Ad vectors to specific cells. In this regard, Everts *et al.* fused the ectodomain of CAR, sCAR, with a scFv directed against carcino-embryonic antigen (CEA), which is over-expressed in the adenocarcinomas of the gastrointestinal tract, lung and breast. This bifunctional adapter successfully re-targeted Ad vectors to CEA artificially expressed in the lungs after intravenous administration (Everts et al., 2005).

Using these bifunctional adapters, Ad vectors have been efficiently retargeted to desired cells or tissues. In addition, the retargeting and accompanying ablation of native tropism also reduced the Ad vector sequestration in liver, leading to reduced toxicity. However, binding a bifunctional adapter to the viral vector requires an incubation step before infection can be achieved. In addition, even though genetic bifunctional adapter molecules themselves are of a homogenous nature, the incubation of them with Ad vectors will still result in batch-to-batch variations, which are undesirable for clinical application. Moreover, there is always a possibility that the bifunctional adapter does not attach to all the viral sites, thereby sustaining the possibility of viral infection in unintended target cells. In order to resolve these issues, genetic transductional targeting approaches have been developed.

Genetic transductional targeting

A variety of vectors and methods have been used to genetically modify viral vectors in order to achieve the required targeting. For example, Girod *et al.* inserted a 14-amino-acid targeting peptide, L14, into the capsid of AAV-2. The resulting capsid modified

virus was demonstrated to efficiently infect previously resistant cell lines that display the integrin receptor recognized by L14 (Girod et al., 1999). Although insertion of a targeting moiety against a particular target cell receptor into the viral capsid is an efficient way of targeting the virus, it is very time consuming to incorporate a specific targeting ligand into the viral capsid for a cell type of interest. Thus, a more general targeting approach might be more beneficial, especially for screening purposes. In this regard, Ried *et al.* incorporated the immunoglobulin G (IgG) binding domain of protein A, Z34C, into the AAV-2 capsid. The resulting AAV-2 mutants could be targeted to distinct hematopoietic cell lines using an antibody against CD29 (β_1-integrin), CD117 (c-kit receptor) and CXCR4 (Ried et al., 2002). Another example of a general targeting approach is provided by genetically modified Ad vectors. In this regard, Noureddinni *et al.* also fused the Fc-binding domain of Staphylococcus aureus protein A into a chimeric fiber expressed on Ad vectors. This modified Ad vector can now be utilized to infect a broad range of target cells, depending on the monoclonal antibody that is coupled to the Fc-binding domain on the Ad vector (Noureddini et al., 2006).

In addition to genetically incorporating the targeting ligands in the capsid of the viral vectors, another approach that has been proposed is pseudotyping. It involves substituiting the receptor binding proteins of one virus for those of another virus. For example, an AAV-2 genome encapsidated into a parvovirus B19 capsid can provide a new tool for AAV-2 targeting to specific cells, this is because based on the natural tropism for human erythroid progenitor cells of parvovirus B19 (Ponnazhagan et al., 1998).

One of the most advanced forms of genetic transductional targeting is to directly

incorporate antibodies recognizing the target cell antigens into the viral capsid. This has recently been achieved for Ad vectors. Hedley *et al.* genetically incorporated a scFv into the fiber of Ad vectors and demonstrated successful targeting to receptors on the surface of target cells (Hedley et al., 2006). It will be of interest to see the targeting capacity of these genetically modified vectors in an *in vivo* context, and determine their translational potential.

Similar genetic approaches have also been applied for targeting of other viruses. For example, scFV against CD38 and EGFR have been genetically incorporated into measles virus (MV) (Nakamura et al., 2005). More recently, Hasegawa *et al.* genetically modified the tropism of MV for targeted virotherapy of ovarian cancer. For this purpose, they incorporated the scFv specific for α-folate receptor (FRα), which is over-expressed on 90% of nonmucinous ovarian cancer, into the attachment protein of MV. This virus reduced the tumor volume and also increased the overall survival of mice as much as the parental virus, but without the side effects of the untargeted virus (Hasegawa et al., 2006).

Transcriptional targeting in combination with transductional targeting

The above examples illustrate the approaches that have been developed for targeting viral vectors to specific cells. However, a strategy to supplement the tranductional targeting is to involve transcriptional targeting as well. For this purpose, cell specific promoter elements have been incorporated into the genome of viral vectors to limit viral gene expression in specific cell types. For example, Muller *et al.* used AAV-2 devoid of binding to their primary receptor heparin sulfate proteoglycan. In this virus, they

incorporated a luciferase reporter gene under the control of 1.5-kb cardiac myosin light chain promoter, fused to the cytomegalovirus immediate early enhancer. The combined transductional and transcriptional targeting with this virus resulted in efficient gene transfer to cardiac cells *in vivo* and also had a significantly reduced hepatic sequestration (Muller et al., 2006).

Another example for combined transductional and transcriptional targeting is provided by Ad vector targeting to endothelial cells. To achieve this targeting, Reynolds *et al.* utilized a chemically linked bifunctional adapter. For this, a Fab fragment against Ad knob was chemically coupled to an antibody against angiotensin converting enzyme (9B9), which is a membrane-bound ectopeptidase expressed on pulmonary vascular endothelium. For transcriptional targeting, the promoter for vascular endothelial growth factor receptor type-1 (flt-1), which has high activity in endothelial cells, was utilized to drive the expression of a luciferase reporter gene. The combined transductional and transcriptional approaches resulted in a synergistic 300,000-fold improvement in the selectivity of transgene expression for lungs as compared to the liver, which is the usual vector sequestration site (Reynolds et al., 2001). Thus, combined targeting approaches have been shown to be useful for cell type specific viral vector delivery and therapeutic gene expression, for improved gene therapy.

Targeting of the viral vectors to the appropriate cells is crucial for development of an efficient gene therapy regimen and as illustrated by above examples, many unique strategies have been developed for this purpose. Though specific target cell delivery increases the therapeutic gene transfer to target cells, unfortunately an immune response elicited against the viral vector still limits full utilization of targeting approaches.

Strategies for Immune System Evasion by Viral Vectors

Viral vectors utilized for gene therapy are recognized as foreign by the host in which they are injected, and are therefore countered by an immune response. The immune response consists of innate and adaptive responses. The innate response is elicited upon recognition of the foreign viral capsid components by the immune system. The innate response leads to clearance of the viral vector before the viruses have had a chance for primary infection (Bessis et al., 2004; Muruve, 2004). This diminishes the efficiency of the transgene delivery to target host cells. Following successful viral infection of host cells, the adaptive arm of the host immune system is activated against the viral proteins that are produced in the host cells and the therapeutic gene if it is foreign to the host. The adaptive response also results in the development of immune memory, which further limits viral re-administration (Bessis et al., 2004). Also, pre-existing immunity against the viral vector further compounds the problem of efficient therapeutic transgene delivery by the viral vector. For example, Ads are one of the causative agents of the "common cold" and thus, many patients have pre-existing humoral immunity against the viral vector. This leads to rapid clearance of the therapeutic viral vector from the blood stream, prevents re-administration of the viral vector and results in overall reduction in the efficacy of the viral vector based gene therapy. This suggests that suppression or avoidance of the immune system would be needed to achieve sufficient viral vector based therapeutic effects. However, the immune response generated against the viral vector and/or the delivered transgene can also be exploited for manipulating the host immune system in developing an effective immune response against tumor cells. The following examples illustrate these points in more

detail.

Immuno-suppression

To circumvent the immune system mediated removal of the viral vector, a variety of approaches have been developed. In this regard, immuno-suppressants have been used to blunt the immune system of the host, thereby increasing the transgene delivery and expression by the viral vector. For example, Jooss *et al.* administered an Ad vector along with different doses of cyclophosphamide, which suppresses T cells. They demonstrated an effective blockade of both T and B cell responses in the liver and the lungs of C7BL/6 mice using this strategy. This resulted in prolonged transgene expression, reduced inflammation and allowed re-administration of the Ad vector (Jooss et al., 1996). However, the use of immunosuppressive drugs, which diminish the immune response capacity of the patient against foreign pathogens, causes concern.

Another strategy that has been utilized for immune system modulation involves perturbation of the host immune system at the level of cross-talk among different immune cell types. Disruption of the co-stimulatory interactions between antigen presenting cells (APCs) and B and T cells has been shown to be successful for reducing the cellular as well as humoral response generated against the viral vector. APCs present processed foreign antigens in association with major histocompatibilty complex (MHC) molecules to T cells for their activation. In addition to the antigenic peptide and MHC interaction with the T cell receptor (TCR), other co-stimulatory molecules also play an important role in T cell activation. In this regard, B7 proteins on APCs bind to CD28 on T cells, providing a critical second co-stimulatory signal, especially for the primary response of

the naïve T cells to novel antigens. B7 also binds to CTLA4 on the T cell surface, which primarily dampens T cell activation. Thus, blocking the interaction of B7 with CD28 will inhibit T cell priming, which will inhibit downstream immune responses activated by T cells. In this regard, it has been shown that the extracellular domain of CTLA4 fused to an immunoglobulin IgGFc domain (CTLA4Ig) binds to B7 with 20-fold higher affinity as compared to CD28. A consequence of the interaction of antigen-MHC with TCR in the absence of B7-CD28 interaction can be the induction of T cell anergy or prolonged unresponsiveness (Kay et al., 1997).

Another immune system interaction that has been disrupted is the interaction between activated T cells and B cells. Activated T cells express CD40, which binds to CD40 ligand on the surface of B cells, which is critical for the development of a humoral B cell response. This interaction can be blocked by a monoclonal antibody, MR-1, against CD40 ligand. Blockade of this interaction results in immunodeficiency in antibody response (Kay et al., 1997). A combination of CTLA4Ig with MR-1 has been utilized for suppressing the host immune system. For example, it has been shown that administration of MR-1 protein along with CTLA4Ig allowed for re-administration of AAV in lung (Halbert et al., 1998) and Ad in the liver (Kay et al., 1997).

An alternate strategy that has been utilized for immuno-suppression is incorporation of immune system suppressor genes in the viral vector itself. Immune system suppressing genes have been used to blunt the immune response even when the viral vector encoded proteins are produced in the host cells. For instance, Haralambieva *et al.* incorporated the P gene from a wild type measles virus (MV) strain into an oncolytic MV. The P gene product inhibits interferon (IFN) induction and/or response. The resulting chimeric

oncolytic virus armed with the P gene exhibited reduced IFN sensitivity, diminished IFN induction capacity and enhanced oncolytic potency as compared to the control oncolytic MV (Haralambieva et al., 2007).

Modification of the viral vector for immune system evasion

In order to prevent immune rejection of the viral vectors, various strategies have been employed for their modification in addition to immunosuppression. One of the strategies involves deletion of the unnecessary viral genome sequences resulting in reduced viral protein expression. The reduced viral protein production results in less immune stimulation. This strategy has been successfully applied for reducing the immune response against the viral vector. For example, as described in another section, gutless Ad vectors devoid of most of the genome sequences have been reported to have improved transgene expression and enhanced safety profile (Morsy et al., 1998; Schiedner et al., 1998).

Another strategy for immune evasion is based upon serotype change of the viral vectors. Serotype specificity is one of the ways to classify subtypes of viruses. Per definition, antibodies generated against one viral serotype do not recognize another viral serotype. Based on this consideration, Riviere *et al.* demonstrated that different recombinant AAV serotypes, AAV type 1, 2 and 5, can be utilized for repeated cross-administration for transgene delivery (Riviere et al., 2006). This is because pre-existing immunity against one serotype of a viral vector does not prevent administration of another serotype of that viral vector. Another such example is provided by Ad vectors that express capsid proteins derived from two different serotypes, so called chimeric

vectors. In this regard, it has been reported that the major antibody response is generated against the hexon capsid protein of Ad vectors. Based on this consideration, Wu *et al.* constructed a chimeric adenovirus, Ad5/H3, by replacing the Ad5 hexon gene with the hexon gene of Ad serotype 3 (Figure 3). They demonstrated that antibodies against either the parent virus with the Ad5 hexon protein (Ad5/H5) or the chimeric virus with Ad3 hexon protein (Ad5/H3) did not cross-neutralize the other virus. In addition, pre-immunization of C57BL/6 mice with either of the viruses did not prevent subsequent infection by the other virus (Wu et al., 2002a). Thus, serotype switching strategies can be utilized for re-administration of the viral vectors. However, for each re-administration, a vector with different serotype will be required. Generation of these serotype viral vectors requires much effort and they may not transducer the same target cell population.

In addition to the above genetic modification strategies, viral vectors have also been modified through chemical strategies, most notably by the use of poly(ethylene glycol) (PEG) to mask the antigenic epitopes on the viral surface. This is also known as 'stealthing' (Figure 3). PEG is a hydrophilic molecule, which physically masks the capsid proteins, thereby resulting in reduced innate immune response generated against the viral vector (Mok et al., 2005). Croyle *et al.* showed that PEGylated gutless Ad vectors could be re-administered with efficient transgene expression. Thus PEGylation can be utilized for improving the safety and efficacy profile of the viral vectors (Croyle et al., 2005). However, immune response will still be generated against the new viral progeny produced in infected cells.

Recently, PEGylation-based immune evasion has been combined with molecules utilized for retargeting of the viral vectors to the desired cell types. For example, folate

was chemically conjugated to PEG. The resulting folate-PEG was subsequently coupled to Ad vectors. This approach increased the transgene expression in folate receptor over-expressing cell line (KB cells) as compared to the folate receptor deficient cell line (A549 cells). In addition, PEGylation significantly reduced the innate immune response against the Ad vector (Oh et al., 2006). Thus, this combinatorial approach efficiently protects viral vectors from the innate immune system and also aids in efficient transgene delivery to specific target cells.

The examples listed above illustrate the various strategies that have been utilized for protecting the viral vector from the host immune system. However, the immune response generated against the viral vector and/or the delivered transgene can also be utilized in substituting immunity against the tumor cells. Although in general an immune response should be avoided to achieve a sufficient therapeutic effect, in the context of cancer immunotherapy this response is actually desired to efficiently utilize the capacity of the host immune system to kill the tumor cells. In this regard, viral vectors have been utilized for developing immunity against tumor-associated self antigens and thereby break tolerance. For example, AAV-2 was utilized to deliver BA46 to dendritic cells. BA46 is a membrane-associated glycoprotein that is expressed in most breast tumor cells, but not in general hematopoietic cell populations. The AAV-2 mediated BA46 delivery to dendritic cells resulted in generation of cytotoxic T lymphocytes against BA46 populations, which could potentially kill the breast cancer cells (Liu et al., 2005). Another example is provided by an Ad vector encoding HER2. The HER2/*neu* oncogene encodes for a protein p185 (C-erbB2). This protein is over-expressed in 30-50% of human breast cancer and in several other types of carcinomas. p185 has high oncogenic potential and

its increased expression correlates with tumor aggressiveness. Ad-HER2 was injected intra-muscularly in BALB/c mice that are transgenic for the transforming form of the *neu* oncogene. These mice spontaneously develop carcinomas in all mammary glands. The Ad-HER2 vaccination resulted in both T and B cell responses against HER2, thereby preventing tumorigenesis (Gallo et al., 2005). Thus, viral vectors can potentially be utilized for generating immune response against the tumor cells.

The above examples highlight a few of the strategies that have been successfully used to counter the immune response that is generated upon viral vector administration such as immunosuppression, expression of immune suppression genes and genetic as well as chemical vector modifications. In addition, the immune response generated against the viral vector and its transgene has been exploited for developing patient's immunity against the tumor cells.

Cell-based strategies for cancer gene therapy

In addition to the virus-based strategies described above, viruses have also been utilized for cell-based strategies aimed at cancer gene therapy. Many of these strategies are centered on using cells as factories to produce angiogenesis inhibitors or cytokines that prime the immune system. Other strategies are aimed at using cells as "trojan horses" to deliver suicide genes or oncolytic viruses directly within the tumor stroma. Cell vehicles used as factories can result in the localized and sustained production of therapeutic proteins, the length of which depends on the type of vectors used for gene transfer, the cellular targets transduced, and the immunogenicity of the therapeutic proteins produced.

Therapeutic effector molecules for cell-based therapy

Angiogenesis inhibitors, such as angiostatin (O'Reilly et al., 1994) and endostatin (O'Reilly et al., 1997), are effective at limiting tumor growth and metastasis, but the fact that micrometastatic lesions can lay dormant may require continuous production to prevent future tumor outgrowth (Scappaticci, 2002). Gene therapy approaches may be ideal for these situations, since these strategies allow for localized and sustained production, and avoids the need for the doses required for systemic efficacy (Persano et al., 2007). Mesenchymal stem cell mediated delivery of IL-12 was recently reported to reduce the formation of lung metastasis in a murine melanoma model, although NK and T cell mediated responses were also involved in the outcome (Elzaouk et al., 2006). A recent study by Jin *et al.* describes the combined use of an Ad vector that targets expression of an anti-angiogenic factor to the tumor endothelium along with a conditionally-replicating oncolytic Ad vector containing a tumor-specific promoter (Jin et al., 2005). A similar approach can be envisioned, using cell-mediated delivery of both therapeutic and oncolytic vectors. Combined therapeutic strategies for a disease marked by such vast epigenetic differences will likely be required. The true potential of angiogenesis inhibitors may be in the fact that they allow time for additional therapeutic avenues to take effect.

Cytokines are also favored as key therapeutic products for cell vehicle mediated delivery. As with angiogenesis inhibitors, large doses are often required to achieve therapeutically relevant concentrations. However, unlike angiogenesis inhibitors, elevated cytokine concentrations can have adverse effects (Lejeune et al., 1998; Neri et al., 2006). Thus, cellular vehicles may also serve to express and secrete the requisite cytokines for

localized production at concentrations that limit untoward complications to the host. These cellular factories also abrogate the need for recombinant protein production and purification techniques. Minuzzo *et al.* recently provided a detailed review of the combined use of viral vectors with cell-mediated delivery of cytokines (Minuzzo et al., 2007).

Cancer gene therapy studies have also evaluated the use of prodrug activating enzymes, or suicide genes, that convert an exogenously provided substrate into a cytotoxic molecule. The herpes simplex virus thymidine kinase gene (HSV-TK) acts as a suicide gene in the presence of the guanosine analog, gancyclovir (GCV) (Elion, 1980; Moolten, 1986). Cell vehicles that express these suicide genes and engraft tumors can cause a 'bystander effect', or collateral damage to surrounding tumor cells upon addition of the prodrug (Freeman et al., 1993). Tumor cells, endothelial cells, progenitor cells, and mesothelial cells have all been evaluated as vehicles to deliver the HSV-TK/GCV mediated bystander effect to tumors (Coukos et al., 1999; Pereboeva et al., 2003; Rancourt et al., 2003; Rancourt et al., 1998).

Recent studies have centered on the use of cell vehicles to deliver oncolytic adenovirus vectors. This strategy avoids complications and the marked inefficiency associated with systemic introduction of viruses, such as pre-existing neutralizing antibodies, non-specific vector sequestration in the liver or blood, and the inability to cross the endothelial barrier (Figure 4) (Chirmule et al., 1999; Franceschi, 2005; Shayakhmetov et al., 2005; Shayakhmetov et al., 2004; Tsujinoue et al., 2001). The list of naturally occurring, or recombinant oncolytic viruses includes adenovirus, herpes (Martuza et al., 1991), vaccinia, reovirus (Coffey et al., 1998), poliovirus, and Newcastle

Disease Virus (Bischoff et al., 1996; Cassel et al., 1965; Coffey et al., 1998; Gromeier et al., 2000; Martuza et al., 1991; Timiryasova et al., 1999). Various cellular vehicles have also been employed to deliver these agents to tumors. Tumor cells infected with oncolytic parvovirus (Raykov et al., 2004) or adenovirus (Garcia-Castro et al., 2005) vectors have been shown to engraft and deliver the oncolytic payload to pre-existing metastatic nodules. Others have used mesenchymal progenitors cells to deliver oncolytic agents to lung (Stoff-Khalili et al., 2007a) or intraperitoneal (Komarova et al., 2006) tumor xenografts. Cytokine induced killer cells have inherent tumor killing activity that is enhanced if the cells are preloaded with oncolytic vaccinia virus (Thorne et al., 2006). Iankov *et al.* recently reported the comparison of several cell vehicles as oncolytic measles virus carriers (Iankov et al., 2007). This strategy transferred the virus via a heterofusion mechanism, even in the presence of neutralizing antibodies, further demonstrating the true potential of this approach.

Cell types used in cell-based therapy

Along with the genetic payload to be used, the cell types suited or available for use as vehicles for cancer gene therapy will be critical. Different cell types have unique characteristics that may be required for efficient cancer gene therapy. In general, ideal cell vehicles are non-invasively accessible, can be purified and expanded to therapeutic levels, are susceptible to genetic manipulation, and home and engraft therapeutically-relevant target sites. Cell size is often a limiting factor due to the fact that systemic administration requires that the cells are capable of circulating through the lung microvasculature. Thus, the cells meeting most of the cell vehicle criteria are of

hematopoietic origin, as these cell types are innately geared for systemic circulation. Further, many of the other characteristics defining ideal cell vehicles are natural properties of hematopoietic cells, including their ability to infiltrate tumor tissues.

Of the many leukocyte subsets found within the tumor stroma, tumor-associated macrophages (TAMs) are the most abundant, and are typically associated with poor prognosis (Leek et al., 1996; O'Sullivan et al., 1994; Takanami et al., 1999). Macrophages are essential components of innate immunity, acting as both antigen presenting and effector cells that protect the body against invading pathogens. Macrophages arise from progenitors in the bone marrow, entering circulation as promonocytes, where they differentiate into monocytes. Monocytes infiltrate tissues, further differentiating into resident macrophages. Macrophage infiltration and accumulation is a normal part of the inflammatory processes resulting from wounds and infection, as well as chronic inflammatory disease. Tumor cells secrete chemotactic molecules such as CCL2, macrophage-colony stimulating factor, and vascular endothelial growth factor that act to recruit TAM precursors. The tumor cells also secrete cytokines that polarize TAM into type II macrophages, which act to suppress adaptive immunity (reviewed by Mantovani *et al.* (Mantovani et al., 2002)). Hypoxic conditions within tumors also induce expression of TAM genes associated with tumor cell proliferation, invasiveness, and angiogenesis (Murdoch et al., 2005). Although TAM are localized at the site of the tumor and play a part in tumor development, they lack the ability to home to tumors if isolated and systemically re-infused (Ben-Efraim et al., 1994; Wiltrout et al., 1983).

Many other leukocyte subsets are also found within the tumor stroma, including

tumor-infiltrating lymphocytes (TILs). TILs have been shown to have either tumor-suppressing or tumor-promoting activity. $CD4^+CD25^+FOXP3^+$ regulatory T cells (Tregs) suppress antitumoral immunity and thus promote tumor growth, while $CD8^+$ cytotoxic T lymphocytes (CTLs) have direct tumor cell killing activity (Chen et al., 2005; Nishikawa et al., 2005). Unlike TAMs, TILs can be isolated, expanded *ex vivo*, and home to tumors when systemically reimplanted into the patient. This adoptive transfer approach has recently been shown to be an effective strategy for the treatment of melanoma. Interestingly, unmodified (Dudley et al., 2002) tumor-reactive T cells, and T cells engineered with viral vectors to be tumor reactive (Morgan et al., 2006) have both demonstrated effective tumor regression in melanoma patients.

Several other non-hematopoietic cell types have also been evaluated as cell vehicles for cancer therapy. Progenitor cells are widely used for this strategy. These cells are rapidly recruited to sites of injury where they differentiate into the cellular components required to repair the damaged tissue (Mackenzie et al., 2001). The architecture of a rapidly developing tumor closely resembles damaged tissue in that it is often disorganized, inflamed, and hypoxic (Haroon et al., 2000). Not surprisingly, mesenchymal and endothelial progenitor cells are recruited to the site of the tumor and can contribute to malignant growth (Studeny et al., 2004).

The specific cell types used will largely depend on the types of tumors being targeted and the types of therapeutics intended for delivery. Systemic injection of cells, unless specifically targeted to the lung, should be restricted to hematopoietic cell lineages that can circulate through the microvasculature. Locoregional, or intratumoral injection of cell vehicles may utilize additional cell types. In the rare circumstances in which natural

tumor-homing T cells are attainable, delivery of lytic viruses may not be the best option, as these cells have inherent tumor-killing activity. As previously mentioned, many non-tumor cells contribute to tumor cell growth. Cell mediated delivery of agents that target elimination of Tregs or TAMs within the tumor may also prove to be therapeutically useful.

Future Perspectives

The above mentioned examples highlight the crucial role viral vectors play in gene therapy applications. However, problems related to efficient delivery of the transgene to target cells, long-term transgene expression and immune responses against the viral vector and infected cells have prevented utilization of the full potential of viral vectors. As noted above, various strategies have been employed to enhance the transgene delivery and expression and reduce viral toxicity. In future, continued progress in these respects will further improve overall efficiency of the viral vector based gene therapy.

Cell based therapy has utilized the many advances in viral vector mediated gene expression technology for concentrated, but localized delivery of therapeutic products. Although the idea of cell-based delivery of therapeutics has been around for quite a while, practical application has been limiting. Realization that particular cell types have true homing potential has led to revitalized interest in this technology. Much of the transcriptional and targeting knowledge obtained for both viruses and cells can now be combined for multifaceted cancer treatment approaches.

One of the interesting aspects related to tumor therapy is that combination of gene therapy with radiotherapy (Rogulski et al., 2000) or chemotherapy (Khuri et al., 2000)

has shown synergistic effects for tumor treatment. Thus, a combinatorial approach has been determined to be optimal for tumor treatment. Therefore, most likely in future viral vectors will be combined with both existing treatments for cancer, as well as new treatment opportunities offered by nanotechnology. As an example, gold nanoparticles (AuNPs), can be used for hyperthermic tumor cell ablation using laser irradiation (O'Neal et al., 2004). Everts *et al.* have attached AuNPs to Ad vectors to deliver these nanoparticles specifically to tumor cells (Everts et al., 2006). This complex of Ad vectors with AuNPs can potentially be used for simultaneous tumor treatment with gene therapy and nanotechnology approaches. These viral vectors with coupled nanoparticles have been previously defined as viro-nano therapy agents (Saini et al., 2006).

In conclusion, viral vectors as well as genetically modified cells are important for cancer gene therapy. Technological advances will further increase the utility of viral vectors for efficient gene and cell therapy in future, and much progress can be expected in the coming years, now that major roadblocks have been identified and strategies to overcome these roadblocks have shown promise in pre-clinical models.

Acknowledgements

This work was supported by the following grants: 1 R21 CA115568 (Dr. Larisa Pereboeva) and W81XWH-06-1-0630 (Dr. Maaike Everts).

References

Akusjarvi G (1993). Proteins with transcription regulatory properties encoded by human adenoviruses. *Trends Microbiol* **1**, 163-170.

Alba R, Bosch A, and Chillon M (2005). Gutless adenovirus: Last-generation adenovirus for gene therapy. *Gene Ther* **12 Suppl 1**, S18-27.

Amalfitano A, Hauser MA, Hu H, Serra D, Begy CR, and Chamberlain JS (1998). Production and characterization of improved adenovirus vectors with the e1, e2b, and e3 genes deleted. *J Virol* **72**, 926-933.

Ben-Efraim S, Tak C, Romijn JC, Fieren MJ, and Bonta IL (1994). Therapeutical effect of activated human macrophages on a human tumor line growing in nude mice. *Med Oncol* **11**, 7-12.

Bessis N, GarciaCozar FJ, and Boissier MC (2004). Immune responses to gene therapy vectors: Influence on vector function and effector mechanisms. *Gene Ther* **11 Suppl 1**, S10-17.

Bett AJ, Prevec L, and Graham FL (1993). Packaging capacity and stability of human adenovirus type 5 vectors. *J Virol* **67**, 5911-5921.

Bischoff JR, Kirn DH, Williams A, Heise C, Horn S, Muna M, Ng L, Nye JA, Sampson-Johannes A, Fattaey A, and McCormick F (1996). An adenovirus mutant that replicates selectively in p53-deficient human tumor cells. *Science* **274**, 373-376.

Bogdanovich S, Perkins KJ, Krag TO, and Khurana TS (2004). Therapeutics for duchenne muscular dystrophy: Current approaches and future directions. *J Mol Med* **82**, 102-115.

Bridge E, and Ketner G (1989). Redundant control of adenovirus late gene expression by early region 4. *J Virol* **63**, 631-638.

Cassel WA, and Garrett RE (1965). Newcastle disease virus as an antineoplastic agent.

Cancer **18**, 863-868.

Chang LJ, and He J (2001). Retroviral vectors for gene therapy of aids and cancer. *Curr Opin Mol Ther* **3**, 468-475.

Chen ML, Pittet MJ, Gorelik L, Flavell RA, Weissleder R, von Boehmer H, and Khazaie K (2005). Regulatory t cells suppress tumor-specific cd8 t cell cytotoxicity through tgf-beta signals in vivo. *Proc Natl Acad Sci U S A* **102**, 419-424.

Chirmule N, Propert K, Magosin S, Qian Y, Qian R, and Wilson J (1999). Immune responses to adenovirus and adeno-associated virus in humans. *Gene Ther* **6**, 1574-1583.

Coffey MC, Strong JE, Forsyth PA, and Lee PW (1998). Reovirus therapy of tumors with activated ras pathway. *Science* **282**, 1332-1334.

Coukos G, Makrigiannakis A, Kang EH, Caparelli D, Benjamin I, Kaiser LR, Rubin SC, Albelda SM, and Molnar-Kimber KL (1999). Use of carrier cells to deliver a replication-selective herpes simplex virus-1 mutant for the intraperitoneal therapy of epithelial ovarian cancer. *Clin Cancer Res* **5**, 1523-1537.

Croyle MA, Le HT, Linse KD, Cerullo V, Toietta G, Beaudet A, and Pastore L (2005). Pegylated helper-dependent adenoviral vectors: Highly efficient vectors with an enhanced safety profile. *Gene Ther* **12**, 579-587.

Dong Y, Wen P, Manome Y, Parr M, Hirshowitz A, Chen L, Hirschowitz EA, Crystal R, Weichselbaum R, Kufe DW, and Fine HA (1996). In vivo replication-deficient adenovirus vector-mediated transduction of the cytosine

deaminase gene sensitizes glioma cells to 5-fluorocytosine. *Hum Gene Ther* **7**, 713-720.

Dudley ME, Wunderlich JR, Robbins PF, Yang JC, Hwu P, Schwartzentruber DJ, Topalian SL, Sherry R, Restifo NP, Hubicki AM, Robinson MR, Raffeld M, Duray P, Seipp CA, Rogers-Freezer L, Morton KE, Mavroukakis SA, White DE, and Rosenberg SA (2002). Cancer regression and autoimmunity in patients after clonal repopulation with antitumor lymphocytes. *Science* **298**, 850-854.

Dyson N (1998). The regulation of e2f by prb-family proteins. *Genes Dev* **12**, 2245-2262.

Elion GB (1980). The chemotherapeutic exploitation of virus-specified enzymes. *Adv Enzyme Regul* **18**, 53-66.

Elzaouk L, Moelling K, and Pavlovic J (2006). Anti-tumor activity of mesenchymal stem cells producing il-12 in a mouse melanoma model. *Exp Dermatol* **15**, 865-874.

Etoh T, Himeno Y, Matsumoto T, Aramaki M, Kawano K, Nishizono A, and Kitano S (2003). Oncolytic viral therapy for human pancreatic cancer cells by reovirus. *Clin Cancer Res* **9**, 1218-1223.

Everts M, Kim-Park SA, Preuss MA, Passineau MJ, Glasgow JN, Pereboev AV, Mahasreshti PJ, Grizzle WE, Reynolds PN, and Curiel DT (2005). Selective induction of tumor-associated antigens in murine pulmonary vasculature using double-targeted adenoviral vectors. *Gene Ther* **12**, 1042-1048.

Everts M, Saini V, Leddon JL, Kok RJ, Stoff-Khalili M, Preuss MA, Millican CL, Perkins G, Brown JM, Bagaria H, Nikles DE, Johnson DT, Zharov VP, and Curiel DT (2006). Covalently linked au nanoparticles to a viral vector: Potential

for combined photothermal and gene cancer therapy. *Nano Lett* **6**, 587-591.

Flint J, and Shenk T (1997). Viral transactivating proteins. *Annu Rev Genet* **31**, 177-212.

Franceschi RT (2005). Biological approaches to bone regeneration by gene therapy. *J Dent Res* **84**, 1093-1103.

Freeman SM, Abboud CN, Whartenby KA, Packman CH, Koeplin DS, Moolten FL, and Abraham GN (1993). The "Bystander effect": Tumor regression when a fraction of the tumor mass is genetically modified. *Cancer Res* **53**, 5274-5283.

Fueyo J, Gomez-Manzano C, Alemany R, Lee PS, McDonnell TJ, Mitlianga P, Shi YX, Levin VA, Yung WK, and Kyritsis AP (2000). A mutant oncolytic adenovirus targeting the rb pathway produces anti-glioma effect in vivo. *Oncogene* **19**, 2-12.

Gallo P, Dharmapuri S, Nuzzo M, Maldini D, Iezzi M, Cavallo F, Musiani P, Forni G, and Monaci P (2005). Xenogeneic immunization in mice using her2 DNA delivered by an adenoviral vector. *Int J Cancer* **113**, 67-77.

Garcia-Castro J, Martinez-Palacio J, Lillo R, Garcia-Sanchez F, Alemany R, Madero L, Bueren JA, and Ramirez M (2005). Tumor cells as cellular vehicles to deliver gene therapies to metastatic tumors. *Cancer Gene Ther* **12**, 341-349.

Girod A, Ried M, Wobus C, Lahm H, Leike K, Kleinschmidt J, Deleage G, and Hallek M (1999). Genetic capsid modifications allow efficient re-targeting of adeno-associated virus type 2. *Nat Med* **5**, 1052-1056.

Gromeier M, Lachmann S, Rosenfeld MR, Gutin PH, and Wimmer E (2000). Intergeneric poliovirus recombinants for the treatment of malignant glioma. *Proc*

Natl Acad Sci U S A **97**, 6803-6808.

Haisma HJ, Grill J, Curiel DT, Hoogeland S, van Beusechem VW, Pinedo HM, and Gerritsen WR (2000). Targeting of adenoviral vectors through a bispecific single-chain antibody. *Cancer Gene Ther* **7**, 901-904.

Halbert CL, Rutledge EA, Allen JM, Russell DW, and Miller AD (2000). Repeat transduction in the mouse lung by using adeno-associated virus vectors with different serotypes. *J Virol* **74**, 1524-1532.

Halbert CL, Standaert TA, Wilson CB, and Miller AD (1998). Successful readministration of adeno-associated virus vectors to the mouse lung requires transient immunosuppression during the initial exposure. *J Virol* **72**, 9795-9805.

Haralambieva I, Iankov I, Hasegawa K, Harvey M, Russell SJ, and Peng KW (2007). Engineering oncolytic measles virus to circumvent the intracellular innate immune response. *Mol Ther* **15**, 588-597.

Haroon ZA, Raleigh JA, Greenberg CS, and Dewhirst MW (2000). Early wound healing exhibits cytokine surge without evidence of hypoxia. *Ann Surg* **231**, 137-147.

Hasegawa K, Nakamura T, Harvey M, Ikeda Y, Oberg A, Figini M, Canevari S, Hartmann LC, and Peng KW (2006). The use of a tropism-modified measles virus in folate receptor-targeted virotherapy of ovarian cancer. *Clin Cancer Res* **12**, 6170-6178.

Hashiro G, Loh PC, and Yau JT (1977). The preferential cytotoxicity of reovirus for certain transformed cell lines. *Arch Virol* **54**, 307-315.

Hedley SJ, Auf der Maur A, Hohn S, Escher D, Barberis A, Glasgow JN, Douglas

JT, Korokhov N, and Curiel DT (2006). An adenovirus vector with a chimeric fiber incorporating stabilized single chain antibody achieves targeted gene delivery. *Gene Ther* **13**, 88-94.

Huang MM, and Hearing P (1989). Adenovirus early region 4 encodes two gene products with redundant effects in lytic infection. *J Virol* **63**, 2605-2615.

Iankov ID, Blechacz B, Liu C, Schmeckpeper JD, Tarara JE, Federspiel MJ, Caplice N, and Russell SJ (2007). Infected cell carriers: A new strategy for systemic delivery of oncolytic measles viruses in cancer virotherapy. *Mol Ther* **15**, 114-122.

Ji L, Bouvet M, Price RE, Roth JA, and Fang B (1999). Reduced toxicity, attenuated immunogenicity and efficient mediation of human p53 gene expression in vivo by an adenovirus vector with deleted e1-e3 and inactivated e4 by gal4-tata promoter replacement. *Gene Ther* **6**, 393-402.

Jin F, Xie Z, Kuo CJ, Chung LW, and Hsieh CL (2005). Cotargeting tumor and tumor endothelium effectively inhibits the growth of human prostate cancer in adenovirus-mediated antiangiogenesis and oncolysis combination therapy. *Cancer Gene Ther* **12**, 257-267.

Jooss K, Yang Y, and Wilson JM (1996). Cyclophosphamide diminishes inflammation and prolongs transgene expression following delivery of adenoviral vectors to mouse liver and lung. *Hum Gene Ther* **7**, 1555-1566.

Kanerva A, Bauerschmitz GJ, Yamamoto M, Lam JT, Alvarez RD, Siegal GP, Curiel DT, and Hemminki A (2004). A cyclooxygenase-2 promoter-based conditionally replicating adenovirus with enhanced infectivity for treatment of

ovarian adenocarcinoma. *Gene Ther* **11**, 552-559.

Kay MA, Meuse L, Gown AM, Linsley P, Hollenbaugh D, Aruffo A, Ochs HD, and Wilson CB (1997). Transient immunomodulation with anti-cd40 ligand antibody and ctla4ig enhances persistence and secondary adenovirus-mediated gene transfer into mouse liver. *Proc Natl Acad Sci U S A* **94**, 4686-4691.

Khuri FR, Nemunaitis J, Ganly I, Arseneau J, Tannock IF, Romel L, Gore M, Ironside J, MacDougall RH, Heise C, Randlev B, Gillenwater AM, Bruso P, Kaye SB, Hong WK, and Kirn DH (2000). A controlled trial of intratumoral onyx-015, a selectively-replicating adenovirus, in combination with cisplatin and 5-fluorouracil in patients with recurrent head and neck cancer. *Nat Med* **6**, 879-885.

Komarova S, Kawakami Y, Stoff-Khalili MA, Curiel DT, and Pereboeva L (2006). Mesenchymal progenitor cells as cellular vehicles for delivery of oncolytic adenoviruses. *Mol Cancer Ther* **5**, 755-766.

Krasnykh VN, Mikheeva GV, Douglas JT, and Curiel DT (1996). Generation of recombinant adenovirus vectors with modified fibers for altering viral tropism. *J Virol* **70**, 6839-6846.

Kreppel F, and Kochanek S (2004). Long-term transgene expression in proliferating cells mediated by episomally maintained high-capacity adenovirus vectors. *J Virol* **78**, 9-22.

Lam JT, Hemminki A, Kanerva A, Lee KB, Blackwell JL, Desmond R, Siegal GP, and Curiel DT (2007). A three-dimensional assay for measurement of viral-induced oncolysis. *Cancer Gene Ther*.

Leek RD, Lewis CE, Whitehouse R, Greenall M, Clarke J, and Harris AL (1996). Association of macrophage infiltration with angiogenesis and prognosis in invasive breast carcinoma. *Cancer Res* **56**, 4625-4629.

Lejeune FJ, Ruegg C, and Lienard D (1998). Clinical applications of tnf-alpha in cancer. *Curr Opin Immunol* **10**, 573-580.

Liu Y, Chiriva-Internati M, You C, Luo R, You H, Prasad CK, Grizzi F, Cobos E, Klimberg VS, Kay H, Mehta JL, and Hermonat PL (2005). Use and specificity of breast cancer antigen/milk protein ba46 for generating anti-self-cytotoxic t lymphocytes by recombinant adeno-associated virus-based gene loading of dendritic cells. *Cancer Gene Ther* **12**, 304-312.

Mackenzie TC, and Flake AW (2001). Human mesenchymal stem cells persist, demonstrate site-specific multipotential differentiation, and are present in sites of wound healing and tissue regeneration after transplantation into fetal sheep. *Blood Cells Mol Dis* **27**, 601-604.

Mantovani A, Sozzani S, Locati M, Allavena P, and Sica A (2002). Macrophage polarization: Tumor-associated macrophages as a paradigm for polarized m2 mononuclear phagocytes. *Trends Immunol* **23**, 549-555.

Marini FC, Shayakhmetov D, Gharwan H, Lieber A, and Andreeff M (2002). Advances in gene transfer into haematopoietic stem cells by adenoviral vectors. *Expert Opin Biol Ther* **2**, 847-856.

Martuza RL, Malick A, Markert JM, Ruffner KL, and Coen DM (1991). Experimental therapy of human glioma by means of a genetically engineered virus mutant. *Science* **252**, 854-856.

McCarty DM, Young SM, Jr., and Samulski RJ (2004). Integration of adeno-associated virus (aav) and recombinant aav vectors. *Annu Rev Genet* **38**, 819-845.

Miller CR, Buchsbaum DJ, Reynolds PN, Douglas JT, Gillespie GY, Mayo MS, Raben D, and Curiel DT (1998). Differential susceptibility of primary and established human glioma cells to adenovirus infection: Targeting via the epidermal growth factor receptor achieves fiber receptor-independent gene transfer. *Cancer Res* **58**, 5738-5748.

Minuzzo S, Moserle L, Indraccolo S, and Amadori A (2007). Angiogenesis meets immunology: Cytokine gene therapy of cancer. *Mol Aspects Med*.

Mok H, Palmer DJ, Ng P, and Barry MA (2005). Evaluation of polyethylene glycol modification of first-generation and helper-dependent adenoviral vectors to reduce innate immune responses. *Mol Ther* **11**, 66-79.

Moolten FL (1986). Tumor chemosensitivity conferred by inserted herpes thymidine kinase genes: Paradigm for a prospective cancer control strategy. *Cancer Res* **46**, 5276-5281.

Morgan RA, Dudley ME, Wunderlich JR, Hughes MS, Yang JC, Sherry RM, Royal RE, Topalian SL, Kammula US, Restifo NP, Zheng Z, Nahvi A, de Vries CR, Rogers-Freezer LJ, Mavroukakis SA, and Rosenberg SA (2006). Cancer regression in patients after transfer of genetically engineered lymphocytes. *Science* **314**, 126-129.

Morsy MA, Gu M, Motzel S, Zhao J, Lin J, Su Q, Allen H, Franlin L, Parks RJ, Graham FL, Kochanek S, Bett AJ, and Caskey CT (1998). An adenoviral vector deleted for all viral coding sequences results in enhanced safety and

extended expression of a leptin transgene. *Proc Natl Acad Sci U S A* **95**, 7866-7871.

Muller OJ, Leuchs B, Pleger ST, Grimm D, Franz WM, Katus HA, and Kleinschmidt JA (2006). Improved cardiac gene transfer by transcriptional and transductional targeting of adeno-associated viral vectors. *Cardiovasc Res* **70**, 70-78.

Murdoch C, Muthana M, and Lewis CE (2005). Hypoxia regulates macrophage functions in inflammation. *J Immunol* **175**, 6257-6263.

Muruve DA (2004). The innate immune response to adenovirus vectors. *Hum Gene Ther* **15**, 1157-1166.

Nakamura T, Peng KW, Harvey M, Greiner S, Lorimer IA, James CD, and Russell SJ (2005). Rescue and propagation of fully retargeted oncolytic measles viruses. *Nat Biotechnol* **23**, 209-214.

Naldini L, and Verma IM (2000). Lentiviral vectors. *Adv Virus Res* **55**, 599-609.

Neri S, Pulvirenti D, and Bertino G (2006). Psychiatric symptoms induced by antiviral therapy in chronic hepatitis c: Comparison between interferon-alpha-2a and interferon-alpha-2b. *Clin Drug Investig* **26**, 655-662.

Nettelbeck DM, and Curiel DT (2003). Tumor-busting viruses. *Sci Am* **289**, 68-75.

Nettelbeck DM, Rivera AA, Kupsch J, Dieckmann D, Douglas JT, Kontermann RE, Alemany R, and Curiel DT (2004). Retargeting of adenoviral infection to melanoma: Combining genetic ablation of native tropism with a recombinant bispecific single-chain diabody (scdb) adapter that binds to fiber knob and hmwmaa. *Int J Cancer* **108**, 136-145.

Nishikawa H, Jager E, Ritter G, Old LJ, and Gnjatic S (2005). Cd4+ cd25+ regulatory t cells control the induction of antigen-specific cd4+ helper t cell responses in cancer patients. *Blood* **106**, 1008-1011.

Norman KL, Coffey MC, Hirasawa K, Demetrick DJ, Nishikawa SG, DiFrancesco LM, Strong JE, and Lee PW (2002). Reovirus oncolysis of human breast cancer. *Hum Gene Ther* **13**, 641-652.

Norman KL, Hirasawa K, Yang AD, Shields MA, and Lee PW (2004). Reovirus oncolysis: The ras/ralgef/p38 pathway dictates host cell permissiveness to reovirus infection. *Proc Natl Acad Sci U S A* **101**, 11099-11104.

Noureddini SC, Krendelshchikov A, Simonenko V, Hedley SJ, Douglas JT, Curiel DT, and Korokhov N (2006). Generation and selection of targeted adenoviruses embodying optimized vector properties. *Virus Res* **116**, 185-195.

O'Neal DP, Hirsch LR, Halas NJ, Payne JD, and West JL (2004). Photo-thermal tumor ablation in mice using near infrared-absorbing nanoparticles. *Cancer Lett* **209**, 171-176.

O'Reilly MS, Boehm T, Shing Y, Fukai N, Vasios G, Lane WS, Flynn E, Birkhead JR, Olsen BR, and Folkman J (1997). Endostatin: An endogenous inhibitor of angiogenesis and tumor growth. *Cell* **88**, 277-285.

O'Reilly MS, Holmgren L, Shing Y, Chen C, Rosenthal RA, Moses M, Lane WS, Cao Y, Sage EH, and Folkman J (1994). Angiostatin: A novel angiogenesis inhibitor that mediates the suppression of metastases by a lewis lung carcinoma. *Cell* **79**, 315-328.

O'Sullivan C, and Lewis CE (1994). Tumour-associated leucocytes: Friends or foes in

breast carcinoma. *J Pathol* **172**, 229-235.

Oh IK, Mok H, and Park TG (2006). Folate immobilized and pegylated adenovirus for retargeting to tumor cells. *Bioconjug Chem* **17**, 721-727.

Parks RJ, Chen L, Anton M, Sankar U, Rudnicki MA, and Graham FL (1996). A helper-dependent adenovirus vector system: Removal of helper virus by cre-mediated excision of the viral packaging signal. *Proc Natl Acad Sci U S A* **93**, 13565-13570.

Pereboeva L, Komarova S, Mikheeva G, Krasnykh V, and Curiel DT (2003). Approaches to utilize mesenchymal progenitor cells as cellular vehicles. *Stem Cells* **21**, 389-404.

Persano L, Crescenzi M, and Indraccolo S (2007). Anti-angiogenic gene therapy of cancer: Current status and future prospects. *Mol Aspects Med*.

Ponnazhagan S, Weigel KA, Raikwar SP, Mukherjee P, Yoder MC, and Srivastava A (1998). Recombinant human parvovirus b19 vectors: Erythroid cell-specific delivery and expression of transduced genes. *J Virol* **72**, 5224-5230.

Rancourt C, Bergeron C, Lane D, Garon G, and Piche A (2003). Delivery of herpes simplex thymidine kinase bystander effect by engineered human mesothelial cells for the treatment of ovarian cancer. *Cytotherapy* **5**, 509-522.

Rancourt C, Robertson MW, 3rd, Wang M, Goldman CK, Kelly JF, Alvarez RD, Siegal GP, and Curiel DT (1998). Endothelial cell vehicles for delivery of cytotoxic genes as a gene therapy approach for carcinoma of the ovary. *Clin Cancer Res* **4**, 265-270.

Raykov Z, Balboni G, Aprahamian M, and Rommelaere J (2004). Carrier cell-

mediated delivery of oncolytic parvoviruses for targeting metastases. *Int J Cancer* **109**, 742-749.

Reynolds PN, Nicklin SA, Kaliberova L, Boatman BG, Grizzle WE, Balyasnikova IV, Baker AH, Danilov SM, and Curiel DT (2001). Combined transductional and transcriptional targeting improves the specificity of transgene expression in vivo. *Nat Biotechnol* **19**, 838-842.

Ried MU, Girod A, Leike K, Buning H, and Hallek M (2002). Adeno-associated virus capsids displaying immunoglobulin-binding domains permit antibody-mediated vector retargeting to specific cell surface receptors. *J Virol* **76**, 4559-4566.

Ring CJ (2002). Cytolytic viruses as potential anti-cancer agents. *J Gen Virol* **83**, 491-502.

Riviere C, Danos O, and Douar AM (2006). Long-term expression and repeated administration of aav type 1, 2 and 5 vectors in skeletal muscle of immunocompetent adult mice. *Gene Ther* **13**, 1300-1308.

Rogulski KR, Freytag SO, Zhang K, Gilbert JD, Paielli DL, Kim JH, Heise CC, and Kirn DH (2000). In vivo antitumor activity of onyx-015 is influenced by p53 status and is augmented by radiotherapy. *Cancer Res* **60**, 1193-1196.

Saini V, P. Zharov V, S. Brazel C, E. Nikles D, T. Johnson D, and Everts M (2006). Combination of viral biology and nanotechnology:New applications in nanomedicine. *Nanomedicine: Nanotechnology, Biology, and Medicine* **2**, 200-206.

Sakhuja K, Reddy PS, Ganesh S, Cantaniag F, Pattison S, Limbach P, Kayda DB, Kadan MJ, Kaleko M, and Connelly S (2003). Optimization of the generation

and propagation of gutless adenoviral vectors. *Hum Gene Ther* **14**, 243-254.

Scappaticci FA (2002). Mechanisms and future directions for angiogenesis-based cancer therapies. *J Clin Oncol* **20**, 3906-3927.

Schiedner G, Morral N, Parks RJ, Wu Y, Koopmans SC, Langston C, Graham FL, Beaudet AL, and Kochanek S (1998). Genomic DNA transfer with a high-capacity adenovirus vector results in improved in vivo gene expression and decreased toxicity. *Nat Genet* **18**, 180-183.

Shayakhmetov DM, Gaggar A, Ni S, Li ZY, and Lieber A (2005). Adenovirus binding to blood factors results in liver cell infection and hepatotoxicity. *J Virol* **79**, 7478-7491.

Shayakhmetov DM, Li ZY, Ni S, and Lieber A (2004). Analysis of adenovirus sequestration in the liver, transduction of hepatic cells, and innate toxicity after injection of fiber-modified vectors. *J Virol* **78**, 5368-5381.

Shin EJ, Wanna GB, Choi B, Aguila D, 3rd, Ebert O, Genden EM, and Woo SL (2007). Interleukin-12 expression enhances vesicular stomatitis virus oncolytic therapy in murine squamous cell carcinoma. *Laryngoscope* **117**, 210-214.

Shinozaki K, Ebert O, and Woo SL (2005). Treatment of multi-focal colorectal carcinoma metastatic to the liver of immune-competent and syngeneic rats by hepatic artery infusion of oncolytic vesicular stomatitis virus. *Int J Cancer* **114**, 659-664.

Stevenson AJ, Giles MS, Hall KT, Goodwin DJ, Calderwood MA, Markham AF, and Whitehouse A (2000). Specific oncolytic activity of herpesvirus saimiri in pancreatic cancer cells. *Br J Cancer* **83**, 329-332.

Stoff-Khalili MA, Rivera AA, Mathis JM, Banerjee NS, Moon AS, Hess A, Rocconi RP, Numnum TM, Everts M, Chow LT, Douglas JT, Siegal GP, Zhu ZB, Bender HG, Dall P, Stoff A, Pereboeva L, and Curiel DT (2007a). Mesenchymal stem cells as a vehicle for targeted delivery of crads to lung metastases of breast carcinoma. *Breast Cancer Res Treat*.

Stoff-Khalili MA, Rivera AA, Stoff A, Michael Mathis J, Rocconi RP, Matthews QL, Numnum MT, Herrmann I, Dall P, Eckhoff DE, Douglas JT, Siegal GP, Zhu ZB, and Curiel DT (2007b). Combining high selectivity of replication via cxcr4 promoter with fiber chimerism for effective adenoviral oncolysis in breast cancer. *Int J Cancer* **120**, 935-941.

Stojdl DF, Lichty B, Knowles S, Marius R, Atkins H, Sonenberg N, and Bell JC (2000). Exploiting tumor-specific defects in the interferon pathway with a previously unknown oncolytic virus. *Nat Med* **6**, 821-825.

Studeny M, Marini FC, Dembinski JL, Zompetta C, Cabreira-Hansen M, Bekele BN, Champlin RE, and Andreeff M (2004). Mesenchymal stem cells: Potential precursors for tumor stroma and targeted-delivery vehicles for anticancer agents. *J Natl Cancer Inst* **96**, 1593-1603.

Takanami I, Takeuchi K, and Kodaira S (1999). Tumor-associated macrophage infiltration in pulmonary adenocarcinoma: Association with angiogenesis and poor prognosis. *Oncology* **57**, 138-142.

Takayama K, Reynolds PN, Adachi Y, Kaliberova L, Uchino J, Nakanishi Y, and Curiel DT (2007). Vascular endothelial growth factor promoter-based conditionally replicative adenoviruses for pan-carcinoma application. *Cancer*

Gene Ther **14**, 105-116.

Thomas MA, Spencer JF, La Regina MC, Dhar D, Tollefson AE, Toth K, and Wold WS (2006). Syrian hamster as a permissive immunocompetent animal model for the study of oncolytic adenovirus vectors. *Cancer Res* **66**, 1270-1276.

Thorne SH, Negrin RS, and Contag CH (2006). Synergistic antitumor effects of immune cell-viral biotherapy. *Science* **311**, 1780-1784.

Timiryasova TM, Li J, Chen B, Chong D, Langridge WH, Gridley DS, and Fodor I (1999). Antitumor effect of vaccinia virus in glioma model. *Oncol Res* **11**, 133-144.

Trapnell BC, and Gorziglia M (1994). Gene therapy using adenoviral vectors. *Curr Opin Biotechnol* **5**, 617-625.

Tsujinoue H, Kuriyama S, Tominaga K, Okuda H, Nakatani T, Yoshiji H, Tsujimoto T, Akahane T, Asada K, and Fukui H (2001). Intravenous readministration of an adenoviral vector performed long after the initial administration failed to induce re-expression of the original transgene in rats. *Int J Oncol* **18**, 575-580.

Van der Vliet PC (1995). Adenovirus DNA replication. *Curr Top Microbiol Immunol* **199 (Pt 2)**, 1-30.

Vile R, Ando D, and Kirn D (2002). The oncolytic virotherapy treatment platform for cancer: Unique biological and biosafety points to consider. *Cancer Gene Ther* **9**, 1062-1067.

Watkins SJ, Mesyanzhinov VV, Kurochkina LP, and Hawkins RE (1997). The 'adenobody' approach to viral targeting: Specific and enhanced adenoviral gene

delivery. *Gene Ther* **4**, 1004-1012.

Wilcox ME, Yang W, Senger D, Rewcastle NB, Morris DG, Brasher PM, Shi ZQ, Johnston RN, Nishikawa S, Lee PW, and Forsyth PA (2001). Reovirus as an oncolytic agent against experimental human malignant gliomas. *J Natl Cancer Inst* **93**, 903-912.

Wiltrout RH, Brunda MJ, Gorelik E, Peterson ES, Dunn JJ, Leonhardt J, Varesio L, Reynolds CW, and Holden HT (1983). Distribution of peritoneal macrophage populations after intravenous injection in mice: Differential effects of eliciting and activating agents. *J Reticuloendothel Soc* **34**, 253-269.

Wold WS, Doronin K, Toth K, Kuppuswamy M, Lichtenstein DL, and Tollefson AE (1999). Immune responses to adenoviruses: Viral evasion mechanisms and their implications for the clinic. *Curr Opin Immunol* **11**, 380-386.

Wold WS, Tollefson AE, and Hermiston TW (1995). E3 transcription unit of adenovirus. *Curr Top Microbiol Immunol* **199 (Pt 1)**, 237-274.

Wong RJ, Chan MK, Yu Z, Kim TH, Bhargava A, Stiles BM, Horsburgh BC, Shah JP, Ghossein RA, Singh B, and Fong Y (2004). Effective intravenous therapy of murine pulmonary metastases with an oncolytic herpes virus expressing interleukin 12. *Clin Cancer Res* **10**, 251-259.

Wu H, Dmitriev I, Kashentseva E, Seki T, Wang M, and Curiel DT (2002a). Construction and characterization of adenovirus serotype 5 packaged by serotype 3 hexon. *J Virol* **76**, 12775-12782.

Wu H, Seki T, Dmitriev I, Uil T, Kashentseva E, Han T, and Curiel DT (2002b). Double modification of adenovirus fiber with rgd and polylysine motifs improves

coxsackievirus-adenovirus receptor-independent gene transfer efficiency. *Hum Gene Ther* **13**, 1647-1653.

Yamamoto M, Davydova J, Wang M, Siegal GP, Krasnykh V, Vickers SM, and Curiel DT (2003). Infectivity enhanced, cyclooxygenase-2 promoter-based conditionally replicative adenovirus for pancreatic cancer. *Gastroenterology* **125**, 1203-1218.

Yang Y, Nunes FA, Berencsi K, Furth EE, Gonczol E, and Wilson JM (1994). Cellular immunity to viral antigens limits e1-deleted adenoviruses for gene therapy. *Proc Natl Acad Sci U S A* **91**, 4407-4411.

Young LS, Dawson CW, and Eliopoulos AG (1997). Viruses and apoptosis. *Br Med Bull* **53**, 509-521.

Figure Legends

Figure 1. Diagram of viral genomes corresponding to the wild type Ad genome and three generations of Ad vectors. Deleted genes are shown in gray. The function of the deleted genes is delivered *in trans* by complementing cell lines or a helper virus. Each generation has tolerated larger insert sizes, culminating in gutless vectors that can package inserts up to 36kB. An example of how these gutless vectors are produced is the use of a helper virus that incorporates loxP sites that flank the packaging signal (ψ) in its genome. When this virus infects cells that express the Cre recombinase and are transfected with the gutless genome, the packaging signal will be deleted from the helper virus genome that will thus not be incorporated into the new virions, resulting instead in packaging of the gutless genome that has the packaging signal.

Figure 2. Modification of replicating viruses into non-replicating gene therapy vectors. Left: Adenovirus and Herpes Simplex Virus are examples of viruses that can be modified into replication incompetent gene therapy vectors by deleting the genes necessary for viral replication (gray rectangles) from the viral genome (green rectangles). Right: The deletion of genes essential for viral replication provides space for therapeutic genes of interest (blue rectangle), which can be incorporated into the genome. For vector production, the gene products necessary for viral replication (gray rectangles) are provided *in trans* in a complementing cell line, resulting in replication incompetent vectors that carry the therapeutic gene of interest.

Figure 3. Strategies employed for immune system evasion. Pre-existing immunity against gene therapy vectors is a major limitation to effective gene transfer. Strategies to overcome this hurdle include serotype switching (top) and physical masking of antigenic epitopes (bottom). Top: Serotype switching encompasses the construction of vectors containing capsid proteins from different serotypes. For example, a chimeric Ad5 vector expressing hexon protein of Ad3 was constructed. This vector was not recognized by antibodies against the hexon protein of Ad5, thereby allowing vector re-administration. Bottom: Alternative strategies have included physical masking of antigenic epitopes on viral vectors. For example, poly(ethylene glycol) molecules can be chemically conjugated to Ad vectors, which protect the vectors against antibody recognition.

Figure 4. Fate of systemically delivered Ad vectors. Systemically administered Ad vectors are not able to escape the circulatory system and are thus rapidly sequestered by cells of the reticuloendothelial system. Furthermore, Ad targeting is limited by soluble

immune factors, such as complement and neutralizing antibodies, and non-specific interactions with erythrocytes, neutrophils, and monocytes. In contrast, cells that have intrinsic or engineered targeting activity can be loaded with Ad vectors and serve as site-specific delivery vehicles that protect virions from inactivation, while amplifying the payload in transit.

Figure 1

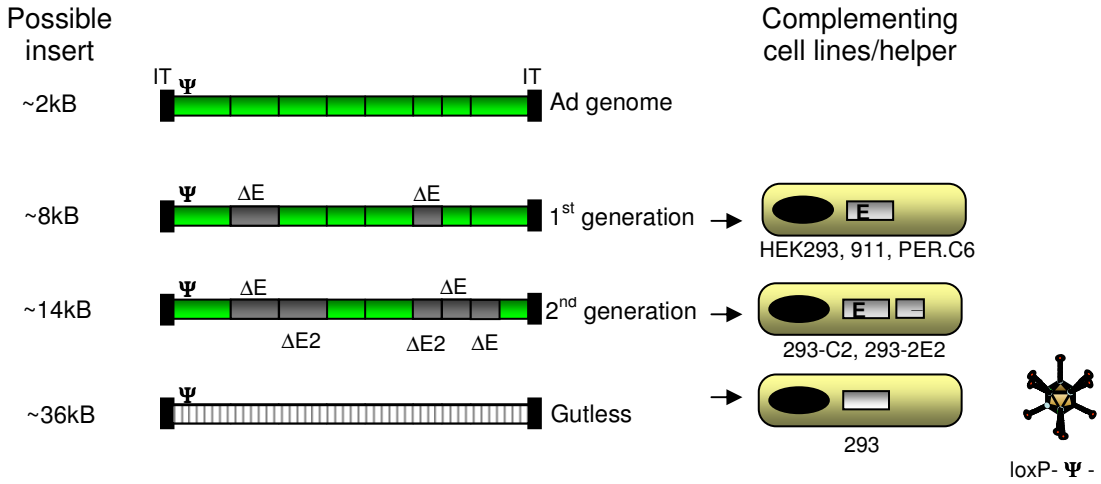
Possible insert
Complementing cell lines/helper
IT
Ψ
IT
~2kB
Ad genome
~8kB
ΔE
ΔE
1st generation
E
HEK293, 911, PER.C6
~14kB
ΔE
ΔE
2nd generation
E
ΔE2
ΔE2
ΔE
293-C2, 293-2E2
~36kB
Gutless
293
loxP- Ψ -

Figure 2

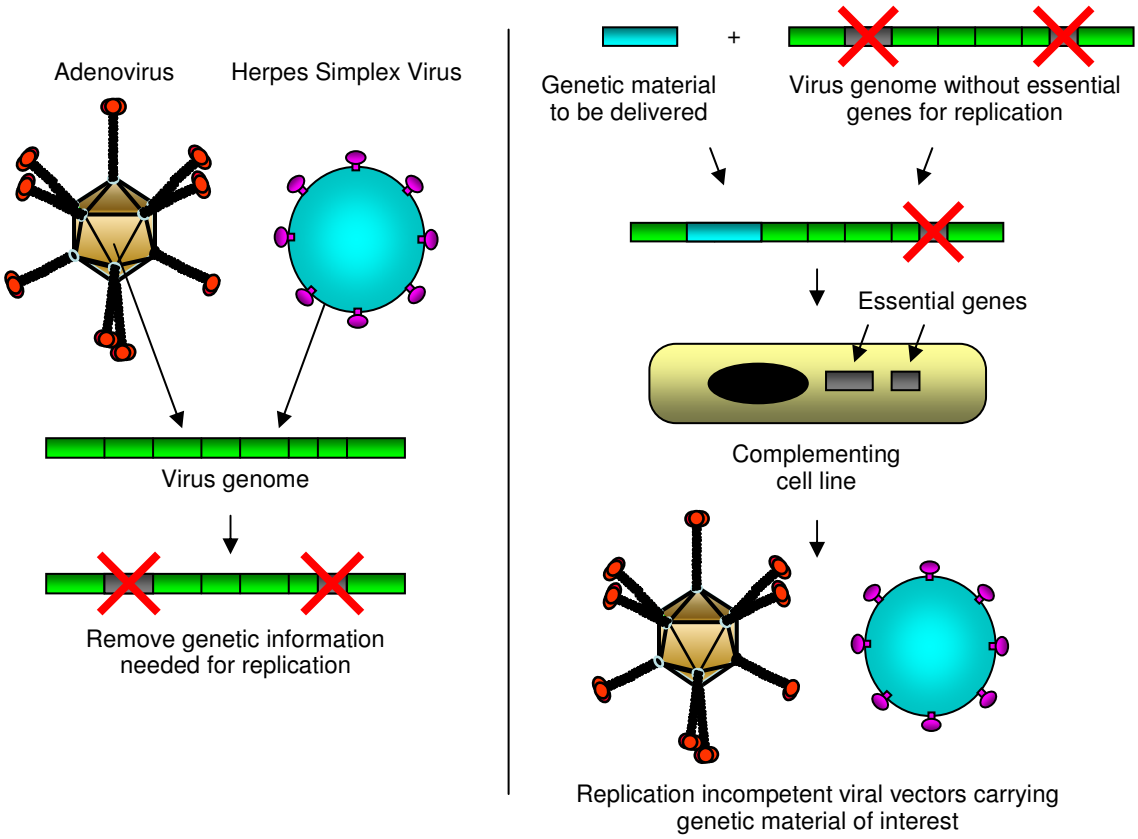
Adenovirus
Herpes Simplex Virus
Virus genome
Remove genetic information needed for replication
+
Genetic material to be delivered
Virus genome without essential genes for replication
Essential genes
Complementing cell line
Replication incompetent viral vectors carrying genetic material of interest

Figure 3

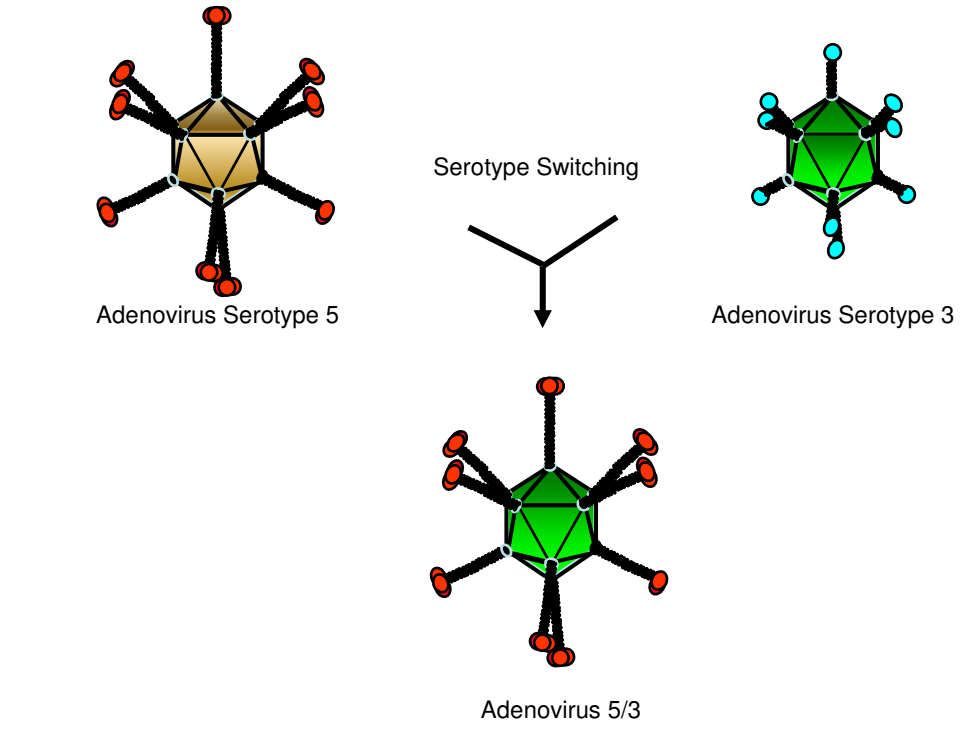
Adenovirus Serotype 5
Serotype Switching
Adenovirus Serotype 3
Adenovirus 5/3
Adenovirus Serotype 5
+
PEG
Stealthing
Adenovirus coated With PEG

Figure 4

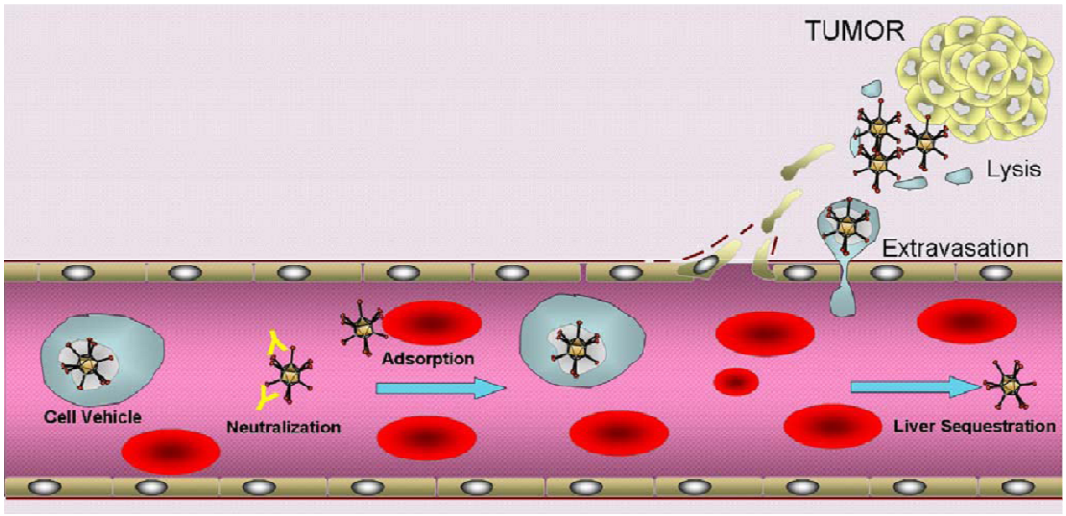
TUMOR
Lysis
Extravasation
Cell Vehicle
Neutralization
Adsorption
Liver Sequestration

PART TWO

COMBINATION OF VIRAL BIOLOGY AND NANOTECHNOLOGY: NEW APPLICATIONS IN NANOMEDICINE

by

VAIBHAV SAINI[1,2], VLADIMIR P. ZHAROV[3], CHRISTOPHER S. BRAZEL[4], DAVID E. NIKLES[4], DUANE T. JOHNSON[4], MAAIKE EVERTS[1,5]

[1]Division of Human Gene Therapy, Departments of Medicine, Obstetrics and Gynecology, Pathology, Surgery, and the Gene Therapy Center, [2]Department of Physiology and Biophysics, [5]Division of Molecular and Cellular Pathology, Pathology, University of Alabama at Birmingham (UAB), Birmingham, Alabama, USA, [3]Philips Classic Laser Laboratories, University of Arkansas for Medical Sciences, Little Rock, Arkansas, USA, [4]Center for Materials for Information Technology (MINT), University of Alabama, Tuscaloosa, Alabama, USA

Nanomedicine: Nanotechnology, Biology, and Medicine 2, 200–206

Abstract

Viruses are well known for their ability to cause disease, but their beneficial utilities as vectors for gene therapy have been noted as well. As an extension of their use in a gene therapy context, their combination with nanotechnology is starting to benefit many areas of science and medicine. These include nanofabrication and medical diagnostics, to name a few, as well as viro-nano therapy, here defined as the combination of viral biology with nanotechnology to create new therapeutic avenues to treat disease. This review provides examples of areas where viruses in combination with nanotechnology are being used to either advance scientific knowledge or accelerate the development of new diagnostics and therapeutics for human pathological conditions.

Introduction

Viruses have been studied extensively for their role as pathogenic agents causing disease. They have a simple structure consisting of an outer protein coat - the capsid - protecting the inner core consisting of the viral genome. This deceivingly simple structure enables viruses to exist as entities on the borderline between living and non-living things. It was not realized until late in the 20th century that the inherent disease-causing characteristics of the virus could be manipulated and utilized for the treatment of disease. This realization lead to the concept of using viruses as agents for gene therapy approaches. After the initial enthusiasm, however, it was realized that viruses needed more significant modifications as initially conceptualized in order to serve as effective and safe gene therapy agents. Nonetheless, the promise of this field inspired many scientific endeavors that have lead to technological breakthroughs such as the ability to

modify viral tropism to target them to specific cells or tissues.

While the field of gene therapy was becoming established and its potentials and pitfalls becoming more defined, the field of nanotechnology was gaining ground as the technology of future. The opportunities offered by the developments of nanotechnology are abundant, many being relevant to the field of medicine. For example, they embody a promise for the selective destruction of the tumor cells in cancer. However, as with all new fields in science, limitations of the technology are becoming more apparent over time. For instance, selective delivery to diseased tissue remains an obstacle to be overcome. In this regard, the lessons learned and technologies obtained from the viral gene therapy field can be applied to the field of nanotechnology. As an example that will be discussed in more detail below, viruses can be utilized as tumor selective delivery vehicles for nanoparticles. In addition to this direct combination of fields, there has been an increasing convergence of viral biology and nanotechnology that benefit diverse areas of science such as nanofabrication and medical diagnostics (Figure 1).

In this review we will first discuss the use of viruses for nanofabrication. This is based on the realization that virus assembly is an example of "bottom-up" construction of a nanoscale structure. In this regard, viruses can be utilized as templates for spatial organization of nanoparticles and the construction of nanowires, among other things. The next section will provide more examples of the ways science has progressed by the interdisciplinary link between the fields of viral biology and nanotechnology. Next, relevant examples will be discussed where nanotechnology has been useful in developing assays for detection and hence diagnosis of viral diseases. This is followed by a description of the potential of a combination of viral biology and nanotechnology for the

development of novel therapies to treat diseases like cancer, defined as viro-nano therapy. We will end with a brief discussion of issues that must be resolved before viro-nano therapy can become a reality for clinical application.

Nanofabrication

Viruses are inherently structured nanoparticles. The assembly of the viral capsid from constituent proteins and packaging of genetic material inside the capsid is a complex process. It is therefore an important demonstration of precise assembly of functional nanoscale biological materials carried out efficiently by nature, which can be capitalized on to create non-biological nanostructures. In the assembly process, biological molecular recognition plays a key role. This molecular recognition can be rationally altered, either chemically or genetically. Being a reproducing biological entity, any modification incorporated in the genome of the virus is represented in the progeny viral particles. These modified viruses provide a multitude of opportunities for nanofabrication and can be exploited for controlling inorganic material nucleation, phase stabilization, assembly and pattern formation at a molecular scale [1-6]. This is mainly attributable to the characteristics of viruses that overlap with those expected from an ideal nanotemplate, including pre-determined composition, surface chemistry amenable to genetic manipulation, monodispersity, accessibility to its interior and extensive chemical tailorability [7].

In a series of elegant experiments by Angela M. Belcher's group, the principle of rational assembly of nanostructures on a genetically manipulated viral template was demonstrated using the M13 bacteriophage. This phage has been used as a template for

synthesizing inorganic nanowires of semiconductors [8] as well as magnetic materials [2, 9, 10]. In these studies, an affinity peptide for inorganic materials was displayed randomly on the genetically manipulated major capsid protein pVIII. To elaborate on one such study, Huang *et al.* genetically modified the M13 bacteriophage to express a gold-binding sequence on pVIII (2700 copies in the filamentous capsid) and a streptavidin binding sequence on pIII (~5 copies at the end of bacteriophage). These modified viruses expressing substrate-specific peptides served as a template for programmable assembly of complex nanostructures. Binding of 5 nm gold nanoparticles to pVIII resulted in one-dimensional (1D) gold nanocrystal arrays. These 1D arrays were shown to further grow into continuous metallic nanowires of ~40 nm diameter after 5 min of electroless deposition time [6]. The expression of two different affinity peptides in the same virus allowed the assembly of more complex nanostuctures as compared to the homo-nanoparticle arrays of gold. In particular, binding of streptavidin coated CdSe quantum dots to pIII and gold nanoparticles to pVIII produced hetero-nanoparticle arrays [6]. More complex structures like linear wire-dot-wire constructs were created when more than one phage bound to the same streptavidin-coated nanoparticle. Application of such nanowires templated on pVIII include routing of electrical carriers to the nanostructures templated on pIII in a precise and controlled way. This provides an approach to solve the interconnecting problem in studies of quantum objects [6].

More recently, in the beginning of 2006, another study by the Belcher group demonstrated metal-ion mediated bundle formation of genetically modified M13 having affinity to a metal ion and defined inorganic placement on these phage particles in the bundle structure. This allowed for a consistent assembly that was lacking in previous

studies [10]. The above examples highlight the use of genetically modified viruses as templates for nanoconstruction. Similarly, unmodified viruses with an inherent chemical functionality of a constituent protein can provide a scaffold for nanofabrication. One such virus is chilo iridescent virus (CIV), which provides a bioscaffold for 2-5 nm gold nanoparticles on the viral capsid. These gold nanoparticles then act as nucleation sites for electroless deposition of gold ions from the solution around the biotemplate. Using this approach, naturally occuring viruses can be used for the fabrication of metallodielectric, plasmonic structures that provide cores with a narrower size distribution and smaller diameters (below 80 nm) than currently used silica. These metallodielectric structures have potential use in surface plasmon sensing, surface-enhanced Raman spectroscopy, enhancement of the nonlinear optical response of organic materials and cancer treatment [7].

Another interesting property of viruses is the ease with which they form crystals. These crystals have been useful in generating long-range three-dimensional (3D) ordered solids of nanostructured materials. Other materials like block copolymers and colloidal crystals can also be used for this purpose, but their use is restricted by the limited number of architectures these materials offer. In contrast, viruses provide a wide variety of porous, highly organized architectures and symmetries. As an example, Cowpea Mosaic Virus (CPMV) has a body centered cubic crystal, which has large nanoscopic cavities and channels occupying about 50% of the crystal's total volume. These cavities and channels were exploited for the production of uniquely regular nanocomposites of palladium and platinum. These represent a monolithic three-dimensionally structured solid with nanometer-scale detail and may find use as sensors and in X-ray optical systems [11].

Based on the examples discussed above, one can understand how the inherent properties of viruses coupled with the ease of genetic manipulation of the viral genome has advanced the use of viruses as templates for nanofabrication.

Symbiotic Relationships between Nanotechnology and Viral Biology

Various branches of science like biochemistry, molecular biology and gene therapy have traditionally been linked to each other, accelerating the progression of each. Similarly, as the science of nanotechnology is currently blossoming, it is rapidly becoming a diversified field having links with many other fields, including viral biology. The various combinations between nanotechnology and viral biology in recent years, as described in more detail below, have been beneficial for the advancement of both fields.

One of the areas in which nanotechnology has helped viral biology is the understanding of the interaction between viruses and cells. Viruses are natural nanosized invaders of our body and have a profound effect on the host. However, our understanding of the initial critical event of recognition and attachment of the virus to the host cells is incomplete. This event is governed by the proteins that constitute the viral capsid, which has many functions including protection of the viral genome, molecular recognition, nucleic acid release upon infection, reassembly and externalization of progeny virions [12]. For each of these functions, major structural changes must occur in the capsid proteins, and it is thus important to gain clarity about these molecular transitions. Methods currently used to study these events include X-ray diffraction and cryoelectron microscopy, combined with image reconstruction. However, these methods have various limitations, including un-physiological sample preparation and the requirement of a synchronous virus

population. Other methods like optical spectroscopy have a limitation of averaging information about a pool of virions. The way out of this quagmire would be to study single viral particles and collect time-resolved structural information under physiological conditions, while avoiding averaging effects of different subpopulations. However, due to the exceedingly small amount of sample, spectroscopic enhancement is required to study single viruses. In this regard, nanoparticles have been of great utility. For example, gold nanoparticles have been encapsulated inside viruses and thus provided a means for spectroscopic enhancement [13]. This has been achieved by covering 2.5-4.5 nm Au particles with citrate, thus adding a negative charge on their surface. Since the brome mosaic virus (BMV) capsid assembles by interaction of positively charged amino-terminals of the capsomeres with negatively charged RNA, the negatively charged Au nanoparticles could be utilized as cores instead of the RNA. These Au encapsulating BMVs were able to be studied using Rayleigh resonance, providing information about transitions of the viral capsid [13]. This approach is thus an example of how nanotechnology can help us unravel issues related to viral biology.

Another example where the latest technology has paved the way to study viral biology is the construction of nanometric biomolecular arrays that can be used to study inter-viral molecular interactions. In this respect, the size of most viruses is on the scale of nanometers; supermolecular assemblies of viruses are hence often in the order of tens of nanometers in size. Moreover, these assemblies can be produced with atomic precision and are ideal monodisperse, nanometric building blocks that can aid in the study of molecularly directed assembly of biomolecular arrays [14]. In particular, Cowpea Mosaic Virus (CPMV) was genetically modified to present a cysteine residue at geometrically

equivalent positions on the viral caposomer. The thiol in this cysteine residue was able to bind to a reactive nanometric chemical template with dimensions close to the diameter of the mutated virus (ca. 30 nm). This template was created by scanning probe lithography and can be used to study the role played by intervirion interactions on assembly morphology and kinetics. Fabrication of these nanometric biomolecular arrays has potential for proteomic analysis using protein arrays, genomic analysis using DNA arrays and studies of protein structure using 2D or 3D crystalline arrays [14].

Another area where viruses have been applied in medicine is the field of gene therapy, where viruses represent natural nanoscale gene delivery vectors. In this regard, an emerging area in the field of nanobiotechnology is the construction of artificial viruses that are able to deliver genes. For example, artificial glycoviruses have been constructed that are capable of gene transfection. These artificial viruses were constructed by assembling glycocluster nanoparticles (GNPs) on plasmid DNA in a number, size and shape controlled manner. This construction of glycoviruses is an example of the 'bottom-up" nature of the assembly of nanostructures [15].

The above mentioned studies are examples in which nanotechnology and viruses have mutually assisted each other in increasing the understanding of these two different fields of scientific literature. However, in addition, the combination of viral biology and nanotechnology can aid in deducing more information about basic cellular mechanisms like endocytosis. Endocytosis has also been called 'cell drinking', with the size of endosomes being $\leq$ 100 nm [16]. This size puts an upper limit in place for the potential particles that can be used to study endocytosis. Glycoviruses (~50 nm) were initially used as guest particles in the endosome [16]. However, it would be beneficial to study

endocytic guest particles in the subviral size region (≤50 nm). In this regard, nanoparticles such as quantum dots (QDs) have been extremely useful. QDs are inorganic semicondustor nanocrystals of 2-6 nm in size, and have been used to study the effect of size variability in the process of endocytosis [16]. QDs are particularly good biolabels because of their unique fluorescence properties (strong, sharp, stable and size-tunable emission). In detail, a QD-conjugated sugar ball with a diameter of 15 nm was used as an endosome marker, in addition to smaller glycocluster nanoparticles of 5 nm in size and the aforementioned glycoviruses of 50 nm in size. This study revealed that endocytosis is highly size dependent, with 50 nm being optimal and anything on either side of 50 nm being less efficient as potential endocytic material [16]. Hence, in designing artificial molecular (drug, gene, probe etc.) delivery systems, size is an issue that should be seriously considered. This is an example where both viral biology and nanotechnology were utilized to conduct studies in a basic science realm, providing insights for many future applications.

Detection and Diagnosis

In the previous section, we described the use of nanoparticles as agents for spectroscopic enhancement of viruses and as biolabels to study cellular functions such as endocytosis. In this section, we will elaborate on the use of nanoparticles to improve detection of viruses with possible applications in the diagnosis of viral diseases. Accurate detection of a disease-causing pathogen is crucial before any treatment regimen can be designed and successful therapy can be achieved. Moreover, unfortunately we are living in a world that is coming to terms with the realities of terrorism and biological warfare.

Since many viruses cause human disease and can possibly be utilized as distinct terror threats, new methods for viral detection are being actively pursued, in which nanotechnology has started to play a significant role.

In general, viruses can be detected either by their antigens (immunoassays) or genomic sequences (PCR based methods). However, sensitivity of detection remains a problematic issue for immunoassays, whereas PCR based methods are plagued by ease of contamination as well as tedious processing. In this regard, nanoparticles, as expected, have paved a way for faster, sensitive and less tedious detection of virulent viruses. For example, Valanne *et al.* have designed a sandwich ELISA method for direct detection of adenoviruses by covalently coating monoclonal anti-hexon antibodies onto highly fluorescent europium(III)-chelate-doped nanoparticles of 107 nm in diameter [17]. In this assay, microtiter wells coated with a first anti-hexon monoclonal antibody are exposed to either purified adenoviruses or nasopharyngeal patient samples, followed by incubation with the antibody-coated nanoparticles of which the fluorescence can readily be detected. Since one nanoparticle can occupy multiple antibodies - theoretically up to 159 – the avidity for the hexon protein is greatly increased. This, combined with the high specific fluorescence of the nanoparticle results in a 10-1000 fold improved detection limit as compared to traditional immunofluorometric assays [17].

In addition to fluorescent europium nanoparticles as described above, nanoparticles based on other metals can be utilized for improved detection of viruses as well. For instance, Wang *et al.* have used gold nanoparticles of 8-15 nm in diameter coupled to oligonucleotide detection probes for visual detection of hepatitis B virus (HBV) and hepatitis C virus (HCV) in serum samples of infected patients [18]. For this,

they utilized a novel method for DNA detection as reported by Taton *et al.*, which is based on sandwich hybridization and gold nanoparticle enhancement techniques using silver [19]. This visual gene chip detection methodology is less expensive than existing fluorophore based methods, as no specialized equipment is required for recording signals, and is also less time consuming [18], exemplifying the ability of nanotechnology to enhance detection of viruses in a variety of ways.

A final example of nanoparticles aiding in virus detection is the utilization of magnetic nanoparticles that can be monitored via MRI. This approach is illustrated by the work of Perez *et al.*, who developed a magnetic viral nanosensor composed of a superparamagnetic iron oxide core coated with dextran, to which antibodies against herpes simplex virus (HSV) or adenovirus can be attached [20]. The presence of viruses induces the nanoassembly of the magnetic nanosensors, which can subsequently be recorded as changes in the spin- spin relaxation times ($\delta T2$) of surrounding water molecules. This method is more sensitive than PCR based methods and is able to detect 5 viral particles in 10 μL of a 25% protein solution. In this particular experimental setup the concentration of iron used for the detection was low ($\leq$ 20μg Fe/mL), thus avoiding aggregation and precipitation of the iron clusters [21]. Similar iron oxide nanoparticles have demonstrated limited or no txoicity in clinical studies [22], rationalizing their use for *in vivo* sensing on viruses using Magnetic Resonance Imaging (MRI) [21]. Furthermore, this method does not require any amplification step and obviates the need for protein removal. Other advantages include the absence of interference of optical properties of the media on the detection process, as well as the amenability for virus detection in biological fluids like blood, cell suspensions, culture media, lipid emulsions

and whole tissue [20]. Since both HSV and Ad are utilized as gene therapy vectors, this detection method has the potential to be used for the analysis of the biodistribution of these vectors, in addition to its utilities in the detection of the wild type viruses as pathogens.

Finally, in addition to nanoparticles, larger and more complex entities such as nanowires have been used for direct, real-time electrical detection of virions [23] These nanowires can be configured as field-effect transistors by attaching them to receptors that can bind biological pathogens. This biological interaction is then recorded as a change in conductance. In particular, Patolsky *et al.* conjugated antibodies against hemagglutinnin of the influenza A virus to silicon nanowires and recorded the conductance changes in the presence and absence of the virus. These recordings were characteristic for influenza A virus but not for paramyxovirus or adenovirus, indicating the selectivity of this approach [23]. These examples illustrate the utility of nanotechnology to improve detection and diagnosis of disease-causing agents like viruses.

Viro-nano Therapy

As introduced in the previous section, viruses are responsible for many pathologic conditions in the human body. In this section we will describe how nanotechnology can improve on therapeutic strategies that have been designed to fight unwarranted infections. First we will describe how nanotechnology can be applied for improving the efficacy of vaccines, which are still the most effective therapeutic tools available to prevent viral diseases. Additionally, we will discuss how nanotechnology can be utilized to remove viruses from various important biological liquids such as blood plasma and water, via a

process called nanofiltration. Finally we will deliberate how, in addition to their harmful potential for causing disease, it has been realized that viruses themselves can be utilized as tools to treat diseases like cancer, especially in combination with various types of nanoparticles. These areas where nanotechnology is used to fight disease in conjunction with viruses fall under the emerging field of viro-nano therapy.

As mentioned above, nanotechnology can be used to improve vaccination strategies against viruses. For example, an effective vaccination strategy against Human Immunodeficiency Virus (HIV) is greatly desired, ever since the Acquired Immune Deficiency Syndrome (AIDS) pandemic began [24]. This is particularly true since available treatment strategies for AIDS are expensive and do not cure the disease. In this regard, a DNA vaccine against HIV might be the optimal preventive strategy since such vaccines are both stable and affordable [25, 26]. However, DNA immunization strategies have major drawbacks, including low immunogenicity and the requirement of immunostimulants. To overcome these drawbacks, Locher *et al.* designed a nanoparticle formulation of HIV DNA sequences. Briefly, a plasmid containing the HIV-2 gp140 *env* gene was electrostatically complexed with a polycationic adjuvant, resulting in a DNA-polymer composite nanoparticles with a diameter of 150 nm. This nanocomposite was tested in BALB/c mice and was demonstrated to induce higher levels of systemic antibody responses compared to naked DNA [26]. Another interesting example is provided by the increased immunogenicity observed for the bovine parainfluenza type 3 (BPI-3) virus proteins when incorporated into poly-lactide-co-glycolide (PLGA) nanoparticles. Briefly, mice were immunized with BPI-3 proteins, either incorporated into PLGA nanoparticles, incorporated into polymethylmethacrylate (PMMA)

nanoparticles, or not incorporated in nanoparticles at all. Mice immunized with the PLGA nanoparticles demonstrated higher levels of virus specific antibody response, as compared to PMMA nanoparticles or to the soluble viral proteins alone [27]. Although still in pre-clinical development, these examples illustrate the utility of nanotechnology in the formulation of effective vaccine strategies against a broad spectrum of viral diseases, for both humans and cattle.

In addition to vaccination strategies, reduction of exposure to viral agents would be an effective approach to limit the chance of disease development. In this regard, there are many plasma derived biological products that are routinely used in hospitals around the world that carry a large risk of contaminants such as viruses. This problem of viral contamination has previously been approached in many ways, including chemical inactivation, pasteurization and terminal dry heat [28-32]. However, it is evident that in addition to inactivating viruses, each of these methods affect the plasma proteins as well, resulting in low yields of these proteins of interest. To overcome this problem, nanofiltration is one of the approaches that can remove both enveloped as well as non-enveloped viruses [33]. A representative study by Omar and Kempf demonstrated succesful elimination of IgG-coated non-enveloped viruses including bovine parvovirus (BPV) and bovine enterovirus (BEV) using this method, employing 20 nm and 50 nm filters respectively to filter the solution. This demonstrates that small viral pathogens such as Hepatitis A Virus (HAV) or parvovirus B19, which are abundantly present in plasma pools, can be removed using this method, thus greatly improving the quality of blood-derived products [32]. Similarly, nanofiltration has been used for the removal of viruses from surface water and groundwater, along with other contaminants such as

pesticides or natural organic materials. Such removal of chemical and biological contaminants by nanofiltration has possible applications for the production of drinking water [34]. All these examples establish the utility of nanofiltration for the removal of viruses from vital biological fluids.

Traditionally, viruses have caused disease and are thus viewed as pathogens that need to be eliminated. However, it has been realized that the properties of viruses can also be manipulated to be of benefit to patients, such as in the context of virotherapy and gene therapy. In virotherapy, the lytic capacitiy of certain viruses is used to treat cancer by limiting the replication of viruses to neoplastic tissues [35]. This has for instance been achieved using DNA viruses such as Conditionally Replicating Adenoviruses (CRAds), or RNA viruses such as Measles Virus [36, 37]. In gene therapy, the capacity of viruses to efficiently deliver genetic material to host cells has been exploited for genetic correction of monozygotic inherited diseases, as well as treatment of complex diseases such as cancer [38-40]. Of note, in both cases significant progress has been made in recent years with respect to targeting gene therapy vectors specifically to tumor cells in order to limit toxicity to non-target organs [41]. These virotherapy and gene therapy approaches might be strengthened in therapeutic potency when combined with novel properties of developed nanoparticles. For example, it has been recently shown that gold nanoparticles (AuNPs) can be used for hyperthermia therapy of tumors upon laser irradiation [42]. It has therefore recently been proposed to attach these AuNPs to viral capsid proteins of targeted gene therapy vectors, leading to targeted delivery of AuNPs to the tumor tissue that expresses the receptor recognized by the virus [43]. This strategy would thus combine tumor killing using AuNP mediated hyperthermia with the

therapeutic gene incorporated in the viral vector, possibly leading to synergistic therapeutic effects (Figure 2).

Nanoparticles can also be used for imaging of tumors. Magnetic nanoparticles can be attached to the capsid of tumor directed viruses and these viruses can be monitored with the application of non-invasive technique of MRI. In addition to imaging, an alternating magnetic field can also be used to heat the magnetic nanoparticles, thus feasibilizing hyperthermia treatment of tumors [44] (Figure 2).This approach therefore has potential to be used simultaneously for diagnosis and treatment of patients

This combination of viral biology with nanotechnology, defined here as viro-nano therapy, will still need to overcome several hurdles before clinical application can be realized, which will briefly be discussed in the next section. However, as outlined by these examples, this combination offers many opportunities for new avenues of treatment of disease.

Future Directions of Viro-nano Therapy

As described above, there are still many issues in viro-nano therapy that need to be resolved before translation to a clinical setting can be achieved. For example, basic questions remain regarding the optimal interaction between nanoparticles and virions, such as the nature of the coupling - covalent or non-covalent - , the optimal number of nanoparticles per virus to achieve therapeutic effects and the degree to which coupling of nanoparticles perturbs the natural tropism of the virus to target cells. Moreover, there are many issues related to the body's immune responses to viral vectors, as has been realized in the field of gene therapy. However, now that the first pre-clinical and clinical gene

therapy successes have become apparent, research efforts directed towards overcoming this hurdle have intensified, and great progress in this regard is to be expected in the near future. Along these lines, the body's immune responses to nanoparticles coupled to viral vectors remain obscure, as do general issues related to toxicity of nanoparticles. Analysis of these factors will be crucial in determining the therapeutic window of developed viro-nano therapy agents. Concrete answers are needed for all such questions, before the true potential of viro-nano therapy can be realized.

References

1. Douglas T, Young M. Host-guest encapsulation of materials by assembled virus protein cages. Nature 1998;393(6681):152-5.
2. Mao C, Solis DJ, Reiss BD, et al. Virus-based toolkit for the directed synthesis of magnetic and semiconducting nanowires. Science 2004;303(5655):213-7.
3. Hartgerink JD, Beniash E, Stupp SI. Self-assembly and mineralization of peptide-amphiphile nanofibers. Science 2001;294(5547):1684-8.
4. Reches M, Gazit E. Casting metal nanowires within discrete self-assembled peptide nanotubes. Science 2003;300(5619):625-7.
5. Weizmann Y, Patolsky F, Lioubashevski O, Willner I. Magneto-mechanical detection of nucleic acids and telomerase activity in cancer cells. J Am Chem Soc 2004;126(4):1073-80.
6. Huang Y, Chiang CY, Lee SK, et al. Programmable assembly of nanoarchitectures using genetically engineered viruses. Nano Lett 2005;5(7):1429-34.

7. Radloff C, Vaia RA, Brunton J, Bouwer GT, Ward VK. Metal nanoshell assembly on a virus bioscaffold. Nano Lett 2005;5(6):1187-91.

8. Mao C, Flynn CE, Hayhurst A, et al. Viral assembly of oriented quantum dot nanowires. Proc Natl Acad Sci U S A 2003;100(12):6946-51.

9. Reiss BD, Mao C, Solis DJ, Ryan KS, Thomson T, Belcher AM. Biological Routes to Metal Alloy Ferromagnetic Nanostructures. Nano Lett 2004;4(6):1127-32.

10. Lee SK, Yun DS, Belcher AM. Cobalt ion mediated self-assembly of genetically engineered bacteriophage for biomimetic co-pt hybrid material. Biomacromolecules 2006;7(1):14-7.

11. Falkner JC, Turner ME, Bosworth JK, et al. Virus crystals as nanocomposite scaffolds. J Am Chem Soc 2005;127(15):5274-5.

12. Chiu W, Burnett, R. M., Garcea, R. . Structural Biology of Viruses: Oxford University Press: New York, 1997.

13. Dragnea B, Chen C, Kwak ES, Stein B, Kao CC. Gold nanoparticles as spectroscopic enhancers for in vitro studies on single viruses. J Am Chem Soc 2003;125(21):6374-5.

14. Cheung CL, Camarero JA, Woods BW, Lin T, Johnson JE, De Yoreo JJ. Fabrication of assembled virus nanostructures on templates of chemoselective linkers formed by scanning probe nanolithography. J Am Chem Soc 2003;125(23):6848-9.

15. Aoyama Y. Macrocyclic glycoclusters: from amphiphiles through nanoparticles to glycoviruses. Chemistry 2004;10(3):588-93.

16. Osaki F, Kanamori T, Sando S, Sera T, Aoyama Y. A quantum dot conjugated sugar ball and its cellular uptake. On the size effects of endocytosis in the subviral region. J Am Chem Soc 2004;126(21):6520-1.

17. Valanne A, Huopalahti S, Soukka T, Vainionpaa R, Lovgren T, Harma H. A sensitive adenovirus immunoassay as a model for using nanoparticle label technology in virus diagnostics. J Clin Virol 2005;33(3):217-23.

18. Wang YF, Pang DW, Zhang ZL, Zheng HZ, Cao JP, Shen JT. Visual gene diagnosis of HBV and HCV based on nanoparticle probe amplification and silver staining enhancement. J Med Virol 2003;70(2):205-11.

19. Taton TA, Mirkin CA, Letsinger RL. Scanometric DNA array detection with nanoparticle probes. Science 2000;289(5485):1757-60.

20. Perez JM, Simeone FJ, Saeki Y, Josephson L, Weissleder R. Viral-induced self-assembly of magnetic nanoparticles allows the detection of viral particles in biological media. J Am Chem Soc 2003;125(34):10192-3.

21. Perez JM, Josephson L, Weissleder R. Use of magnetic nanoparticles as nanosensors to probe for molecular interactions. Chembiochem 2004;5(3):261-4.

22. Harisinghani MG, Barentsz J, Hahn PF, et al. Noninvasive detection of clinically occult lymph-node metastases in prostate cancer. N Engl J Med 2003;348(25):2491-9.

23. Patolsky F, Zheng G, Hayden O, Lakadamyali M, Zhuang X, Lieber CM. Electrical detection of single viruses. Proc Natl Acad Sci U S A 2004;101(39):14017-22.

24. Sahloff EG. Current issues in the development of a vaccine to prevent human

immunodeficiency virus: insights from the society of infectious diseases pharmacists. Pharmacotherapy 2005;25(5):741-7.

25. Ulmer JB, Sadoff JC, Liu MA. DNA vaccines. Curr Opin Immunol 1996;8(4):531-6.

26. Locher CP, Putnam D, Langer R, Witt SA, Ashlock BM, Levy JA. Enhancement of a human immunodeficiency virus env DNA vaccine using a novel polycationic nanoparticle formulation. Immunol Lett 2003;90(2-3):67-70.

27. Shephard MJ, Todd D, Adair BM, Po AL, Mackie DP, Scott EM. Immunogenicity of bovine parainfluenza type 3 virus proteins encapsulated in nanoparticle vaccines, following intranasal administration to mice. Res Vet Sci 2003;74(2):187-90.

28. Scheidler A, Rokos K, Reuter T, Ebermann R, Pauli G. Inactivation of viruses by beta-propiolactone in human cryo poor plasma and IgG concentrates. Biologicals 1998;26(2):135-44.

29. Preuss T, Kamstrup S, Kyvsgaard NC, Nansen P, Miller A, Lei JC. Comparison of two different methods for inactivation of viruses in serum. Clin Diagn Lab Immunol 1997;4(5):504-8.

30. Ng PK, Dobkin MB. Pasteurization of antihemophilic factor and model virus inactivation studies. Thromb Res 1985;39(4):439-47.

31. Savage M, Torres J, Franks L, Masecar B, Hotta J. Determination of adequate moisture content for efficient dry-heat viral inactivation in lyophilized factor VIII by loss on drying and by near infrared spectroscopy. Biologicals 1998;26(2):119-24.

32. Omar A, Kempf C. Removal of neutralized model parvoviruses and enteroviruses in human IgG solutions by nanofiltration. Transfusion 2002;42(8):1005-10.

33. Burnouf T, Radosevich M. Nanofiltration of plasma-derived biopharmaceutical products. Haemophilia 2003;9(1):24-37.

34. Van der Bruggen B, Vandecasteele C. Removal of pollutants from surface water and groundwater by nanofiltration: overview of possible applications in the drinking water industry. Environ Pollut 2003;122(3):435-45.

35. Stoff-Khalili MA, Dall P, Curiel DT. From gene therapy to virotherapy for ovarian cancer. Minerva Ginecol 2004;56(6):503-14.

36. Ono HA, Davydova JG, Adachi Y, et al. Promoter-controlled infectivity-enhanced conditionally replicative adenoviral vectors for the treatment of gastric cancer. J Gastroenterol 2005;40(1):31-42.

37. Bateman A, Bullough F, Murphy S, et al. Fusogenic membrane glycoproteins as a novel class of genes for the local and immune-mediated control of tumor growth. Cancer Res 2000;60(6):1492-7.

38. Flotte TR. Adeno-associated virus-based gene therapy for inherited disorders. Pediatr Res 2005;58(6):1143-7.

39. Blankinship MJ, Gregorevic P, Chamberlain JS. Gene Therapy Strategies for Duchenne Muscular Dystrophy Utilizing Recombinant Adeno-associated Virus Vectors. Mol Ther 2006;13(2):241-9.

40. Gerolami R, Uch R, Brechot C, Mannoni P, Bagnis C. Gene therapy of hepatocarcinoma: a long way from the concept to the therapeutical impact. Cancer Gene Ther 2003;10(9):649-60.

41. Everts M, Curiel DT. Transductional targeting of adenoviral cancer gene therapy. Curr Gene Ther 2004;4(3):337-46.

42. O'Neal DP, Hirsch LR, Halas NJ, Payne JD, West JL. Photo-thermal tumor ablation in mice using near infrared-absorbing nanoparticles. Cancer Lett 2004;209(2):171-6.

43. Zharov VP, Kim JW, Curiel DT, Everts M. Self-assembling nanoclusters in living systems: application for integrated photothermal nanodiagnostics and nanotherapy. Nanomedicine 2005;1(4):326-45.

44. Hilger I, Andra W, Hergt R, Hiergeist R, Kaiser WA. Magnetic thermotherapy of breast tumors: an experimental therapeutic approach. Rofo 2005;177(4):507-15.

Figure Legends

Figure 1. Schema of areas of science where viral biology meets nanotechnology. These areas include nanofabrication such as nanowires, basic science applications such as the study of cellular functions, detection and diagnosis of viral pathogens as well as viro-nano therapy.

Figure 2. Therapeutic applications of metal nanoparticles incorporated into viral vectors. Coupling of gold nanoparticles to targeted viral vectors will provide therapeutic opportunities utilizing hyperthermia, whereas coupling of magnetic nanoparticles will provide imaging opportunities via MRI as well as therapeutic opportunities via hyperthermia. These provide examples of the potential utilities of viro-nano therapy agents for clinical use.

Figure 1

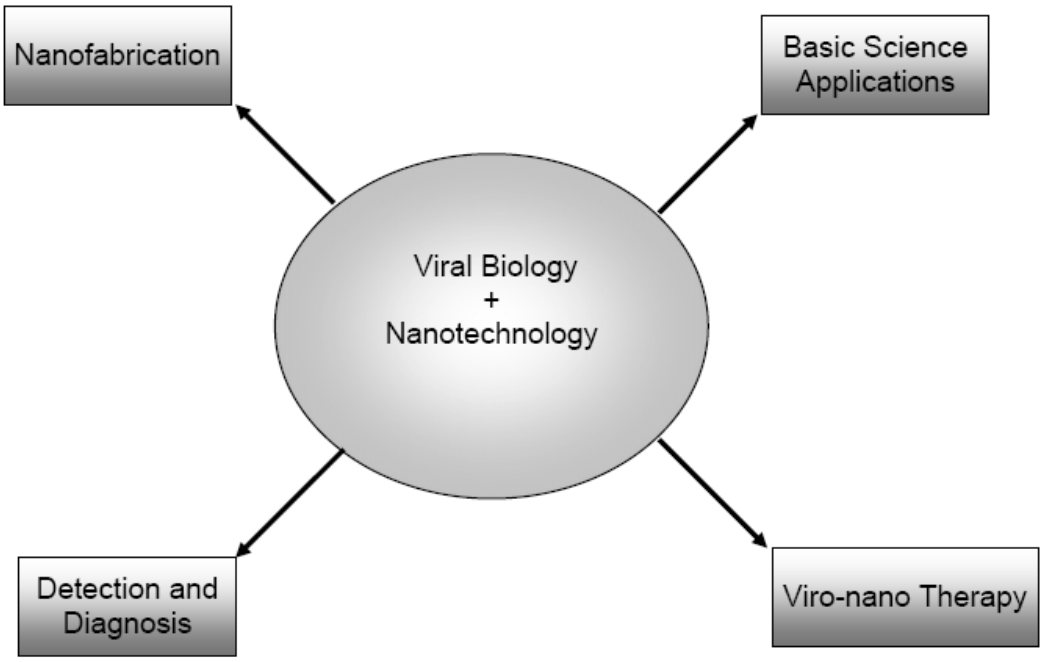
Nanofabrication
Basic Science Applications
Viral Biology
+
Nanotechnology
Detection and Diagnosis
Viro-nano Therapy

Figure 2

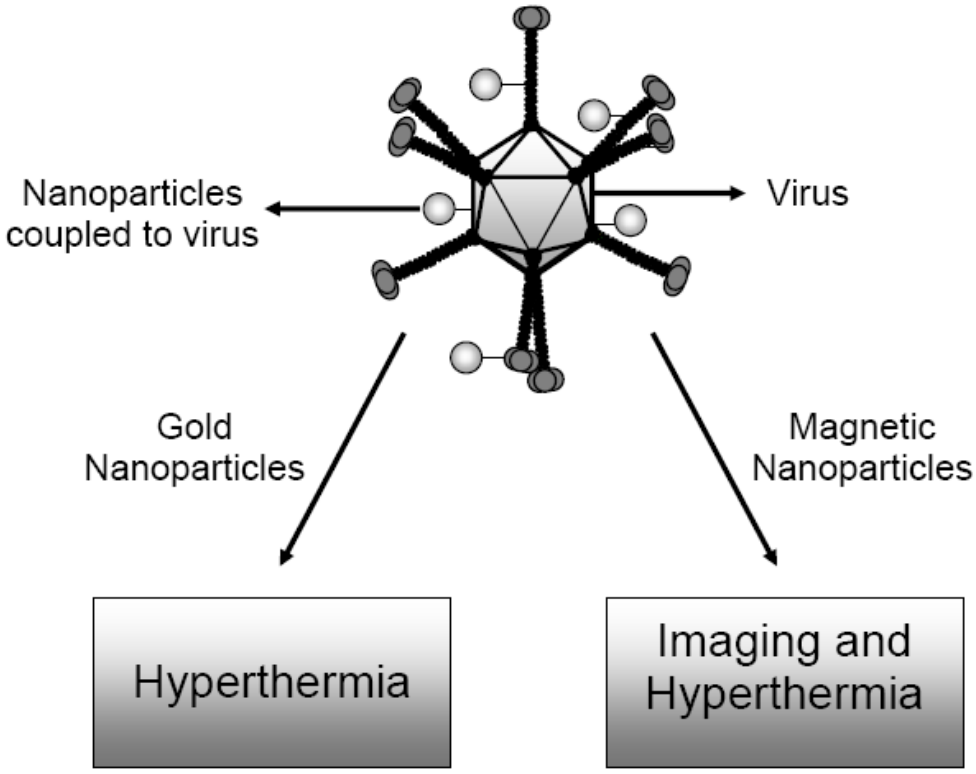
Nanoparticles coupled to virus
Virus
Gold Nanoparticles
Magnetic Nanoparticles
Hyperthermia
Imaging and Hyperthermia

RESEARCH OBJECTIVES

Novel combinatorial treatment strategies are required to achieve tumor eradication. In this regard, viral vector based gene therapy and nanotechnology offer unique possibilities. To combine these two technologies, novel strategies are needed for coupling nanoparticles (NPs) to viral vectors. Towards this goal, we have developed two methods for either non-specific or specific coupling of NPs to adenoviral (Ad) vectors. Upon development of an optimal AuNP-labeled Ad vector, we tested these vectors for their ability for laser-induced hyperthermic tumor cell ablation. Following studies describe these efforts in detail:

Study One: Covalently Linked Au Nanoparticles to a Viral Vector: Potential for Combined Photothermal and Gene Cancer Therapy

In this study, we developed a method for non-specific coupling of AuNPs to Ad vectors. This was the first scientific report that demonstrated NP coupling to a human gene therapeutic viral vector. Following this, we further characterized the impact of non-specific AuNP coupling on Ad vector characteristics, such as native Ad vector infectivity and targeting to tumor cells. We discovered that high AuNP:Ad vector ratios negatively affect Ad vector infectivity as well as tumor targeting ability. Therefore, we endeavored development of an alternate coupling method that could minimize the negative impact on Ad vector characteristics as observed with non-specific coupling.

Study Two: An Adenoviral Platform for Selective Self-Assembly and Targeted Delivery of Nanoparticles

In this study, we developed a method for specific coupling of AuNPs to Ad vectors. Following the coupling, we analyzed the number of AuNPs bound per virion. In addition, we analyzed the impact of specific AuNP coupling on Ad vector characteristics. We observed a significant but moderate decrease in native infectivity of specifically AuNP-labeled Ad vectors. However, this decrease in infectivity was between 1 and 2 orders of magnitude less than that observed with non-specifically AuNP-labeled Ad vectors. Importantly, unlike non-specifically AuNP-labeled Ad vectors, no adverse effects were observed on tumor targeting ability of specifically AuNP-labeled Ad vectors. Thus, we have developed a well characterized specifically AuNP-labeled Ad vector amenable for utilization in downstream studies exploring the applicability of these AuNP-labeled vectors for hyperthermic tumor cell death.

Study Three: Limitations of Adenoviral Vector-Mediated Delivery of Gold Nanoparticles to Tumors for Hyperthermia Induction

Herein, we tested different types of AuNPs for their suitability for hyperthermia induction and observed that 20 nm NPs are optimal for this purpose in our system. In addition, we discovered that AuNPs both on the cell membrane and inside the cytoplasm of cells contribute towards hyperthermia induction. Unfortunately, we did not observe hyperthermic tumor cell killing with 20 nm AuNP-labeled Ad vectors. However, we identified various technical hurdles, which when overcome with future developments, may pave the way for a combined nanotechnology and viral vector based gene therapy for the treatment of tumors.

STUDY ONE

COVALENTLY LINKED Au NANOPARTICLES TO A VIRAL VECTOR: POTENTIAL FOR COMBINED PHOTOTHERMAL AND GENE CANCER THERAPY

by

MAAIKE EVERTS[1], VAIBHAV SAINI[1,2], JENNIFER L. LEDDON[1], ROBBERT J. KOK[3], MARIAM STOFF-KHALILI[1], MEREDITH A. PREUSS[1], C. LEIGH MILLICAN[4], GUY PERKINS[5], JOSHUA M. BROWN[5], HITESH BAGARIA[6], DAVID E. NIKLES[6], DUANE T. JOHNSON[6], VLADIMIR P. ZHAROV[7], DAVID T. CURIEL[1]

[1]Division of Human Gene Therapy, Departments of Medicine, Surgery, Pathology and the Gene Therapy Center, [2]Department of Physiology and Biophysics, [4]High-Resolution Imaging Facility, University of Alabama at Birmingham (UAB), Birmingham, Alabama, USA, [3]Department of Pharmacokinetics and Drug Delivery, University Center for Pharmacy, Groningen University Institute for Drug Exploration (GUIDE), The Netherlands, [5]National Center for Microscopy and Imaging Research, Center for Research on Biological Structure School of Medicine, University of California, San Diego, California, USA, [6]Center for Materials for Information Technology (MINT), University of Alabama, Tuscaloosa, Alabama, USA, [7]Philips Classic Laser Laboratories, University of Arkansas for Medical Sciences, Little Rock, Arkansas, USA

Nano Letters 6 (4), 587 -591

Format adapted for dissertation

Abstract

Hyperthermia can be produced by near-infrared laser irradiation of gold nanoparticles present in tumors and thus induce tumor cell killing via a bystander effect. To be clinically relevant, however, several problems still need to be resolved. In particular, selective delivery and physical targeting of gold nanoparticles to tumor cells are necessary to improve therapeutic selectivity. Considerable progress has been made with respect to retargeting adenoviral vectors for cancer gene therapy. We therefore hypothesized that covalent coupling of gold nanoparticles to retargeted adenoviral vectors would allow selective delivery of the nanoparticles to tumor cells, thus feasibilizing hyperthermia and gene therapy as a combinatorial therapeutic approach. For this, sulfo-N-hydroxysuccinimide labeled gold nanoparticles were reacted to adenoviral vectors encoding a luciferase reporter gene driven by the cytomegalovirus promoter (AdCMVLuc). We herein demonstrate that covalent coupling could be achieved, while retaining virus infectivity and ability to retarget tumor-associated antigens. These results indicate the possibility of using adenoviral vectors as carriers for gold nanoparticles.

Introduction

Cancer targeted therapies rely on exploiting susceptibility parameters of tumor versus normal cells. The increased susceptibility of tumors to heat makes hyperthermia a feasible treatment option.[1] A variety of heat sources have been explored, including laser light, focused ultrasound, as well as microwaves. More recently, the use of near-infrared-absorbing gold nanoparticles has successfully been applied to reduce tumor burden and increase survival in animal experiments.[2] Selectivity of heat induction is based on

enhanced permeability of the tumor vasculature and subsequent retention of the intravenously administered nanoparticles, which can be heated using deep penetrating near-infrared (NIR) laser light.[3] However, enhanced permeability and retention pathophysiology do not occur in all tumors, mandating alternative methods of targeted nanoparticle tumor delivery before successful clinical application can be achieved.

We hypothesized that the recent improvements in targeted adenoviral vectorology might provide the platform for tumor selective delivery of these nanoparticles. We therefore sought to establish the feasibility of covalently coupling gold nanoparticles to adenoviral vectors, as a means to achieve the desired targeted localization. We anticipated that this linkage could be achieved without compromising key adenoviral infectivity properties that constitute the functional basis of its tumor-targeting capabilities. This combination of a targeted viral vector with an amplifying nanoparticle payload thus seeks to exploit favorable aspects of each component to realize an optimized anticancer effect. This type of combinatorial system represents a novel paradigm for the design of tumor-targeted nanoparticles.

Results

Association of gold particles with adenoviral vectors

The sulfo-NHS-ester on the gold nanoparticles employed has reactivity toward primary amines that are abundantly present on the adenoviral capsid lysine residues (Figure 1). For the initial characterization of the feasibility of coupling gold nanoparticles to adenoviral vectors, a ratio of 1000:1 gold:adenovirus (particle:particle) was employed in the synthesis procedure. After the reaction, the mixture was purified using CsCl

gradient centrifugation-a standard method for adenoviral vector purification. Fractions collected from the bottom of the centrifugation tube were analyzed for the presence of virus using an anti-hexon antibody (Figure 2A) and for the presence of gold using silver staining (Figure 2B). Although staining for the presence of virus appears to be more sensitive than detection of gold, a comparison of the staining patterns of both slot blots demonstrated co-localization of virus with gold, indicating co-migration of both components through the CsCl gradient. These results suggested a covalent association between the gold nanoparticles and the adenoviral vectors.

During centrifugation of gold-labeled viral particles in a CsCl gradient, a shift in the height of the viral band in the centrifuge tube was observed, which was dependent on the amount of gold nanoparticles employed in the synthesis procedure, indicating an increased density of the viral particles upon gold labeling (Table 1, Figure 3). To exclude aspecific, noncovalent interaction of gold nanoparticles with the viral vectors, a synthesis procedure employing gold nanoparticles labeled with a nickel-nitrilotriacetic acid (Ni-NTA) instead of a sulfo-NHS reactive group was performed. In this reaction, the shift in vector band localization could not be observed (Table 1, Figure 3), confirming the covalent nature of interaction of the sulfo-NHS particles with the virions. It should be noted, however, that the surface charge of sulfo-NHS labeled particles is neutral, whereas the surface charge of Ni-NTA labeled particles is negative. Since adenoviruses have a net negative charge on their capsid surface as well,[4] nonspecific electrostatic absorption of Ni-NTA labeled particles to the virions could be less than electrostatic absorption of sulfo-NHS particles. Nonetheless, the absence of Ni-NTA labeled particles in CsCl purified virions indicates that association of nanoparticles with virions in the gradient is

not based on the weight of the particles.

Electron microscopy of gold-labeled adenoviral vectors

Electron microscopy was used to visualize gold nanoparticles reacted to the surface of adenoviral vectors that were purified by CsCl centrifugation as above. Vectors were deposited onto carbon-coated copper grids; no staining was used in order to avoid occlusion of the 1.4 nm nanoparticles on the surface of the virions. Gold nanoparticles could not be observed in virus preparations that were either unlabeled (Figure 4A) or labeled with Ni-NTA gold nanoparticles (Figure 4C). One does see some "texture", but this arises from the little bit of underfocus used to better see the virions and is not to be confused with gold particles. In contrast, gold nanoparticles could clearly be observed in the virus preparation labeled with sulfo-NHS gold nanoparticles (Figure 4B, small black dots on the edges of the virions, see magnified insert). The gold particles in Figure 4B have rather sharp boundaries and similar sizes, as opposed to the texture in Figure 4C. This further strengthened the observation of a covalent interaction between the two components.

Gold-labeled adenoviral vectors retain infectivity in HeLa aells

Modification of capsid proteins such as the here-described chemical modification with gold nanoparticles may result in a loss of infectivity of the adenoviral vectors. We therefore evaluated gene transfer of a luciferase encoding adenoviral vector AdCMVLuc, labeled with different amounts of gold in HeLa cells. These cells are previously reported to be readily infected with adenoviral vectors.[5] AdCMVLuc infectivity at a multiplicity

of infection (MOI) of 25 was not affected by the synthesis procedure itself. This was demonstrated by the comparable levels of luciferase activity of sham-labeled versus fresh, unmodified AdCMVLuc (Figure 5). Further, a gold:adenovirus ratio of 100:1 (particle:particle) also did not affect infectivity. However, higher gold:adenovirus ratios did significantly decrease infectivity compared to unlabeled AdCMVLuc (Figure 5). Results were similar for both lower (5) and higher (125) MOIs (data not shown). This suggested a threshold of the number of gold nanoparticles that can be coupled to adenoviral vector without disrupting the natural infectivity mechanism of adenoviral gene transfer.

Gold-labeled adenoviral vectors can be retargeted to CEA expressing tumor cells

A majority of human tumors are deficient in the primary receptor for adenoviral vectors, the Coxsackie adenovirus receptor (CAR), resulting in poor tumor cell transduction. To overcome this hurdle, approaches have been established whereby the adenoviral vector is physically retargeted to alternate receptors on the tumor cell surface. One example is retargeting of adenoviral vectors to the tumor-associated antigen carcino embryonic antigen (CEA), which is overexpressed on several neoplasias such as colon carcinoma. To establish whether gold-labeled adenoviral vectors could still be retargeted to CEA, AdCMVLuc was preincubated with the fusion protein sCAR-MFE, which on one side binds to the adenoviral capsid and on the other side binds to CEA. Gene transfer in MC38-CEA-2 cells, a CEA overexpressing cell line, was markedly increased upon preincubation of fresh, unmodified AdCMVLuc with the sCAR-MFE fusion protein (Figure 6, fresh AdCMVLuc, white versus black bar). Similar to results obtained in HeLa

cells, a gold:adenovirus ratio of 100:1 (particle:particle) did not affect retargeting to and infectivity in CEA expressing cells. A gold:adenovirus ratio of 1000:1 significantly but moderately affected retargeting and infectivity, whereas ratios of 3000:1 and higher resulted in infectivity levels lower than untargeted, unmodified AdCMVLuc (Figure 6). This indicated that up to a ratio of 1000 gold nanoparticles per adenoviral vector in the reaction mixture, retargeting to tumor-associated antigens could still be achieved.

Discussion

It has been recognized that exploitation of multiple treatment modalities will be needed to achieve success in cancer therapy. This has been pioneered using combinations of radiation, surgery, and chemotherapy, which are now standard therapeutic approaches. The addition of gene therapy to the arsenal of available treatment options will lead to a further increase in therapeutic combinatorial opportunities. This has already been demonstrated by synergistic effects between conditionally replicative adenoviruses (CRAds) together with radiation[6] or chemotherapy.[7] To extend this paradigm to a combination of gene therapy and hyperthermia, we herein investigated the possibility to covalently couple gold nanoparticles to adenoviral vectors, without affecting virus infectivity or retargetability. The herein established gold-labeled vectors can thus next be analyzed for hyperthermia-mediated tumor cell death induction.

It has been known that rapidly proliferating cells, such as tumor cells, are more sensitive to heat shock than slowly proliferating cells through a variety of mechanisms, including mitotic delay, cell cycle arrest, and plasma membrane damage.[8,9] The selectivity of hyperthermia for tumors is further conveyed by a tumor's usually limited

blood supply, thus creating an environment with hypoxia and low pH, which is not found in healthy tissue.[1] One of the mechanisms by which hyperthermia has been induced is near-infrared absorption and subsequent heating of gold nanoparticles[10-12] or nanoshells.[3] So far, tumor selectivity of these particles has been achieved based on enhanced permeability and retention of particles due to "leaky" tumor architecture.[3] Although the tumor selectivity obtained by these mechanisms is promising, the specificity that would be obtained by covalent conjugation of the gold nanoparticles to tumor-targeted adenoviral vectors, as demonstrated in this paper, would be beneficial for an increased tumor to healthy tissue ratio and thus a better therapeutic index. This is particularly valid for smaller solid gold nanoparticles that are expected to interfere to a lesser extent with virus infectivity and retargeting compared to gold nanoshells, which have a size between 100 and 140 nm.

In the current work we have employed relatively small gold nanoparticles, for which effective heating will require extremely short (femto- or at least picosecond) laser pulses.[13] Alternatively, "nanoclusters" can be formed, where gold nanoparticles are clustered together, resulting in increased absorption efficiency.[13] Indeed, the proximity of the three-dimensional location of gold nanoparticles within one virus ("bio-nanoclusters") may provide the condition for plasmon-plasmon resonances that accompany increased absorption and a shift to the near-IR range. Nevertheless, we plan to explore the possibility of larger solid gold nanoparticles to be incorporated in the adenoviral platform.

Considerable advancements in tumor-specific targeting of adenoviral vectors for gene therapy have been achieved using both bispecific adapter molecules[14] as well as

genetic capsid modification.[15] Furthermore, adenoviral vectors are compatible with chemical modification, as shown with fluorophores[16] or poly(ethylene glycol) derivatives.[17] This led us to explore the possibility of covalently coupling gold nanoparticles to targeted adenoviral vectors and thus retarget the nanoparticles to tumor-associated antigen expressing tumor cells, as demonstrated in this paper. The achieved targeting to tumor cells now creates the opportunity to test the therapeutic effects of near-infrared (NIR) laser-induced hyperthermia-mediated tumor cell death. These data further provide a rational basis to investigate the synergistic therapeutic gains accrued by a combination of hyperthermia with gene therapy. For example, hyperthermia-sensitive promoters such as hsp70 can drive the expression of cytokines such as interleukin-12 or tumor necrosis factor-alpha.[18] Furthermore, hyperthermia induced viral replication of CRAds might be a feasible strategy, thus combining multiple ways of cell death induction using a single vector.

Another important issue that still needs to be addressed is the optimal spatial location of the particles for most effective cancer cell killing. One option might be a location near the cell membrane (during initial vector binding and internalization) or even inside the membrane itself, since only a low laser energy is required for plasma membrane damage through thermal denaturation or bubble formation phenomena. This will lead to immediate cell death, mainly through necrosis.[19] Another option might be the nucleus (after complete penetration of the vector into the cells), where laser-induced nuclear damage may lead to cell damage through other mechanisms such as apoptosis, cell cycle arrest, etc.[8,9]

Along with adenoviral vectors, other methods of tumor-selective targeting have

been exploited in the literature, such as direct conjugation of therapeutic modalities to antibodies[19] or inclusion of such modalities in liposomal formulations.[20] However, some potential limitations of directly conjugating gold nanoparticles to tumor-targeted antibodies include the limited number of modalities that can be attached without disrupting antibody specificity, whereas liposomes can be modified with particles to a higher extent, forming metallosomes.[21] These metallosomes may have a favorable body distribution and hence tumor specificity, as well as decreased immunogenicity compared to viral vectors. However, efficacy of adenoviral gene transfer is still unparalleled in in vivo systems, favoring the use of adenoviral vectors for possible combinatorial approaches of hyperthermia with gene therapy, as described above.

In addition to gold, we are currently exploring the feasibility of coupling other metal nanoparticles to adenoviral vectors, such as iron-platinum (FePt) nanoparticles. These nanoparticles have magnetic properties that make them ideal for either imaging of particle localization (e.g., using MRI techniques), or magnetic-induced hyperthermia for cell killing, analogous to the gold NIR approach.[22,23]

Finally, to further improve on the herein established gold conjugated adenoviral vector paradigm, other methods of coupling nanoparticles to the adenoviral surface need to be investigated. The relatively nonspecific coupling via the sulfo-N-hydroxysuccinimide reactive group on the gold particle to primary amines of lysine-residues present in the capsid interferes with virus infectivity and retargetability at higher gold-virus ratios. Genetic manipulation of the nanoparticle binding locales will allow us to specifically conjugate particles to capsid proteins not involved in virus infectivity or interaction with targeting methods. Such modifications will allow for an increase in

payload capacity of the virus, i.e., the number of nanoparticles that can be coupled without negatively affecting the virus, and thus create a wider therapeutic window. For example, nickel-nitrilotriacetic acid (Ni-NTA) modified gold particles,[24] used in the here-described experiments as a negative control, would be capable of binding six histidine residues that have carefully been inserted in certain capsid proteins, such as hexon[25] or pIX.[26] Ultimately, combination of multiple modalities within one viral particle, i.e., a targeting site in genetically modified virus capsid proteins allowing physical localization of the vector with the tumor cell, a nanoparticle binding site allowing induction of hyperthermia and imaging opportunities, combined with tumor-specific induction of therapeutic gene expression and viral replication may prove to be an optimal platform for cancer therapy.

Acknowledgments

The authors thank Dr. Kerry Chester for the kind gift of the scFv anti-CEA (MFE-23) encoding plasmid. This work was supported by the following grants: RO1 CA083821, RO1 CA94084, R01 EB000873, RR04050, W81XWH-04-1-0025, and W81XWH-05-1-0035. D. T. Johnson and D. E. Nikles would like to further acknowledge support from the Center for Information Technology and the Alabama NASA-EPSCoR (Grant SUB2002-036).

References

1. van der Zee, J. *Ann. Oncol.* **2002**, *13* (8), 1173-1184.

2. O'Neal, D. P.; Hirsch, L. R.; Halas, N. J.; Payne, J. D.; West, J. L. *Cancer Lett.* **2004**,

209 (2), 171-176.

3. Hirsch, L. R.; Stafford, R. J.; Bankson, J. A.; Sershen, S. R.; Rivera, B.; Price, R. E.; Hazle, J. D.; Halas, N. J.; West, J. L. *Proc. Natl. Acad. Sci. U.S.A.* **2003**, *100* (23), 13549-13554.

4. Konz, J. O.; Lee, A. L.; Lewis, J. A.; Sagar, S. L. *Biotechnol. Prog.* **2005**, *21* (2), 466-472.

5. Wu, H.; Seki, T.; Dmitriev, I.; Uil, T.; Kashentseva, E.; Han, T.; Curiel, D. T. *Hum. Gene Ther.* **2002**, *13* (13), 1647-1653.

6. Rogulski, K. R.; Freytag, S. O.; Zhang, K.; Gilbert, J. D.; Paielli, D. L.; Kim, J. H.; Heise, C. C.; Kirn, D. H. *Cancer Res.* **2000**, *60* (5), 1193-1196.

7. Khuri, F. R.; Nemunaitis, J.; Ganly, I.; Arseneau, J.; Tannock, I. F.; Romel, L.; Gore, M.; Ironside, J.; MacDougall, R. H.; Heise, C.; Randlev, B.; Gillenwater, A. M.; Bruso, P.; Kaye, S. B.; Hong, W. K.; Kirn, D. H. *Nat. Med.* **2000**, *6* (8), 879-885.

8. Maldonado-Codina, G.; Llamazares, S.; Glover, D. M. *J. Cell Sci.* **1993**, *105* (Pt 3), 711-720.

9. Edwards, M. J.; Mulley, R.; Ring, S.; Wanner, R. A. *J. Embryol. Exp. Morphol.* **1974**, *32* (3), 593-602.

10. Zharov, V. P.; Galitovsky, V. *Appl. Phys. Lett.* **2003**, *83*, 4897-4899.

11. Zharov, V. P.; Letfullin, R. R.; Galitovskaya, E. *J. Phys. D*: *Appl. Phys.* **2005**, *38* (15), 2571-2581.

12. El-Sayed, I. H.; Huang, X.; El-Sayed, M. A. *Cancer Lett.* **2005**.

13. Zharov, V. P.; Kim, J. W.; Curiel, D. T.; Everts, M. *Nanomedicine* **2005**, *1* (4), 326-345.

14. Kashentseva, E. A.; Seki, T.; Curiel, D. T.; Dmitriev, I. P. *Cancer Res.* **2002**, *62* (2), 609-616.

15. Bauerschmitz, G. J.; Lam, J. T.; Kanerva, A.; Suzuki, K.; Nettelbeck, D. M.; Dmitriev, I.; Krasnykh, V.; Mikheeva, G. V.; Barnes, M. N.; Alvarez, R. D.; Dall, P.; Alemany, R.; Curiel, D. T.; Hemminki, A. *Cancer Res* **2002**, *62* (5), 1266-11270.

16. Leopold, P. L.; Ferris, B.; Grinberg, I.; Worgall, S.; Hackett, N. R.; Crystal, R. G. *Hum. Gene Ther.* **1998**, *9*, (3), 367-378.

17. Ogawara, K.; Rots, M. G.; Kok, R. J.; Moorlag, H. E.; Van Loenen, A. M.; Meijer, D. K.; Haisma, H. J.; Molema, G. *Hum. Gene Ther.* **2004**, *15* (5), 433-443.

18. Huang, Q.; Hu, J. K.; Lohr, F.; Zhang, L.; Braun, R.; Lanzen, J.; Little, J. B.; Dewhirst, M. W.; Li, C. Y. *Cancer Res.* **2000**, *60* (13), 3435-3439.

19. Zharov, V. P.; Galitovskaya, E. N.; Johnson, C.; Kelly, T. *Lasers Surg. Med.* **2005**, *37* (3), 219-226.

20. Molema, G., Drug targeting: Basic concepts and novel advances. In *Drug Targeting. Organ-Specific Strategies*; Molema, G., Meijer, D. K. F., Eds.; Wiley-VCH Verlag GmbH: Weinheim, 2001; pp 1-22.

21. Hainfeld, J. F.; Powell, R. D. *J. Histochem. Cytochem.* **2000**, *48* (4), 471-480.

22. Moroz, P.; Jones, S. K.; Gray, B. N. *Int. J. Hyperthermia* **2002**, *18*, (4), 267-84.

23. Bagaria, H. G.; Johnson, D. T. *Int. J. Hyperthermia* **2005**, *21* (1), 57-75.

24. Hainfeld, J. F.; Liu, W.; Halsey, C. M.; Freimuth, P.; Powell, R. D. *J. Struct. Biol.* **1999**, *127* (2), 185-198.

25. Wong, J. Y.; Chu, D. Z.; Williams, L. E.; Yamauchi, D. M.; Ikle, D. N.; Kwok, C. S.; Liu, A.; Wilczynski, S.; Colcher, D.; Yazaki, P. J.; Shively, J. E.; Wu, A. M.; Raubitschek, A. A. *Clin. Cancer Res.* **2004**, *10* (15), 5014-5021.

26. Dmitriev, I. P.; Kashentseva, E. A.; Curiel, D. T. *J. Virol.* **2002**, *76* (14), 6893-6899.

Figure Legends

Figure 1. Gold nanoparticles can covalently be attached to primary amines present in capsid proteins. The sulfo-NHS ester attached on the 1.3-nm gold particle will react with primary amines of lysine residues present in the adenoviral capsid, resulting in an amide bond between the gold particle and the adenovirus. There are over 10 000 lysines in the proteins that make up the capsid, although not all of these will be accessible for chemical reaction.

Figure 2. Slotblot analysis demonstrating the presence of adenovirus and gold in fractions collected after virus CsCl purification. Gold nanoparticles were first reacted with adenoviral vectors in a 1000:1 ratio. The reaction mixture was then purified using centrifugation over a CsCl gradient, a standard method of viral vector purification. After the bottom of the centrifugation tube was punctured, 28 fractions were collected and

analyzed for the presence of adenovirus using staining for the hexon capsid protein (A) and the presence of gold nanoparticles using silver enhancement staining (B). The original reaction mixture prior to purification was used as a positive control (+control).

Figure 3. Photograph of gold-labeled adenoviral vectors in a CsCl gradient. 1×10^{12} viral particles were reacted with either no gold nanoparticles (left), 10 000 Ni-NTA gold particles per viral particle (middle) or 10 000 sulfo-NHS gold particles per viral particle. The gold nanoparticles not reacted to the virus in the middle and right tube remain in the upper portion of the gradient (brown color above arrow A). The white band in the area indicated by arrow A consists of remaining unlabeled virions, the light brown band indicated by arrow B indicates gold-labeled virions and can only be observed in the right centrifuge tube.

Figure 4. Electron microscopy identifies gold nanoparticles associated with adenoviral vectors. Vectors were either unlabeled (A), sulfo-NHS gold nanoparticles labeled (B), or Ni-NTA gold nanoparticles labeled (C). Adenoviral vectors were examined using electron microscopy using a JEOL JEM 1200FX operated at 80 kV. Original magnification 100000×, scale bar 100 nm.

Figure 5. Infectivity of gold-labeled adenoviral vectors is retained at lower particle-to-vector ratios. Gold nanoparticles were reacted with AdCMVLuc at ratios of 100:1, 1000:1, 3000:1, and 5000:1. After reaction, HeLa cells were infected with 100 vp/cell and luciferase expression was determined after 24 h. Bars represent mean ± standard

deviation. Asterisks indicate $p < 0.05$.

Figure 6. Retargeting of gold-labeled adenoviral vectors to CEA is retained at lower particle-to-vector ratios. Gold nanoparticles were reacted with AdCMVLuc at ratios of 100:1, 1000:1, 3000:1, and 5000:1. After reaction, MC38-CEA-2 cells were infected with 100 vp/cell of AdCMVLuc without (white bars) or with (black bars) sCAR-MFE fusion protein preincubation, to retarget the viral vector to the expressed CEA. Luciferase expression was determined after 24 h. Bars represent mean ± standard deviation. Asterisks indicate $p < 0.05$.

Table Legends

Table 1. Positions of viral bands in centrifugation tubes after CsCl gradient centrifugation.

Figure 1

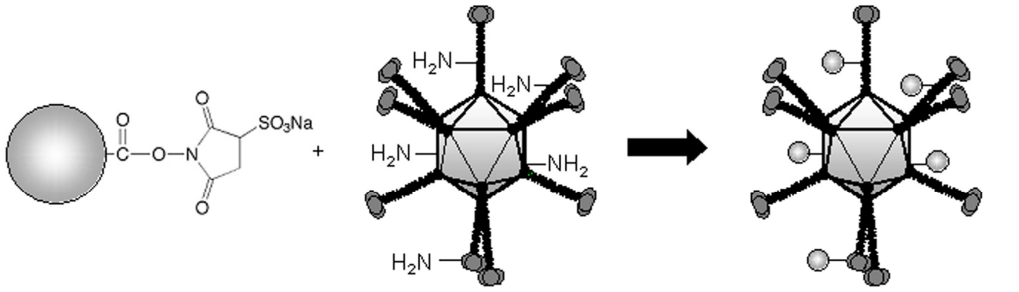

Gold nanoparticle with sulfo-NHS ester

Adenoviral vector with primary amines in capsid

Adenoviral vector with gold nanoparticles coupled to capsid

Figure 2

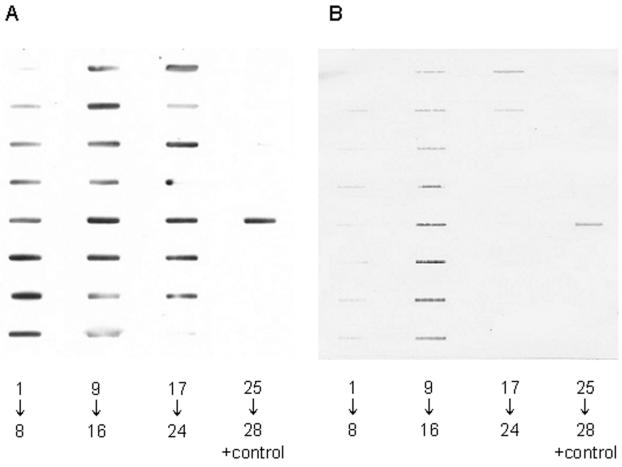

Figure 3

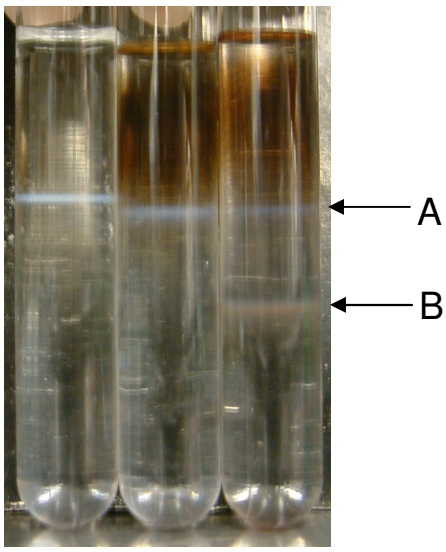

Figure 4

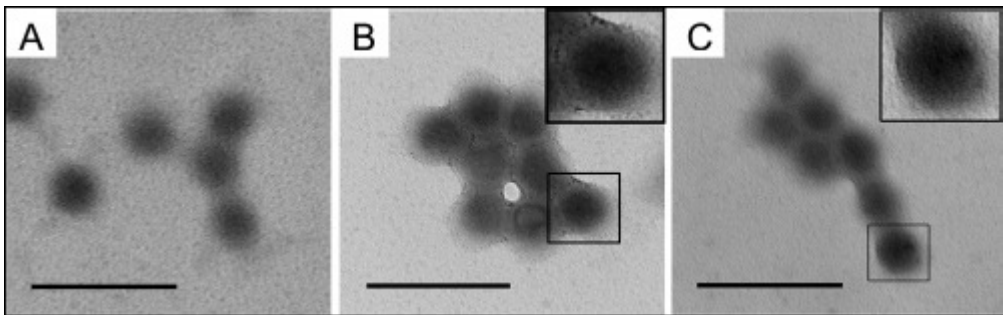

Figure 5

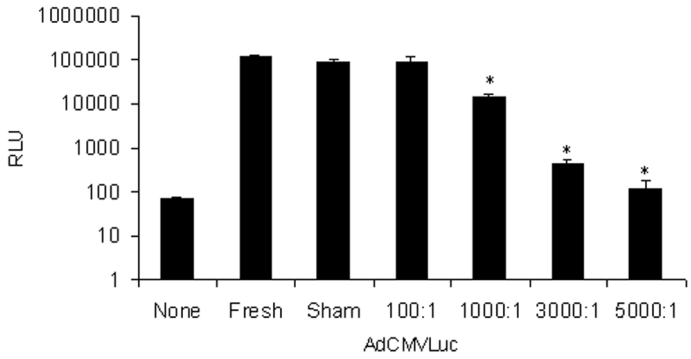
1000000
100000
10000
1000
100
10
1
RLU
*
*
*
None
Fresh
Sham
100:1
1000:1
3000:1
5000:1
AdCMVLuc

Figure 6

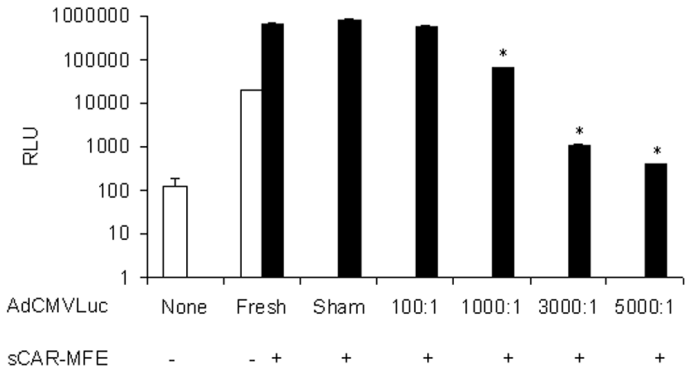
1000000
100000
10000
1000
100
10
1
RLU
*
*
*
AdCMVLuc
None
Fresh
Sham
100:1
1000:1
3000:1
5000:1
sCAR-MFE
- - + + + + + +

Table 1

virus-gold combination	distance from bottom to lower band	distance from bottom to upper band (cm)	total distance gradient (cm)
virus alone, no gold nanoparticles	no lower band	4.3	6.6
virus + 10000 Ni-NTA gold nanoparticles	no lower band	4.2	6.6
virus + 10000 Sulfo-NHS gold nanoparticles	2.8 cm	4.2	6.6

Supporting Information

Detailed description of materials and methods

Adenoviral vector production

The adenoviral vector encoding firefly luciferase (Luc) under transcriptional control of the constitutively active cytomegalovirus (CMV) promoter, AdCMVLuc, was constructed as previously described.[1] Briefly, AdCMVLuc was constructed by amplifying the luciferase reporter gene out of pGL3 basic (Promega, Madison, WI), and ligated downstream of the CMV promoter into the Ad shuttle plasmid pShuttleCMV.[2] Recombinant Ad was generated by homologous recombination with the adenoviral genome plasmid pAdEasy1 (Qbiogene, Carlsbad, CA) in E. coli strain BJ5183, and virus was rescued in HEK-293 cells. For subsequent virus production, cells were infected using growth medium as described below, except containing 2% fetal bovine serum instead of 10%. Following overnight incubation, regular medium was added to the cells and cells were incubated until cytopathic effect was observed. Cells were harvested, frozen and thawed five times. Virus was purified using standard double CsCl gradient centrifugation. Viral particle number was determined by measuring absorbance at 260nm using a conversion factor of 1.1 x 1012 viral particles per absorbance unit.

Cell culture

HEK-293 cells were obtained from Microbix (Toronto, Canada), HeLa cells were obtained from the American Type Culture Collection (ATCC, Manassas, VA, USA) and MC38 cells stably transfected with carcinoembryonic antigen (CEA), MC38-CEA-2, were kindly provided by Dr. Jeffrey Schlom, National Cancer Institute (Bethesda, MD).

All cells were maintained in DMEM:Ham's F12 (1:1 v/v, Mediatech, Herndon, VA) medium, containing 10% fetal bovine serum (Hyclone, Logan, UT), 2 nM L-glutamine, 100 IU/mL penicillin and 25 μg/mL streptomycin (all Mediatech). Medium for MC38-CEA-2 cells additionally contained 500 ug/mL G418 (Mediatech). Cells were grown in a humidified atmosphere with 5% CO2 at 37 °C.

Coupling of gold nanoparticles to the adenoviral vector

Gold nanoparticles with a size of 1.4 nm containing a sulfo-N-hydroxy succinimide reactive group on the surface of the particle were acquired from Nanoprobes (Yaphank, NY, USA). Lyophilized gold nanoparticles were dissolved in DMSO to a final concentration of 200 fM immediately before reaction to the adenoviral vectors. In different syntheses, varying amounts of gold were added to a fixed amount of AdCMVLuc, diluted in 10 mM HEPES buffer containing 10% glycerol and 1 mM MgCl2, pH 7.8. Ratios of gold to adenovirus used in syntheses were 100:1, 1000:1, 3000:1 and 5000:1 (particle:particle). Gold nanoparticles were allowed to react with adenoviral vectors for 2 hours at room temperature. The reaction mixture was subsequently stored at 4 °C until use.

Electron microscopy of gold-labeled adenoviral vectors

Vectors were deposited onto carbon-coated copper grids; no staining was used in order to avoid occlusion of the 1.4 nm nanoparticles on the surface of the virions. Adenoviral vectors were examined using electron microscopy using a JEOL JEM 1200FX operated at 80 kV.

Purification of gold-labeled adenoviral vectors

To determine whether gold was covalently coupled to the adenoviral vector, reaction mixtures were purified using a CsCl gradient, with fractions collected from the bottom of the centrifugation tube. Fractions were analyzed for the presence of adenovirus using slot blot staining for the hexon capsid protein, and the presence of gold using slot blot staining employing silver enhancement. Hexon staining was accomplished by using a polyclonal goat anti-hexon antibody (Chemicon, Temecula, CA, USA), followed by an HRP-conjugated rabbit anti-goat secondary antibody (DakoCytomation, Carpinteria, CA, USA). Signal was detected using Western Lightning chemiluminescence reagent (PerkinElmer Life Sciences, Boston, MA) and Kodak BioMax MR Film (Kodak, Rochester, NY). Gold staining was accomplished by using LI silver enhancement according to manufacturer's instructions (Nanoprobes).

Construction, production and purification of the retargeting adapter molecule sCAR-MFE

A fusion protein capable of retargeting adenoviral vectors to the tumor-associated antigen carcinoembryonic antigen (CEA) was constructed, consisting of the ectodomain of CAR including its own leader sequence (aa 1-236), followed by a 5-aa peptide linker (GGPGS), a 6-histidine tag (for detection/purification), followed by the αCEA single chain antibody MFE-23 (a kind gift from Dr. Kerry Chester, London, UK). To construct sCAR-MFE, first, cDNA encoding sCAR followed by the 6-his tag was amplified out of pFBsCAR6hTf, [3] introducing a HindIII (5') and maintaining the BamHI (3') restriction

site. Second, the scFv MFE-23 was amplified by PCR introducing a BamHI (5') and XhoI (3') restriction site. Both PCR products were simultaneously ligated into the pcDNA3.1 plasmid (Invitrogen, Carlsbad, CA), digested with HindIII and XhoI restriction enzymes, thereby creating pcDNA/sCAR/6h/MFE. The constructed plasmid was verified by sequencing. HEK-293 cells were stably transfected with PvuI linearized plasmid, and clones were selected for high production and secretion of protein in the supernatant. After expansion of a positive clone, medium was collected and protein was purified by immobilized metal-affinity chromatography (Ni-NTA Superflow, Qiagen, Valencia, CA, USA), followed by dialysis with PBS.

In vitro gene transfer

To assess adenovirus infectivity, HeLa cells were plated in triplicate at a density of 1 x 105 cells/well in 24-well plates. The following day, 1 x 107 viral particles (vp) AdCMVLuc (100 vp/cell) were added to the cells in medium containing 2% fetal bovine serum. After 2 hours of incubation, medium containing AdCMVLuc was removed and replaced with regular growth medium. Cells were incubated for an additional 22 hours and were subsequently washed with PBS and lysed using Reporter Lysis Buffer (Promega, Madison, WI). After one freeze-thaw cycle, luciferase activity was measured using the Luciferase Assay System (Promega), according to manufacturer's instructions. To assess retargeting of AdCMVLuc to CEA by the sCAR-MFE fusion protein, MC38-CEA-2 cells were plated and infected as described above, with viral particles being incubated for 15 minutes at room temperature with 75 ng fusion protein, before addition to the cells.

References (Supporting Information)

1. Reynolds, P. N.; Nicklin, S. A.; Kaliberova, L.; Boatman, B. G.; Grizzle, W. E.; Balyasnikova, I. V.; Baker, A. H.; Danilov, S. M.; Curiel, D. T. Nat Biotechnol 2001, 19, 838-842.

2. He, T. C.; Zhou, S.; da Costa, L. T.; Yu, J.; Kinzler, K. W.; Vogelstein, B. Proc Natl Acad Sci U S A 1998, 95, 2509-2514.

3. Zhu, Z. B.; Makhija, S. K.; Lu, B.; Wang, M.; Rivera, A. A.; Preuss, M.; Zhou, F.; Siegal, G. P.; Alvarez, R. D.; Curiel, D. T. Virology 2004, 325, 116-128.

STUDY TWO

AN ADENOVIRAL PLATFORM FOR SELECTIVE SELF-ASSEMBLY AND TARGETED DELIVERY OF NANOPARTICLES

by

VAIBHAV SAINI[1,2], DMITRI V. MARTYSHKIN[3], SERGEI B. MIROV[3], ALEX PEREZ[4], GUY PERKINS[4], MARK H. ELLISMAN[4], VICTORIA D. TOWNER[1], HONGJU WU[1], LARISA PEREBOEVA[1,5], ANTON BOROVJAGIN[1], DAVID T. CURIEL[1], MAAIKE EVERTS[1,5]

[1]Division of Human Gene Therapy, Departments of Medicine, Obstetrics and Gynecology, Pathology, Surgery, and the Gene Therapy Center, [2]Department of Physiology and Biophysics, [3]Department of Physics, [5]Division of Molecular and Cellular Pathology, Pathology, University of Alabama at Birmingham (UAB), Birmingham, Alabama, USA [4]National Center for Microscopy and Imaging Research, Center for Research on Biological Structure School of Medicine, University of California, San Diego, California, USA

Small 4(2), 262-269

Format adapted and errata corrected for dissertation

Abstract

Nanotechnology holds great promise for the treatment of diseases. In this regard, metallic nanoparticles (NPs) can be used for diagnosis, imaging and therapy of tumors and cardiovascular disease. However, targeted delivery of NPs to specific cells remains a major limitation for clinical realization of these potential treatment options. Therefore, we herein define a novel strategy for specific coupling of NPs to a targeted adenoviral (Ad) platform, to deliver NPs to specific cells. The advantage of using this gene therapy vector as a targeting vehicle is the potential combination of nanotechnology and gene therapy for treatment of disease. To achieve the coupling of NPs to the virus, we have combined genetic manipulation of the gene therapy vector with a specific chemical coupling strategy. In particular, we employed a high-affinity interaction between a sequence of six-histidine amino acid residues genetically incorporated into Ad capsid proteins and Nickel (II) Nitrilotriacetic acid on the surface of gold NPs. Our results demonstrate the selective self-assembly of AuNPs and Ad vectors into the envisioned multifunctional platforms. Importantly, compared to previously employed coupling strategies, this selective assembly does not negatively affect targeting of Ad to specific cells. This further opens the possibility of utilizing Ad vectors for targeted NP delivery to specific cells, thereby providing a new type of combinatorial approach for the treatment of diseases, involving both nanotechnology and gene therapy. In addition, the specific NP coupling strategy employed herein can be utilized for coupling other types of NPs or molecules, thereby greatly expanding the utility of Ad as a targeted delivery vehicle. This utility may have broad implications for the fields of nanotechnology, gene therapy and viral biology.

Keywords: cell recognition, gene expression, nanoparticles, self-assembly, viruses

Introduction

Nanotechnology is revolutionizing the field of biomedicine. In this regard, metallic NPs such as quantum dots (QDs), magnetic NPs and gold NPs (AuNPs) can be used for tissue welding, gene regulation, intra-cellular environment studies, diagnosis, imaging, as well as hyperthermic tumor cell killing.[1-6] However, targeted delivery of nanoparticles to specific cells is a major impediment for the successful clinical utilization of the multiple treatment opportunities provided by nanotechnology.

We previously hypothesized that Ad vectors, which are used as targeted vectors for gene therapy,[7] might provide a suitable platform for target-specific delivery of NPs. This would allow a combination of the proven gene delivery capacity of Ad vectors with the imaging and therapeutic potential of NPs for the treatment of disease. Towards this end, we have demonstrated that NPs can be coupled to Ad vectors using a non-specific coupling method. However, non-specific NP coupling to Ad vectors at high NP:Ad ratios resulted in abrogation of Ad vector infectivity in target cells.[8] To circumvent this problem and thereby extend the paradigm of NP targeting via an Ad vector platform, we herein hypothesize that *specific* AuNP coupling to Ad vectors prevents the detrimental effects on Ad vector infectivity and targeting, observed with the non-specific NP coupling. To achieve the specific coupling, we genetically manipulated Ad capsid proteins to introduce NP binding sites at locales not involved in the vector infection and targeting pathway. Validation of this hypothesis paves the way towards realization of a multifunctional nanoscale system that combines gene therapy and nanotechnology approaches for the targeting and treatment of disease. In addition, it serves as a proof-of-principle that Ad vectors can serve as a platform for specific self-assembly of multiple components.

Results

To demonstrate feasibility of specific NP coupling to an Ad vector platform, we used gold NPs (AuNPs) as representative examples.

Ad vectors utilized for NP coupling

To specifically couple NPs to Ad vectors, we exploited the non-covalent affinity of Nickel (II) Nitrilotriacetic acid (Ni-NTA) for a sequence of six-histidine amino acid residues (6-His). In particular, the Ni-NTA-group on the employed AuNPs has a high affinity for a 6-His tag that can be genetically engineered into the Ad capsid at various defined capsid surface locations. We therefore utilized Ads expressing 6-His tags in capsid proteins not essential for Ad infectivity. These include an artificial fiber called 'fiber fibritin' (FF, ~ 9 copies), pIX (240 copies) or hexon (720 copies, Figure 1a). First, the expression of a 6-His tag in the Ad capsid was verified using western blot of purified virions. When stained with an antibody recognizing 6-His, a band with the appropriate size was observed for all the viruses tested, with the expected size of FF being 37 kD, pIX 14.4 kD and hexon 109 kD (Figure 1b). In addition, the relative intensities of the bands depended on the copy number of a particular protein in the Ad capsid. For example, the band intensity of FF (Figure 1b, lane 2, ~ 9 copies) is less than that of pIX (Figure 1b, lane 3, 240 copies) which in turn is less than that of hexon (Figure 1b, lane 4, 720 copies).

Specific coupling of NPs to Ad vectors

In order to couple AuNPs specifically to Ad vectors, Ni-NTA-AuNPs were

reacted with the described Ad vectors that display 6-His tags at specific capsid locales (Figure 1c). For this purpose, a ratio of 2,000:1 AuNP:Ad (particle:particle) was employed in the reaction mixture. After the reaction, the complexes were purified from unreacted AuNPs and Ad using CsCl density gradient ultra-centrifugation - a standard method for Ad vector purification. After centrifugation of AuNP-labeled viral particles in a CsCl gradient, a shift in the viral band position (density) relative to that of unlabeled virus in the gradient was observed. The extent of the band shift in the centrifuge tube was dependent on the type of modified Ad vector used in the coupling procedure.

For a negative control we incubated Ni-NTA-labeled AuNPs with an Ad that did not contain a 6-His tag. The resulting Ad band had the same density in the CsCl gradient as the same unmodified Ad without incubation with Ni-NTA-AuNPs (Figure 2a; Table 1 in supporting information). This indicates that Ni-NTA-AuNPs, as expected, did not bind to Ads in the absence of 6-His sites.

Unexpectedly, when Ni-NTA-AuNPs were incubated with the Ad vectors containing a 6-His tag in either fiber fibritin (FF) or pIX, no change in the virus density i.e. band shift was observed (Figure 2b; Table 1 in supporting information).

In contrast to the control and Ad vectors containing 6-His tag in FF and pIX, a distinct change in the viral band density upon AuNP coupling was observed for the Ad vector containing a 6-His tag in hexon (Figure 2b; Table 1 in supporting information). Hexon has four loop regions (L1 to L4), three of which are located on the outside of the virion being exposed to a solvent. Within these loops there are nine hypervariable regions (HVRs) with no known function.[9] Two of those, HVR2 and HVR5 can display heterologous peptides that are accessible for binding and retargeting of the mature

virion.[10] In this study we used a modified Ad with a 6-His tag incorporated in the HVR2 for coupling to AuNPs. The result shown in Figure 2b confirms the accessibility of this location for the interaction with Ni-NTA-AuNP. To further prove the specificity of the Ni-NTA-AuNP interaction with Ad vector expressing 6-His in HVR2, this reaction was also performed in the presence of 250 mM imidazole, which, as expected, competitively inhibited AuNP binding to the Ad vector (Figure 7 in supporting information).

Thus, based on the buoyant density of the treated Ad vectors it appears that the likelihood of NP coupling to Ad correlates with the number and potential accessibility of the available binding sites on the Ad capsid.

Transmission electron microscopy of NP-labeled Ad vectors

To confirm binding of NPs to the Ad particles, we used Transmission Electron Microscopy (TEM) to visualize AuNPs on the surface of Ad particles that were purified by CsCl centrifugation as described above. As expected, no AuNPs could be detected on either unlabeled Ad vector alone (Figure 3a) or Ad vector without 6-His but treated with AuNPs (Figure 3b). In line with our observations from the CsCl density analysis no AuNPs were seen in the preparations of Ads containing a 6-His tag in either FF or pIX (Figure 3c and d, respectively). In contrast, AuNPs could clearly be observed in the Ad vector containing a 6-His tag in hexon (Figure 3e and f). This result reinforces our conclusion that the selective coupling of NP to the Ad vectors depends on the number and accessibility of the coupling sites on the Ad capsid surface and identifies hexon as an optimal location for such coupling.

Atomic absorption spectroscopy of NP-labeled Ad vectors

To further characterize the AuNP-labeled Ad vectors, atomic absorption spectroscopy was utilized for quantification of the AuNPs coupled to the Ad vectors. The Ad vector with no coupled AuNPs as well as the one containing a 6-His tag in hexon, which showed both the change in the viral band density and presence of AuNPs by TEM upon coupling to Ni-NTA-AuNPs, were subjected to spectroscopy. This analysis demonstrated that on average this vector bound 56±4 AuNPs (see supplementary section), whereas the control Ad vector bound none. This validates the observation that hexon is a good capsid location for coupling NPs to Ad vectors.

Selectively NP-labeled Ad vectors retain infectivity in HeLa cells

In our previously published report, we observed a drastic abrogation of native Ad infectivity upon non-specific AuNP coupling at high AuNP:Ad ratios, possibly due to modification of Ad capsid proteins like fiber and penton base. To circumvent this problem, we envisaged specific coupling of AuNPs to the Ad capsid at locations not implicated in the natural mechanism of Ad infection. As described above, we were able to couple AuNPs specifically to hexon protein, which represents one of such structural proteins of the Ad capsid.

To determine whether our hypothesis was correct, we analyzed transgene expression in cells infected with Ad vectors encoding luciferase, with or without AuNPs coupled to hexon. To this end, we utilized HeLa cells, which have been previously reported to be readily susceptible to infection with Ad vectors. We observed a statistically significant, but only moderate, decrease in viral infectivity in the presence of bound AuNPs, as

compared to the control, where no AuNPs were present (Figure 4a). Despite this moderate loss of infectivity, the specifically AuNP-labeled Ad vectors (2,000 AuNPs per Ad vector input ratio) retain their capability to infect HeLa cells to a greater extent than the previously reported Ad vectors with non-specifically coupled AuNPs, where adding 1,000 AuNPs per Ad vector in the reaction mixture resulted in a decrease of approximately 1 order of magnitude, and 3,000 AuNPs per Ad vector resulted in a decrease of more than 2 orders of magnitude.[8] Thus, specific NP coupling to Ad vectors perturbs Ad vector infectivity to a lesser extent than the non-specific NP coupling reported previously.

Selectively NP-labeled Ad vectors can be retargeted to CEA-expressing tumor cells

The efficiency and specificity of transduction of the Ad vectors to be used as a delivery platform for NPs predicates the efficacy of the NP:Ad complex targeting to target cells. However, a majority of target cells, including tumor, endothelial or dendritic cells are deficient in the primary Ad receptor, the Coxsackie Adenovirus Receptor (CAR), thereby resulting in poor tumor cell transduction. To improve the transduction efficiency, a variety of approaches have been developed whereby the Ad vector is physically retargeted to alternate receptors on the target cell surface.[11] An example is retargeting of Ad vectors to the tumor-associated antigen carcino-embryonic antigen (CEA), which is over-expressed on several neoplasias such as colon and breast carcinoma. We used a bi-functional adapter molecule, sCAR-MFE, for retargeting Ad vectors to CEA-expressing tumor cells. The sCAR-MFE protein binds to the fiber knob in the Ad capsid through the sCAR part of the molecule and to the CEA on tumor cells

through the MFE part of the molecule, which is a single chain antibody (MFE-23) directed to CEA. In our previously published report, we observed detrimental effects on Ad vector retargeting to CEA-expressing tumor cells upon non-specific NP coupling at high NP:Ad ratios. To determine whether specific NP coupling to Ad vectors could reduce the negative effects on Ad retargeting to CEA, Ad vectors coupled and not coupled to AuNPs through the 6-His tag modification in hexon were pre-incubated with the bifunctional adapter molecule sCAR-MFE. To analyze the targeting efficiency of AuNP-coupled Ad vectors complexed with sCAR-MFE, we utilized the CEA-expressing cell line MC38-CEA-2. For various coupling reactions, we used Ad:AuNP input ratio of 1:2,000 and the purified Ad:AuNP complex was incubated with sCAR-MFE in a ratio of 1:85,000 before addition to the cells. We used an excess of AuNPs and sCAR-MFE molecules to saturate all potential binding sites on the Ad vector. Of note, the amount of sCAR-MFE used does not saturate the CEA receptors on the target cells.[12] In contrast to the previously reported decrease in targeted gene transfer using a non-specific NP coupling approach, we observed no statistically significant difference ($p > 0.05$) in the targeted gene transfer for the vectors and containing a 6-His tag in hexon, with and without the prior AuNPs coupling step. In addition, we observed a significant increase ($p < 0.01$) in the level of gene transfer of both AuNP-coupled and non-coupled Ad in the presence of sCAR-MFE as compared to the same viruses that were not pre-incubated with this targeting adapter molecule (Figure 5b). Thus, in contrast to the previously reported *non-specific* coupling strategy, the *specific* NP coupling to Ad capsid has no detrimental effect on Ad retargeting.

Discussion

Nanotechnology presents novel opportunities for imaging and treatment of diseases, such as the use of QDs for visualizing disease processes or gold nanoshells for photothermal therapy of cancer. In this regard, combination of nanotechnology with gene therapy would result in multifunctional nanoscale systems with potential for sophisticated disease treatment, for example in the context of cancer and cardiovascular disease. Towards this end, herein we have developed a methodology for specifically coupling NPs to an Ad vector, which is a well developed human gene therapeutic vector currently in many clinical trials. Importantly, the coupling method does not negatively affect virus infectivity and targeting to specific cells. However, we would like to point out that the observed unperturbed gene transfer ability is only indirect evidence for the cellular uptake of AuNP-labeled Ad vectors, but technical difficulties with observing 1.8 nm AuNPs in a cellular environment prevent observing AuNP-labeled Ad vectors inside an infected cell at this point in time. Coupling larger NPs may resolve this problem in future experiments.

For nanotechnology to become relevant as a treatment option, it is critical to achieve targeted delivery of nanoparticles to specific cells. With regards to NP delivery, NPs have previously been targeted utilizing both passive and active systems. Passive targeting approaches exploit the enhanced permeability and retention (EPR) of "leaky" tumor vasculature, as demonstrated for Au nanoshells.[6] Although passive targeting showed promising results, active targeting to a tumor associated antigen (TAA) is thought to be more effective. For this purpose, antibodies and peptides targeted against TAAs have been utilized to deliver AuNPs specifically to tumor cells[13-16] However, there is a limit

on the number of nanoparticles that can be attached to either an antibody or a peptide, due to their small size as compared to liposomes and Ad vectors. To circumvent this problem, targeted liposomes can be used, in which nanoparticles are encapsulated by a lipid bilayer that has targeting ligands immobilized on its outer surface[17, 18] However, if a combination of nanotechnology with gene therapy is desired, effective delivery of a therapeutic transgene to the target cells is critical. In this regard, Ad vector-mediated gene transfer is still unparalleled in *in vivo* systems, vis-à-vis targeting potential and transduction efficiency, although much progress is being achieved with other vector systems in recent years. Thus, a viral vector platform would be optimal for the assembly and targeted delivery of NPs to specific cells resulting in a combination of gene therapy and nanotechnology for treatment of disease.

In order to serve as a platform for NPs, a suitable method is required for coupling NPs to the viral vector. Towards this end, NPs have been coupled to viral capsids utilizing non-specific as well as specific chemistries. For instance, we have previously non-specifically coupled AuNPs to lysine residues in the capsid of an Ad vector. However, due to the non-specific coupling methodology, at higher NP:Ad vector ratios an abrogation of Ad vector infectivity and targeting to specific cells was observed.[8] Thus, a method for specific coupling of NPs to viral vector platforms would be optimal. In this regard, Belcher's group has coupled NPs specifically to the outer coat of bacteriophage M13.[19, 20] However, phage can not be used for human gene therapy applications, especially with respect to the envisioned combinatorial nanoscale multifunctional system. We therefore herein describe a specific coupling chemistry for human Ad vectors that does not negatively affect the retargeting ability of the virus, thus

making it feasible to combine nanotechnology and gene therapy in one nanoscale system. Furthermore, the methodology described herein to specifically couple NPs to Ad vectors can be easily adapted for other gene therapy vectors, such as adeno-associated virus (AAV), herpes simplex virus (HSV) or lentivirus.

The methodology described herein utilizes the affinity of 6-His for Ni-NTA. This affinity is routinely used to purify recombinant proteins containing a 6-His sequence in laboratories across the world. Moreover, 6-His is non-immunogenic and does not perturb the mature viral assembly. Also, it has been shown previously that a 6-His expressing recombinant Ad12 knob protein binds to Ni-NTA labeled gold. In addition, this AuNP-labeled Ad12 knob protein still bound to purified CAR protein.[21] However, Ad12 is not used for clinical gene therapy due to its oncogenic potential.[22] We therefore used the Ad5 vector, which has been used in multiple gene therapy trials. Although incorporation of a 6-His tag is possible in the Ad5 knob similar to Ad12 knob, we chose herein to not use this AuNP binding locale because of potential interference with targeting strategies, where an adaptor molecule has to bind to the Ad knob and re-target the virus to an antigen expressed on a tumor cell. Based on this, we utilized Ad vectors expressing a 6-His tag in capsid proteins that are not involved in Ad vector infectivity and targeting pathway, including an artificial fiber (FF), pIX and hexon protein.

The absence of observed AuNP binding to the Ad vectors expressing a 6-His tag in FF, as evidenced by unchanged viral band density in the CsCl density gradient, might be explained by the fact that there are only few FF copies (~9) with a 6-His tag available for AuNP binding. We also did not observe any bound AuNPs to the FF protein in the Ad capsid in TEM. However, it must be realized that due to the flexibility of the Ad fibers it

is extremely difficult to visualize these in TEM. We therefore do not completely disregard the notion that AuNPs can be coupled to FF, but judging from the lack of change in density the number of AuNPs per virion will be much less than hexon, should any bind at all.

With regard to the Ad vector containing a 6-His tag in pIX, the pIX protein has been located 65Å below the surface of the Ad capsid in a cavity between hexon proteins[23] and, thus, the 6-His moiety is likely to be inaccessible for AuNP coupling. In addition, the C-terminal domain of the pIX protein has been proposed to exist in two alternate conformations, either bound to the capsid or extended away from the capsid.[24] Thus, the flexibility in the pIX protein conformation might hinder the binding of Ni-NTA-AuNPs to a 6-His tag expressed in pIX.

With regard to the hexon coupling location, it is noteworthy that with an Ad:AuNP input ratio of 1:2,000 and 720 copies of hexon per virus, only 56 AuNPs bound per virion. This leads us to speculate that steric hindrance might play a role in AuNP interaction with the hexon protein in the Ad capsid. One potential reason may be the location of HVR2, where our 6-His tag is inserted, partially underneath the larger HVR1 region.[25] This partial obscuring of HVR2 may result in sub-optimal coupling efficiency of AuNPs. In addition, the spatial location of various adenoviral capsid proteins is still an area of active research, as evidenced by a recently published study by Marsh *et al.*[26] Based on their results, these investigators have reassigned the position earlier thought to be occupied by the protein IIIa to the pIX protein. The capsid proteins surrounding the hexon protein might therefore impose additional steric constrains. As the details of the Ad capsid structure are determined with greater accuracy, the issues pertaining to the

steric hindrance to interaction of various capsid proteins with molecules like AuNPs will be better understood.

The specificity of the 6-His – Ni-NTA coupling is demonstrated by our results in which Ni-NTA-labeled NPs bound to Ad vectors only at those accessible capsid locations which expressed a 6-His tag in high numbers as well as the ability of the imidazole to prevent the coupling reaction. Another interaction that could be utilized instead of 6-His - Ni-NTA is that of biotin with (strept)avidin. Viral vectors, such as Ad[27] AAV[28] and lentivirus[29] that are metabolically biotinylated during virus production in specific capsid locations, including hexon, have already been constructed by other groups. These viral vectors could be coupled to NPs with surface attached (strept)avidin or coupled to biotinylated NPs via a (strept)avidin bridge.

The specific AuNP coupling to Ad vectors demonstrated here can be exploited for coupling of other types of NPs to gene therapy vectors. For example, magnetic NPs can be utilized for either magnetic resonance based imaging or magnetic field-mediated tumor cell hyperthermic ablation.[5] Another example would be the use of QDs, which have excellent imaging applicability. With regard to imaging, QDs are superior to traditional fluorescent labels owing to a their consistent and prolonged signal strength.[30] Not only would QD-labeled Ad vectors be of use for imaging tumors, it would also be a sophisticated tool to track Ad vector biodistribution in pre-clinical animal models, illustrating the versatility of this approach.

In the aggregate, the specific coupling methodology realized herein for attaching NPs to Ad vectors provides an opportunity for specific assembly and delivery of NPs to target cells. In addition, the specific labeling of Ad vectors by NPs realized in this study

represents a unique combination of gene therapy and nanotechnology approaches, which has the potential for simultaneous targeting, imaging and therapy of disease. This multifunctional nanoscale system capable of incorporating multiple modalities in a single particle provides an important basis for the development of new generation diagnostics and therapies.

Conclusions

For successful utilization of the various treatment options offered by nanotechnology, target cell specific delivery of NPs is crucial. In this regard, here we have demonstrated that NPs can be specifically coupled to distinct Ad capsid proteins and targeted to tumor cells. In addition, specific NP-labeled Ad vectors displayed the same level of infectivity and targeting capability to tumor cells as unlabeled Ad vectors. Thus, Ad vectors can serve as the platform for selective self-assembly and targeted delivery of NPs to target cells. This paves the way for realization of a multifunctional nano-scale device for the treatment of disease by combining gene therapy and nanotechnology approaches.

Materials and Methods

Ad vector production

The Ad vectors encoding a firefly luciferase (Luc) and/or green fluorescence protein (GFP) under transcriptional control of the constitutively active cytomegalovirus (CMV) promoter and displaying a 6-His tag in fiber fibritin[31] and hexon (HVR2)[10] were constructed as described previously. The Ad vector displaying a 6-His tag on pIX was

generated as follows. First we constructed a modified pShuttle CMV vector[32] encoding Ad capsid protein IX (pIX) fused to a short linker peptide P(SA)4-PGSRGS followed by a 6His tag downstream of the pIX-Flag open reading frame. The 15 amino acid linker with 6-His were amplified by PCR from pBS.F5.RGS6HSL[33] and cloned into the shuttle vector plasmid pSlLucIXflag[32] at the unique NheI site downstream of the pIX-flag coding sequence. Recombinant Ad was generated by homologous recombination with the adenoviral genome plasmid pAdEasy1 (Qbiogene, Carlsbad, CA) in E. coli strain BJ5183, and virus was rescued in HEK-293 cells. For subsequent virus production, cells were infected using growth medium as described below, except containing 2% fetal bovine serum instead of 10%. Following overnight incubation, regular medium was added to the cells and cells were incubated until cytopathic effect was observed. Cells were harvested, and lysates obtained by 4 consecutive freeze-thaw cycles. Virus was purified using standard double CsCl gradient centrifugation. Viral particle number was determined by measuring absorbance at 260 nm using a conversion factor of 1.1×10^{12} viral particles per absorbance unit.[34]

Cell culture

HEK-293 cells were obtained from Microbix (Toronto, Canada), HeLa cells were obtained from the American Type Culture Collection (ATCC, Manassas, VA, USA) and MC38 cells stably transfected with carcinoembryonic antigen (CEA), MC38-CEA-2, were kindly provided by Dr. Jeffrey Schlom, National Cancer Institute (Bethesda, MD). All cells were maintained in DMEM:Ham's F12 (1:1 v/v, Mediatech, Herndon, VA) medium, containing 10% fetal bovine serum (Hyclone, Logan, UT), 2 nM L-glutamine,

100 IU/mL penicillin and 25 μg/mL streptomycin (all Mediatech). Medium for MC38-CEA-2 cells additionally contained 500 ug/mL G418 (Mediatech). Cells were grown in a humidified atmosphere with 5% CO2 at 37 °C.

Western blot

A total of 10^9 viral particles (vp) of each viral vector was mixed with Laemmli sample buffer containing 10mM β-mercaptoethanol. Samples were boiled for 10 minutes at 95 °C and were separated in a 4-15% polyacrylamide gradient sodium dodecyl sulfate-polyacrylamide gel by electrophoresis (SDS-PAGE) and transferred onto a polyvinylidene difluoride (PVDF) membrane (Bio-Rad, Hercules, CA, USA). The membranes were probed with an anti-His tag monoclonal antibody (Molecular probes, Invitrogen, Eugene, OR, USA). This was followed by an HRP-conjugated goat anti-mouse secondary antibody (DakoCytomation, Carpinteria, CA, USA). Signal was detected using Western Lightning chemiluminescence reagent (PerkinElmer Life Sciences, Boston, MA) and Kodak BioMax MR Film (Kodak, Rochester, NY).

Coupling of AuNPs to the Ad vector

AuNPs with a size of 1.8 nm containing a Ni-NTA reactive group on the surface of the particle were acquired from Nanoprobes (Yaphank, NY, USA). As per the information received from Nanoprobes, elemental analysis for nickel and gold suggests an average between 15 and 20 NTA-Ni(II) per Nanogold®. Also, the compound is supplied as the Ni(II) chelate. The reaction of AuNPs with Ad vectors was carried out at a ratio of 1:2,000 (Ad:AuNPs) in a buffer of pH 7.5 containing 20 mM Tris and 150 mM

NaCl for 30 minutes at room temperature, with 10^{12} vp of Ad used for each reaction. The reaction mixture was subsequently loaded onto a CsCl density gradient.

Purification of AuNP-labeled Ad vectors

To determine whether AuNPs were coupled to the Ad vectors, reaction mixtures were purified using a CsCl density gradient with ultra-centrifugation at 25,000 rpm for 3 hours at 4° C. Following ultra-centrifugation, the distance of viral bands was measured from the bottom of the tube (Table 1). For further experiments, viral bands were collected from the bottom of the centrifuge tube.

Electron microscopy of AuNP-labeled Ad vectors

Unmodified or AuNP-labeled Ad vectors were deposited onto carbon-coated copper grids, washed with double-distilled water, stained for 10 s with Nano-Van (Nanoprobes, Yaphank, NY, USA) and were examined using a JEOL JEM 1200FX electron microscope with a point resolution no worse than 0.45 nm. The microscope was operated at 80 kV and carefully aligned according to Nanoprobes' instructions to directly visualize the 1.8 nm gold particles. Negatives were recorded at 100,000 magnification and subsequently digitized with a Nikon SuperCoolScan scanner at 1800 dpi, producing a pixel resolution of 0.14 nm in images of size 4033x6010 pixels.

Atomic absorption spectroscopy of AuNP-labeled Ad vectors

The gold (Au) atomic absorption standard solution (1 mg/mL in 0.5N HCl) was obtained from Acros Organics (Belgium) and diluted to make standards ranging from 10

to 100 ppb. The obtained Au atomic absorption standard solutions were used for instrument calibration as well as for a quality control measurement. The atomic absorption measurements were performed at Atomspec DF Workstation (Thermo Jarrell Ash Corporation). Atomic absorption of Au was measured at 242.8 nm using the Smith-Hieftje background correction method. Before measuring the Ad:Au samples, they were dialyzed to remove CsCl and replace it with water. Following this, the viral particle number was determined as described earlier. The number of AuNPs per virion was calculated by comparing the atomic absorption readings for the viral samples with the Au standard, assuming 180 atoms of Au per AuNP. For calculation details, please see the supplemental section.

Construction, production and purification of the retargeting adapter molecule sCAR-MFE

A fusion protein capable of retargeting adenoviral vectors to the tumor-associated antigen carcinoembryonic antigen (CEA), consisting of the ectodomain of CAR, followed by a 5-aa peptide linker (GGPGS), a 6-histidine tag (for detection/purification), followed by the anti-CEA single chain antibody MFE-23 (a kind gift from Dr. Kerry Chester, London, UK) was constructed, produced and purified as described previously.[8]

***In vitro* gene transfer**

To assess Ad infectivity, HeLa cells were plated in triplicates at a density of 105 cells/well in 24-well plates. The following day, 107 viral particles (vp) of Ad vectors (100 vp/cell) were added to the cells in medium containing 2% fetal bovine serum. After

2 hours of incubation, medium containing Ad vectors was removed and replaced with regular growth medium. Cells were incubated for an additional 22 hours and were subsequently washed with PBS and lysed using Reporter Lysis Buffer (Promega, Madison, WI). After one freeze-thaw cycle, luciferase activity was measured using the Luciferase Assay System (Promega), according to manufacturer's instructions. To assess retargeting of Ad vectors to CEA by the sCAR-MFE fusion protein, MC38-CEA-2 cells were plated and infected as described above, with viral particles being incubated for 15 minutes at room temperature with 75 ng fusion protein (Ad:sCAR-MFE = 1:85,000), before addition to the cells.

Statistics

Statistical analysis for significance was performed using a 2-tailed t-test assuming equal variance in Excel (Microsoft Office 2003).

Acknowledgements

The authors thank Dr. Kerry Chester, Royal Free & University College Medical School (London, UK) for the kind gift of the anti-CEA scFv (MFE-23) encoding plasmid and Dr. Jeffrey Schlom, National Cancer Institute (Bethesda, MD, USA) for providing us with the carcinoembryonic antigen (CEA) expressing cell line MC38-CEA-2. We also acknowledge Hadiyah N. Green and Jonathan Hartwell for technical assistance. This work was supported by the following grants: P41RR04050 (Dr. Mark H. Ellisman), R01CA111569, 5R01CA090547, W81XWH-05-1-0035 (Dr. David T. Curiel) and W81XWH-06-1-0630 (Dr. Maaike Everts).

References

[1] A. M. Gobin, D. P. O'Neal, D. M. Watkins, N. J. Halas, R. A. Drezek ,J. L. West, *Lasers Surg Med* **2005**, *37*, 123-9.

[2] N. L. Rosi, D. A. Giljohann, C. S. Thaxton, A. K. Lytton-Jean, M. S. Han ,C. A. Mirkin, *Science* **2006**, *312*, 1027-30.

[3] J. Kneipp, H. Kneipp, M. McLaughlin, D. Brown ,K. Kneipp, *Nano Lett* **2006**, *6*, 2225-31.

[4] X. Gao, Y. Cui, R. M. Levenson, L. W. Chung ,S. Nie, *Nat Biotechnol* **2004**, *22*, 969-76.

[5] C. Alexiou, R. Jurgons, C. Seliger ,H. Iro, *J Nanosci Nanotechnol* **2006**, *6*, 2762-8.

[6] L. R. Hirsch, R. J. Stafford, J. A. Bankson, S. R. Sershen, B. Rivera, R. E. Price, J. D. Hazle, N. J. Halas ,J. L. West, *Proc Natl Acad Sci U S A* **2003**, *100*, 13549-54.

[7] H.-J. Li, M. Everts, L. Pereboeva, S. Komarova, A. Idan, D. T. Curiel ,H. R. Herschman, *Cancer Res 67*, In press.

[8] M. Everts, V. Saini, J. L. Leddon, R. J. Kok, M. Stoff-Khalili, M. A. Preuss, C. L. Millican, G. Perkins, J. M. Brown, H. Bagaria, D. E. Nikles, D. T. Johnson, V. P. Zharov ,D. T. Curiel, *Nano Lett* **2006**, *6*, 587-91.

[9] J. J. Rux, P. R. Kuser ,R. M. Burnett, *J Virol* **2003**, *77*, 9553-66.

[10] H. Wu, T. Han, N. Belousova, V. Krasnykh, E. Kashentseva, I. Dmitriev, M. Kataram, P. J. Mahasreshti ,D. T. Curiel, *J Virol* **2005**, *79*, 3382-90.

[11] M. Everts ,D. T. Curiel, *Curr Gene Ther* **2004**, *4*, 337-46.

[12] H. J. Li, M. Everts, L. Pereboeva, S. Komarova, A. Idan, D. T. Curiel ,H. R. Herschman, *Cancer Res* **2007**, *67*, 5354-61.

[13] I. H. El-Sayed, X. Huang ,M. A. El-Sayed, *Cancer Lett* **2006**, *239*, 129-35.

[14] L. Loo, R. H. Guenther, V. R. Basnayake, S. A. Lommel ,S. Franzen, *J Am Chem Soc* **2006**, *128*, 4502-3.

[15] A. G. Tkachenko, H. Xie, D. Coleman, W. Glomm, J. Ryan, M. F. Anderson, S. Franzen ,D. L. Feldheim, *J Am Chem Soc* **2003**, *125*, 4700-1.

[16] A. G. Tkachenko, H. Xie, Y. Liu, D. Coleman, J. Ryan, W. R. Glomm, M. K. Shipton, S. Franzen ,D. L. Feldheim, *Bioconjug Chem* **2004**, *15*, 482-90.

[17] W. J. Mulder, G. J. Strijkers, J. W. Habets, E. J. Bleeker, D. W. van der Schaft, G. Storm, G. A. Koning, A. W. Griffioen ,K. Nicolay, *Faseb J* **2005**, *19*, 2008-10.

[18] D. B. Kirpotin, D. C. Drummond, Y. Shao, M. R. Shalaby, K. Hong, U. B. Nielsen, J. D. Marks, C. C. Benz ,J. W. Park, *Cancer Res* **2006**, *66*, 6732-40.

[19] S. W. Lee, C. Mao, C. E. Flynn ,A. M. Belcher, *Science* **2002**, *296*, 892-5.

[20] C. Mao, C. E. Flynn, A. Hayhurst, R. Sweeney, J. Qi, G. Georgiou, B. Iverson ,A. M. Belcher, *Proc Natl Acad Sci U S A* **2003**, *100*, 6946-51.

[21] J. F. Hainfeld, W. Liu, C. M. Halsey, P. Freimuth ,R. D. Powell, *J Struct Biol* **1999**, *127*, 185-98.

[22] J. F. Williams, Y. Zhang, M. A. Williams, S. Hou, D. Kushner ,R. P. Ricciardi, *Curr Top Microbiol Immunol* **2004**, *273*, 245-88.

[23] J. Vellinga, M. J. Rabelink, S. J. Cramer, D. J. van den Wollenberg, H. Van der Meulen, K. N. Leppard, F. J. Fallaux ,R. C. Hoeben, *J Virol* **2004**, *78*, 3470-9.

[24] S. D. Saban, M. Silvestry, G. R. Nemerow ,P. L. Stewart, *J Virol* **2006**, *80*,

12049-59.

[25] D. M. Roberts, A. Nanda, M. J. Havenga, P. Abbink, D. M. Lynch, B. A. Ewald, J. Liu, A. R. Thorner, P. E. Swanson, D. A. Gorgone, M. A. Lifton, A. A. Lemckert, L. Holterman, B. Chen, A. Dilraj, A. Carville, K. G. Mansfield, J. Goudsmit ,D. H. Barouch, *Nature* **2006**, *441*, 239-43.

[26] M. P. Marsh, S. K. Campos, M. L. Baker, C. Y. Chen, W. Chiu ,M. A. Barry, *J Virol* **2006**, *80*, 11881-6.

[27] S. K. Campos ,M. A. Barry, *Hum Gene Ther* **2004**, *15*, 1125-30.

[28] G. S. Arnold, A. K. Sasser, M. D. Stachler ,J. S. Bartlett, *Mol Ther* **2006**, *14*, 97-106.

[29] D. Nesbeth, S. L. Williams, L. Chan, T. Brain, N. K. Slater, F. Farzaneh ,D. Darling, *Mol Ther* **2006**, *13*, 814-22.

[30] H. E. Grecco, K. A. Lidke, R. Heintzmann, D. S. Lidke, C. Spagnuolo, O. E. Martinez, E. A. Jares-Erijman ,T. M. Jovin, *Microsc Res Tech* **2004**, *65*, 169-79.

[31] L. Pereboeva, S. Komarova, P. J. Mahasreshti ,D. T. Curiel, *Virus Res* **2004**, *105*, 35-46.

[32] I. P. Dmitriev, E. A. Kashentseva ,D. T. Curiel, *J Virol* **2002**, *76*, 6893-9.

[33] J. T. Douglas, C. R. Miller, M. Kim, I. Dmitriev, G. Mikheeva, V. Krasnykh ,D. T. Curiel, *Nat Biotechnol* **1999**, *17*, 470-5.

[34] J. V. Maizel, Jr., D. O. White ,M. D. Scharff, *Virology* **1968**, *36*, 115-25.

Figure Legends

Figure 1. NPs can be specifically coupled to distinct Ad capsid locations. a)

Schematic representation of the location of various structural proteins in the Ad capsid. Ad vectors used in this study contain a 6-His tag genetically incorporated in either modified fiber (fiber-fibritin (FF) mosaic, ~9 copies), pIX (240 copies) or hexon (720 copies) proteins. b) Western blot analysis demonstrating the presence of 6-His tags in the Ad vectors in either FF (lane 2), pIX (lane 3) or hexon (lane 4). An unmodified Ad vector without a 6-His tag was used as a negative control (lane 1). c) AuNPs can be non-covalently coupled to specific locations on the Ad capsid. It is hypothesized that the Ni-NTA attached to the surface of 1.8 nm gold nanoparticles will react with the Ad capsid proteins that display a 6-His tag, resulting in a specific high affinity binding of AuNPs to Ad particles. This figure schematically shows Ad vectors expressing a 6-His tag in the hexon protein. There are 720 potential sites for Ni-NTA-AuNPs coupling to the Ad corresponding to the number of hexon molecules present in the Ad capsid.

Figure 2. NP-labeled Ad vectors demonstrate a change in density in CsCl gradients. a) Ni-NTA-AuNPs do not bind to Ad vectors in the absence of 6-His tag as revealed by density analysis in the CsCl gradient. Equal number of unmodified Ad particles (10^{12} vp) were analyzed by CsCl gradient centrifugation either without AuNPs (left tube) or following incubation with AuNPs at a Ad ratio of 2,000:1 (AuNPs:Ad, right tube). The unbound AuNPs in the right tube remain in the upper part of the gradient forming a diffuse zone. The sharp white band material seen at the same position in both tubes contains uncoupled Ad vectors. b) Relative positioning of the AuNP-coupled and uncoupled Ad vectors in the CsCl density gradient. Equal numbers of Ad particles (10^{12} vp) without or with a 6-His tag in FF, pIX or hexon were incubated either with Ni-NTA-

AuNPs at the AuNP:Ad input ratio of 2,000 (3 tubes on the right) or no AuNPs (tube on the left). The change in the viral band density seen for the Ad vector expressing a 6-His tag in hexon (rightmost tube) indicates coupling of the AuNPs to Ad.

Figure 3. Visualization of AuNPs coupled to Ad vectors by Transmission Electron Microscopy. Vectors were either unlabeled (a) or labeled with Ni-NTA-AuNPs to 6-His tag expressed in either FF (c), pIX (d) or hexon (e). AuNPs coupled to Ad vectors are only observed for the Ad vector with a 6-His tag in hexon (e, magnified in f with black arrowheads pointing at 1.8 nm AuNPs). The Ad vectors that do not express a 6-His tag do not bind any AuNPs (b). Original magnification is 100,000X, scale bar is 10 nm.

Figure 4. Analysis of infectivity and targeting of NP-labeled Ad vectors. a) Infectivity of Ad vectors is moderately affected upon specific AuNP coupling. A moderate reduction in the infectivity of AuNP-labeled-Ad vectors in HeLa cells was observed as compared to the unlabeled vectors (n=3, $*p = 0.0058$). b) Retargeting efficiency of the AuNP-coupled Ad vector to CEA expressing cells remains unaffected by the site-specific gold-coupling of the virus. The amount of luciferase transgene delivered to MC38-CEA-2 was similar for both unlabeled or AuNP-labeled Ad vectors in the presence of sCAR-MFE fusion protein, which retargets the viral vector to the expressed CEA (n=3, NS (not significant) $p= 0.1054$). For both unlabeled or AuNP-labeled Ad vectors, the amount of luciferase transgene delivered is significantly more in the presence of sCAR-MFE fusion protein (n=3, $*p= 4.482 \times 10^{-6}$, $**p= 0.0001$). Bars represent mean values ± standard deviation.

Figure 5. Atomic absorption calibration curve. The calibration curve was obtained using standard solutions (open circles). The concentration of Au for the Ad vector sample containing a 6-His tag in hexon that was coupled to AuNPs is shown as blue filled circles.

Figure 6. Atomic absorption spectra of a) control sample (Ad5) without AuNPs b) signal obtained from Ad vector sample with a 6-His tag in hexon that was coupled to AuNPs, and c) temperature of the furnace.

Figure 7. NP-labeled Ad vectors demonstrate a change in density in CsCl gradients. To confirm the specificity of interaction between Ni-NTA-AuNPs and the Ad vector expressing a 6-His tag in hexon, the coupling reaction was performed in the presence and absence of 250 mM imidazole. The presence of imidazole competitively inhibited the AuNP binding as no change in Ad band density was observed in the CsCl density gradient (middle tube).

Table Legends

Table 1. Positions of viral bands in centrifugation tubes after CsCl

Table 2. The procedure for measurement of atomic absorption

Table 3. Atomic absorption measurement for Ad vector with AuNPs coupled in hexon

Table 4. Atomic absorption measurement for control Ad5 sample

Figure 1

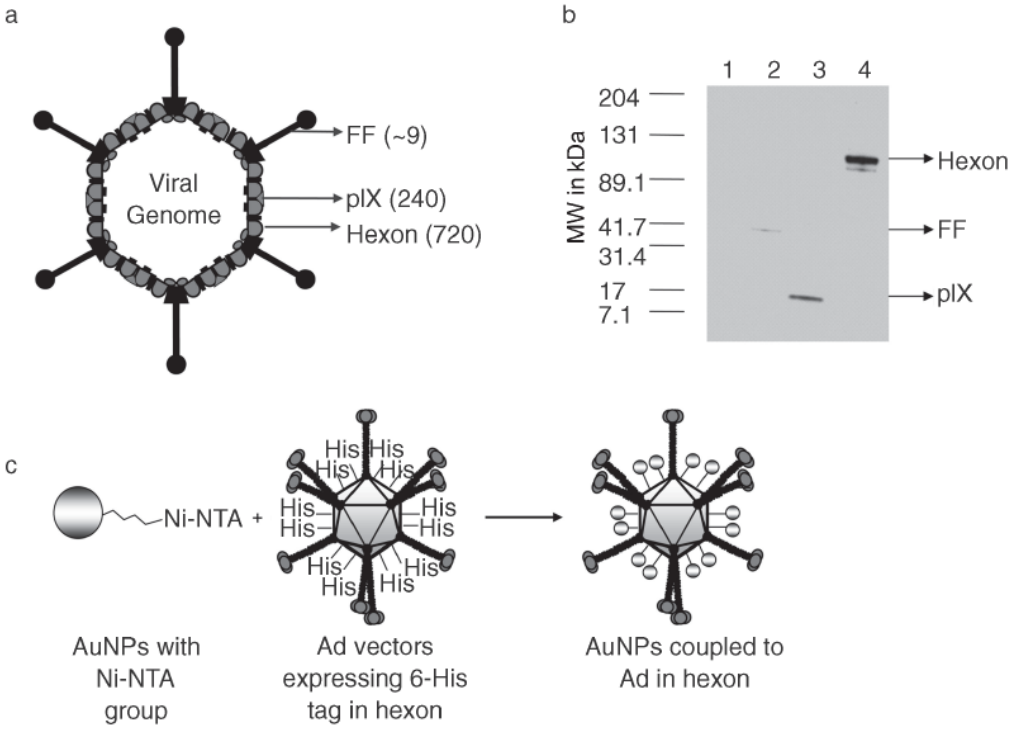
a
FF (~9)
Viral
Genome
pIX (240)
Hexon (720)
b
1 2 3 4
204
131
89.1
41.7
31.4
17
7.1
MW in kDa
Hexon
FF
pIX
c
Ni-NTA +
His
AuNPs with
Ni-NTA
group
Ad vectors
expressing 6-His
tag in hexon
AuNPs coupled to
Ad in hexon

Figure 2

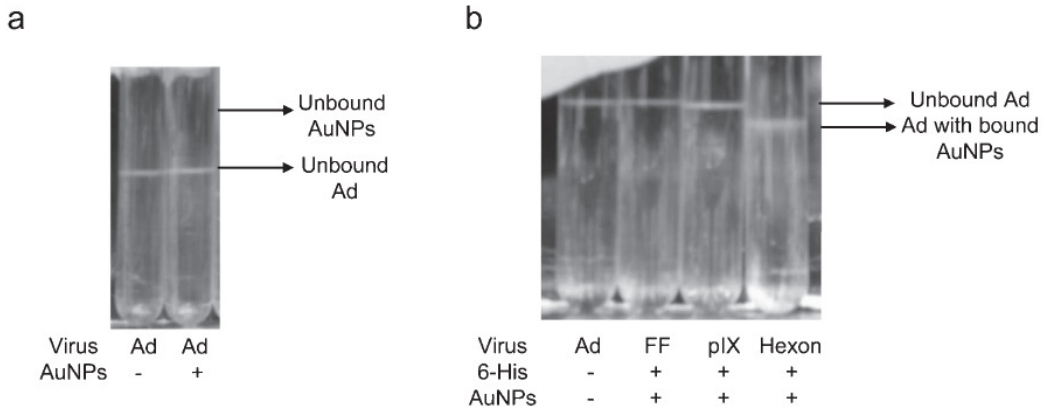
a
Unbound AuNPs
Unbound Ad
Virus Ad Ad
AuNPs - +
b
Unbound Ad
Ad with bound AuNPs
Virus Ad FF pIX Hexon
6-His - + + +
AuNPs - + + +

Figure 3

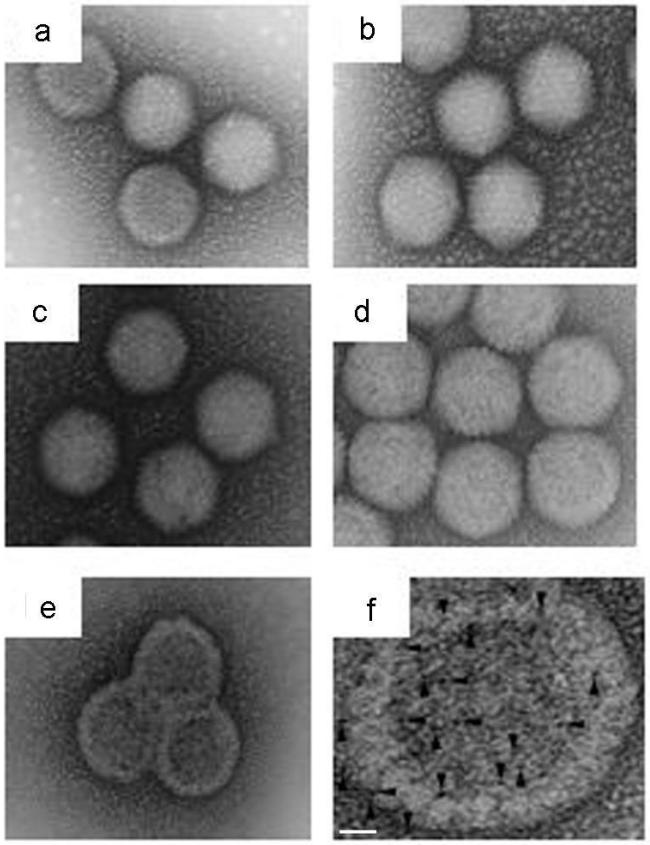

Figure 4

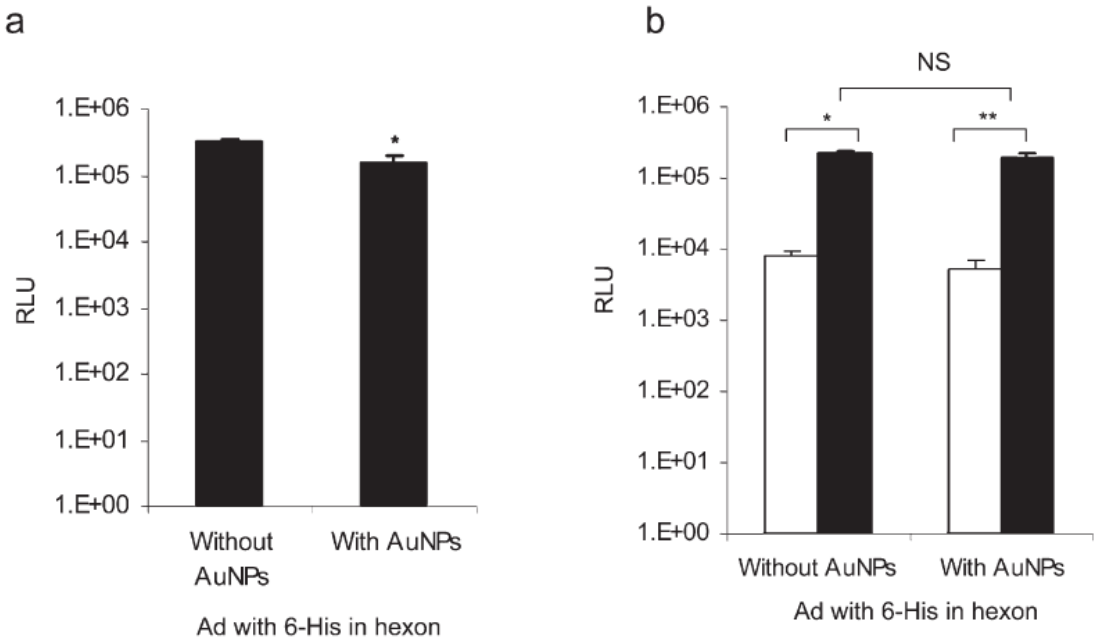
a
1.E+06
1.E+05
1.E+04
1.E+03
1.E+02
1.E+01
1.E+00
RLU
*
Without AuNPs
With AuNPs
Ad with 6-His in hexon
b
NS
*
**
1.E+06
1.E+05
1.E+04
1.E+03
1.E+02
1.E+01
1.E+00
RLU
Without AuNPs
With AuNPs
Ad with 6-His in hexon

Figure 5

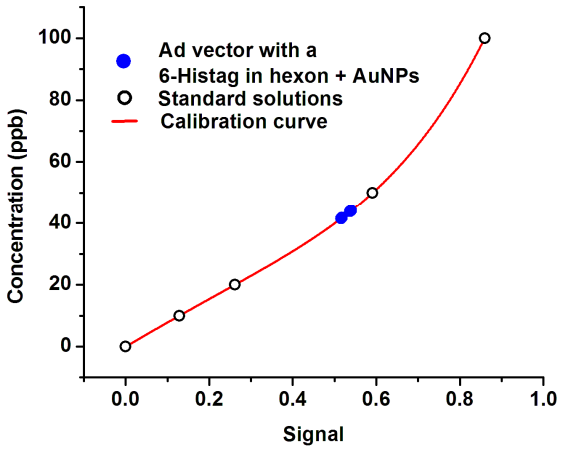
Ad vector with a
6-Histag in hexon + AuNPs
Standard solutions
Calibration curve
Concentration (ppb)
Signal
0
20
40
60
80
100
0.0
0.2
0.4
0.6
0.8
1.0

Figure 6

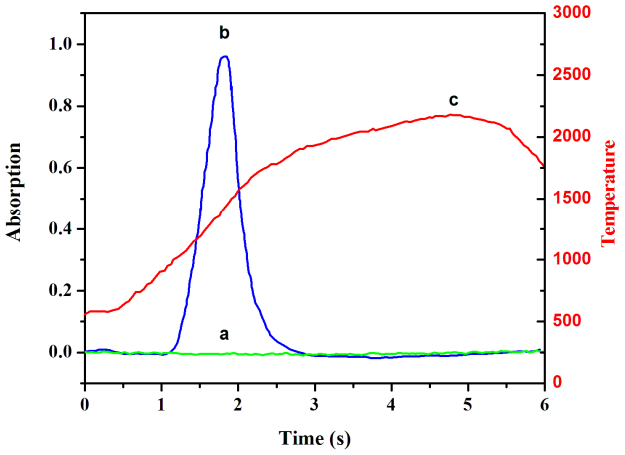
b
c
a
Absorption
Temperature
Time (s)
1.0
0.8
0.6
0.4
0.2
0.0
3000
2500
2000
1500
1000
500
0
0
1
2
3
4
5
6

Figure 7

Virus	Ad	Hexon	Hexon
6-His	-	+	+
AuNPs	-	+	+
Imidazole	-	+	-

Table 1

Ad-AuNP combination	distance from bottom to the viral band (cm)	total height gradient (cm)
Ad5	4.6	7.2
Ad5 + AuNPs	4.6	7.2
Ad5 with 6-His in FF + AuNPs	4.6	7.2
Ad5 with 6-His in pIX + AuNPs	4.6	7.2
Ad5 with 6-His in hexon + AuNPs	3.8	7.2

Table 2

furnace information					
	dry	pyro1	pyro2	atom	clean
temp	150	600	600	2250	2300
ramp	60	10	10	1	0
hold	80	15	5	4	3
purge	low	low	med	off	med

Table 3

Ad vector with 6-His in hexon + AuNPs	
absorption	concentration (ppb)
0.5371	43.77048
0.5178	41.73367
0.517	41.65116
0.54	44.08451
0.5156	41.50713
average	42.54939

Table 4

control sample (Ad5) without AuNPs	
absorption	concentration (ppb)
0.0069	0.54

Supporting Information

Detailed description of materials and methods

Atomic absorption spectroscopy of AuNP-labeled Ad vectors

The gold (Au) atomic absorption standard solution (1 mg/mL in 0.5N HCl) was obtained from Acros Organics (Belgium). It was further diluted in ultra pure HPLC grade water (Chromasolv® Plus, for HPLC, Sigma-Aldrich) containing 0.5N HCl to 10 ppb, 20 ppb, 50 ppb, and 100 ppb concentration respectively. The obtained Au atomic absorption standard solutions were used for instrument calibration as well as for a quality control measurement.

The atomic absorption measurements were performed at Atomspec DF Workstation (Thermo Jarrell Ash Corporation). Atomic absorption of Au was measured at 242.8 nm using the Smith-Hieftje background correction method. The atomic absorption signal corresponds to an integral of the absorbance integrated over time. The instrument was calibrated using Au atomic absorption standard solution prior to virus sample measurements.

The Ad vector samples collected from the CsCl gradients were dialyzed to remove CsCl and replace it with water. Following this, the viral particle number was determined by measuring absorbance at 260 nm using a conversion factor of 1.1×10^{12} viral particles per absorbance unit[34]

Ad vectors containing a 6-His tag in hexon coupled to AuNPs were ultrasonicated for 5 min and diluted 20 times in ultra pure HPLC grade water before measurements due to high initial concentration of Au. The dilution factor (20) and the final concentration of Au in virus sample were carefully chosen in order to fall into a linear response of the

instrument.

The typical measurement procedure consists of 5 stages; sample drying, pyrolysis, another pyrolysis, atomization, and cuvette cleaning. The parameters of each section should be experimentally optimized for each individual analyte. The following analytical protocol has been found to be optimal for measurements of the amount of Au atoms in samples containing viral particles and 1.8 nm AuNPs (Table 2).

For repeatability, five consecutive measurements of the same virus sample have been done followed by the quality control measurement of the atomic absorption standard solution, followed by a control virus sample (Ad5) measurement containing no AuNPs. The Au concentration was determined by using arithmetic average of the results of five measurements (Table 3).

Figure 5 shows the atomic absorption calibration curve obtained using standard solutions and concentration of Au for Ad vector sample containing a 6-His tag in hexon coupled to AuNPs.

The results of atomic absorption measurements of Au concentration in control Ad5 samples are summarized in Table 4. The Ad5 samples contain no Au and the observed signal corresponds to a noise level. Figure 6a shows signal obtained from control Ad5 sample without nanoparticles. As one can see there is no signal associated with gold atoms absorption. The atomic absorption of Au in Ad vector samples with a 6-His tag in hexon coupled to AuNPs and the atomization furnace temperature profile are depicted in Fig. 6b and Fig. 6c respectively.

The number of AuNPs per virion was calculated by comparing the atomic absorption readings for the viral samples with the Au standard, assuming 180 atoms of

Au per AuNP calculated as follows:

Volume of 1.8 nm AuNPs is:

$$V_{nano} = \frac{\pi D^3}{6} = \frac{\pi\left(1.8 \cdot 10^{-9}\right)^3}{6} = 3.052 \cdot 10^{-27} m^3 = 3.052 \cdot 10^{-21} cm^3, \quad (1)$$

where D=1.8 nm is diameter of nanoparticle.

Mass of one 1.8 nm AuNPs is:

$$m_{nano} = V_{nano} \cdot \rho = 58.9 \cdot 10^{-21} g, \quad (2)$$

where ρ=19.3 g/cm^3 is Au density.

Number of Au atoms in one AuNP is:

$$N_{Au} = \frac{m_{nano} \cdot N_A}{M.W.} = 180 \ \ atoms, \quad (3)$$

where M.W=197 g/mol is Au molecular weight and N_A=6.022·10^{-23} is Avogadro's number.

Number of Au atoms per mL in 1 ppb solution is:

$$N_{Au\ 1ppb} = \frac{10^{-9} g}{M.W.} \cdot N_A = 3.06 \cdot 10^{12} atoms / mL. \quad (4)$$

Number of AuNPs requared to produce 1 mL of 1ppb Au solution is:

$$N_{nano\ 1ppb} = \frac{N_{Au\ 1ppb}}{N_{Au}} = 1.7 \cdot 10^{10} nanoparticles. \quad (5)$$

Number of AuNPs coupled to hexon per virus is:

$$N = \frac{c_{Au} \cdot \eta \cdot N_{nano\ 1ppb}}{c_{vp}} = 56 \ \ nanoparticles / virus, \quad (6)$$

where c_{Au}=42.55 ppb is Au concentration found from atomic absorption measurements, η=20 is dilution factor and c_{vp}=0.2607·10^{12} vp/mL is concentration of virus particles.

Error associated with atomic absorption spectroscopy measurements. Atomic absorption spectroscopy is one of the most sensitive techniques designed for trace detection of metal ions in aqueous solutions. It has been used for over three decades as an analytical tool in environmental, industrial and scientific laboratories. Over this extended period of time the analytical methods and data treatment have substantially evolved in order to minimize the errors associated with the method features. We also made great efforts to optimize this method particularly for Au ions detection in an organic biological matrix and achieved signals of ideal shapes without any parasitic backgrounds, as one can see in Fig. 6. Therefore we believe that it is safe to assume that noise associated with method imperfection can be neglected. However noise associated with random signal fluctuation and detection system noise due to electronics and the quantum nature of the photomultiplier tube (PMT) can not be avoided. The rough estimation of noise level was made based on 5 measurements of 20 ppb gold standard solutions used as control measurements throughout the analytical protocol. The relative standard deviation $\%RSD = \frac{s}{x} \cdot 100\%$, where $s = \sqrt{\frac{1}{N-1}\sum_{i}^{N}(x_i - x)^2}$ is the sample variance, N is the number of measurements, and x is the mean value. The RSD was estimated to be 6.5%. The same estimation can be done for the Ad vector sample containing a 6-His tag in hexon that was coupled to AuNPs, resulting in 2.3% relative standard deviation. Taking into account the above error estimations one can find that the number of Au nanoparticles attached to the viruses was 56±4.

STUDY THREE

LIMITATIONS OF ADENOVIRAL VECTOR-MEDIATED DELIVERY OF GOLD NANOPARTICLES TO TUMORS FOR HYPERTHERMIA INDUCTION

by

VAIBHAV SAINI[1,2], M.SC., DMITRI V. MARTYSHKIN [3], PH.D., VICTORIA D. TOWNER[1], B.S., SERGEY B. MIROV[3], PH.D., MAAIKE EVERTS[1,4*], PH.D.

[1]Division of Human Gene Therapy, Departments of Medicine, Obstetrics and Gynecology, Pathology, Surgery, and the Gene Therapy Center, [2]Department of Physiology and Biophysics, [3]Department of Physics, [4]Division of Molecular and Cellular Pathology, Pathology, University of Alabama at Birmingham (UAB), Birmingham, Alabama, USA

Submitted to *Nanomedicine: Nanotechnology, Biology, and Medicine*

Format adapted for dissertation

Abstract

Novel combinatorial treatment strategies are desirable to achieve tumor eradication. In this regard, nanotechnology and gene therapy hold the potential to expand the available tumor treatment options. In particular, gold nanoparticles (AuNPs) have been utilized for hyperthermic tumor cell ablation. Similarly, adenoviral (Ad) vectors have been utilized for targeting, imaging, and cancer gene therapy. Thus, to combine AuNP mediated hyperthermia with Ad vector based gene therapy, we have previously coupled AuNPs to Ad vectors. Herein we tested the capability of these AuNP-labeled Ad vectors for hyperthermic tumor cell ablation. Towards this end, we compared absorption characteristics of different sized AuNPs and determined that in our system 20 nm diameter AuNPs are optimal for laser induced hyperthermic tumor cell killing. In addition, we observed that AuNPs outside and inside the cell contribute differentially towards hyperthermia induction. Unfortunately, due to the limitation of delivery of required amounts of AuNPs to cells, we observed that AuNP-labeled Ad vectors are unable to kill tumor cells via hyperthermia. However, with future technological advances, it may become possible to realize the potential of the multifunctional AuNP-labeled Ad vector system for simultaneous targeting, imaging and combined hyperthermia and gene therapy of tumors.

Keywords: Gold nanoparticles, hyperthermia, tumor treatment, adenovirus

Introduction

Development of new treatment options is crucial to achieve tumor eradication. In this regard, nanotechnology and gene therapy can provide novel opportunities for cancer

therapy. For example, in nanotechnology, gold nanoparticles (AuNPs) have been shown to be useful for drug delivery, targeting, imaging, and hyperthermia therapy of tumors [1-8]. In particular, laser-heated AuNPs have been shown to be effective in killing the tumors via hyperthermia induction, which possibly perturbs the tumor cell machinery at genetic and protein level resulting in cell death [9-11]. Similarly, in gene therapy, adenoviral (Ad) vectors have been developed as multifunctional therapeutic agents, providing applications such as targeting, imaging, and tumor cell killing [12].

With regards to tumor ablation, a combinatorial therapeutic regimen, as opposed to a single component therapy, has been recognized as optimal for successful treatment. In this regard, radiotherapy, chemotherapy, and immunotherapy approaches have been combined with gene therapy for developing more effective tumor ablation strategies [13-15]. Based on this, we have previously proposed to combine nanotechnology-based treatment opportunities with gene therapy for developing novel multifunctional nanoparticles for tumor treatment [16]. To this end, we have labeled Ad vectors with AuNPs, without perturbing the biological interactions of Ad vectors with target cells, to explore the possibility of combining gene therapy with AuNP based hyperthermia for the treatment of cancer [17, 18]. In the current study, we tested the feasibility of utilizing these AuNP-labeled Ad vectors for hyperthermia therapy.

Materials and Methods

Cell Culture

HeLa cells were obtained from the American Type Culture Collection (ATCC, Manassas, VA, USA) and HEK-293 cells were obtained from Microbix (Toronto,

Canada). The cells were maintained in DMEM:Ham's F12 (1:1 v/v, Mediatech, Herndon, VA) medium, containing 10% fetal bovine serum (Hyclone, Logan, UT), 2 nM L-glutamine, 100 IU/mL penicillin and 25 μg/mL streptomycin (all Mediatech) and were grown in a humidified atmosphere with 5% CO_2 at 37 °C.

Ad vector production

The Ad vectors encoding a red fluorescence protein (DsRed) under transcriptional control of the constitutively active cytomegalovirus (CMV) promoter and displaying a biotin acceptor peptide (BAP) in hexon (HVR5) were kindly provided by Dr. Michael A Barry (Mayo Clinic, Rochester, Minnesota, USA). For virus production, HEK-293 cells were infected using growth medium containing 2% fetal bovine serum instead of 10%. Following overnight incubation, regular medium was added to the cells and they were incubated until cytopathic effect was observed. Cells were harvested and lysates were obtained by 4 consecutive freeze-thaw cycles. Virus was purified using standard double CsCl gradient ultracentrifugation. Viral particle number was determined by measuring absorbance at 260 nm using a conversion factor of 1.1 x 10^{12} viral particles per absorbance unit [19]. The biotinylation status of the purified viral particles was determined via western blot (data not shown).

AuNPs

AuNPs with a diameter of 1.8 nm containing a Ni-NTA reactive group on the surface of the particle were acquired from Nanoprobes (Yaphank, NY, USA) and AuNPs with a diameter of 5 nm and 20 nm containing a streptavidin reactive group on the

surface of the particle were acquired from Nanocs (New York, NY, USA). The coupling of 5 nm and 20 nm diameter AuNPs with biotinylated Ad vectors was carried out at a ratio of 280:1 (AuNPs:Ad) for 30 minutes at room temperature, prior to adding the mixture to HeLa cells.

Absorption spectra measurements

The absorption spectra of 1.8 nm, 5 nm, and 20 nm AuNPs were measured in 0.5 cm quartz spectroscopic cell using UV-VIS-NIR scanning spectrophotometer (Shimazdu UV-3101PC). Absorption cross section (σ, cm^2) was calculated according to Lambert-Beer law $T=I_1/I_0=e^{-\sigma nl}$, *or* $\sigma=ln(1/T)/nl$, where T is transmission coefficient, I_0 and I_1 is incident and transmitted light intensities, n is concentration (nanoparticles per mL), and l is a spectroscopic cell length in cm.

Laser treatment

Cells incubated with AuNPs: HeLa cells were plated in triplicates at a density of 50,000 cells/well in 1 ml glass shell vials with a 6 mm internal diameter (Wheaton, NJ, USA). The following day, cells were rinsed with PBS and incubated with AuNPs in medium containing 2% fetal bovine serum for 1 hour at 37°C. Cells were washed or not, as indicated in the description of the respective experimental results.

Cells incubated with AuNPs and Ad vectors: HeLa cells were plated as described above. The following day, cells were incubated with AuNPs and/or Ad vectors for 1 hour at 4°C, then washed or not, and subsequently incubated for another hour at 37°C, and again either washed or not.

Following the incubations, cells were laser irradiated at 532 nm, 600 pulses, 1

minute, 4.2-5.2 W. After irradiation, cells were incubated in a humidified atmosphere with 5% CO_2 at 37 °C for 1 hour, and then trypsinized before being stained with propidium iodide, 25 µg/ml (Invitrogen, Carlsbad, CA) before being subjected to flow cytometry.

Statistics

Statistical analysis for significance was performed using a 2-tailed student's t-test assuming equal variance in Excel (Microsoft Office 2003) and a p value of <0.05 was considered significant.

Results

Small-sized AuNPs are unable to induce laser-mediated hyperthermic tumor cell ablation

In previously published reports, we have coupled AuNPs to Ad vectors to demonstrate the principle of coupling metal NPs to gene therapy vectors to facilitate combination therapy of neoplastic disease [17, 18]. AuNPs have been used for hyperthermic tumor cell killing by other groups [2-5, 7]. Before using AuNP-labeled vectors for 532 nm-laser induced hyperthermic tumor cell ablation, we tested the suitability of 1.8 nm diameter AuNPs for this purpose. To this end, we compared the absorption characteristics of 1.8 nm NPs with other NPs and observed that at 532 nm, the absorption cross section of 1.8 nm NPs is 100 and 1000 times less than 5 nm and 20 nm NPs respectively (Figure 1).

Based on low absorption efficiency of 1.8 nm NPs, we hypothesized that these NPs might not be optimal for hyperthermic tumor cell killing. To test our hypothesis, we

used the experimental set-up based upon a previously published system with minor modifications, including a higher power setting (~5 W vs. 1.9 W), and a longer pulse duration (60 seconds vs. 10 seconds) [7]. Also, to mimic a solid tumor for which hyperthermia therapy would be useful, we irradiated surface-attached cells in a monolayer instead of cells in suspension. The irradiation procedure itself had no negative impact on cell viability, as compared to control cells (Figure 2, a and b). In addition, AuNPs incubated with HeLa cells in the absence of irradiation had no negative impact on cell viability (Figure 2, g). Moreover, upon incubation of HeLa cells with AuNP numbers ranging from 6.02 X 10^{10} to 6.02 X 10^{13} per well in combination with laser irradiation, no change in cell viability was observed (Figure 2, c-f). Thus, as expected, 1.8 nm AuNPs were unable to induce hyperthermic tumor cell death.

AuNPs of 20 nm diameter can induce laser-mediated hyperthermic tumor cell ablation

After observing the higher absorption cross section at 532 nm for 5 and 20 nm diameter AuNPs as compared to 1.8 nm AuNPs, we tested the capability of these bigger NPs for laser-induced hyperthermic tumor cell killing. As observed before, the irradiation procedure had no negative impact on cell viability as compared to the control cells (Figure 3, a and b). Also, the maximum number of 5 nm (Figure 3, f) and 20 nm (Figure 3, j) AuNPs incubated with HeLa cells in the absence of irradiation had no negative impact on cell viability. In addition, when 5 nm AuNPs were incubated with HeLa cells in numbers ranging from 5 X 10^{9} to 5 X 10^{11} vps per well, and subsequently laser irradiated, no change in cell viability was observed (Figure 3, c-e). Similarly, 20 nm

AuNPs did not change HeLa cell viability at either 7 X 10^8 or 7 X 10^9 AuNPs per well (Figure 3, g and h). However, when HeLa cells were incubated with 7 X 10^{10}AuNPs of 20 nm per well, and then laser irradiated, a significant hyperthemic cell death of 50.3±13.6 % was observed (Figure 3, i).

After observing cell death with 20 nm diameter AuNPs, we wanted to discern whether AuNPs should be located either on the surface or inside the cell for hyperthermia induction. To characterize this differential contribution of NPs, we analyzed cell death with or without washing the cells after incubating them with 7 X 10^{10}AuNPs of 20 nm diameter. It has been reported in the literature that cells internalize AuNPs [20]. Thus, after incubating the cells with AuNPs at 37°C for 1 hour, washing removes both the unbound AuNPs in solution and the non-internalized AuNPs attached to the cell surface, leaving only the internalized AuNPs in cells. Although we observed more cell death (79.8±7.6 %) in the sample that was not washed, the washed sample also had significant cell death (31.6±4.0 %) as compared to the control (Figure 4, a, c and d). This indicates that AuNPs in the solution and on the surface as well as inside the cells contribute to hyperthermic killing.

Ad vectors labeled with 20 nm diameter AuNPs tested for hyperthermic cell killing

After determining the suitability of 20 nm AuNPs for 532 nm laser induced hyperthermic cell killing, we proceeded to analyze whether 20 nm AuNP-labeled Ad vectors could be utilized for cell killing as well, as this would pave the way for combining AuNP mediated hyperthermia with Ad vector mediated gene therapy of tumors. Towards this end, we coupled streptavidin-functionalized 20 nm AuNPs to

genetically engineered Ad vectors that are metabolically biotinylated in the hexon capsid protein. This coupling method is conceptually based upon the specific coupling strategy published previously where 1.8 nm Ni-NTA-AuNPs were specifically coupled to Ad vectors expressing a 6-His in hexon [18]. However, due to the bigger size of AuNPs (20 nm vs 1.8 nm), we were unable to use the previously employed CsCl density gradient ultracentrifugation for separating the reactants from the products. Thus, in order to separate unreacted AuNPs from the AuNP-labeled Ad vectors, we utilized the principle of viral interaction with its receptor- coxsackie adenovirus receptor (CAR). While Ad vectors can bind to CAR at 4°C [21], AuNPs have not been observed to bind to a specific receptor and therefore should not interact with the cells at this temperature. We therefore incubated the mixture of unreacted AuNPs and AuNP-labeled Ad vectors with HeLa cells, which express CAR, at 4°C for 1 hour, and then upon washing removed both unreacted AuNPs and AuNP-labeled Ad vectors that did not bind to the CAR (Figure 5). To determine whether washing removes AuNPs after incubation at 4°C for 1 hour, we incubated HeLa cells with 7 X 10^{10}AuNPs of 20 nm diameter and did not observe significant cell death when samples were washed as compared to when they were not washed (Figure 6, d and e). Unfortunately, when cells were incubated with AuNPs coupled to Ad vectors, no significant cell death was observed (Figure 6, g). To understand this inability of AuNP-labeled Ad vectors for hyperthermic cell killing, we theoretically calculated the maximum number of AuNPs that can be delivered to cells utilizing Ad vectors. We plated 50,000 HeLa cells per well and infected these with Ad vectors at a multiplicity of infection (MOI) of 5000 vp/cell. Thus, we added 2.5 x 10^8 vp/well. If only 10% of these added viral particles infect cells, then the number of Ad

vectors infecting cells per well is 2.5 x 10^7. In a previously published report, we were able to couple 56±4 AuNPs of 1.8 nm diameter to Ad vectors [18]. Most likely, steric factors restrict the number of 20 nm AuNPs that can be coupled to Ad vectors. We anticipate that this number is less than the number of 1.8 nm AuNPs that can be coupled per virus. In this regard, Ad vectors have 20 triangular facets, each formed by 12 copies of hexon trimers [22]. Based on this, we hypothesize that we can couple 20 AuNPs of 20 nm diameter to each Ad vector (1 AuNP per facet), resulting in the delivery of 5 x 10^8 AuNPs to the cells per well by Ad vectors. This number is approximately 100X less that the number needed for inducing laser-mediated hyperthermic tumor cell ablation. To confirm the inability of 5 x 10^8 AuNPs/well to induce cell killing, we incubated HeLa cells with 5 x 10^8 AuNPs/well and did not observe cell death (Figure f). Thus, although 20 nm AuNPs can be utilized for hyperthermic tumor cell killing, it is presently not possible to deliver the required number of AuNPs to the tumor cells utilizing Ad vectors.

Discussion

A combinatorial approach has been recognized as optimal for successful tumor treatment. Thus, to combine nanotechnology with gene therapy for developing a novel nanoscale agent for cancer therapy, we have previously labeled Ad vectors with AuNPs [17, 18]. In the current study, we explored the feasibility of utilizing these AuNP-labeled Ad vectors for hyperthermic tumor cell ablation.

The rapid multiplication of tumor cells imposes disadvantages on these cells, which can be utilized for selective therapeutic intervention for killing the neoplastic cells while restricting the damage to the healthy cells of the body. In this regard, due to the

limited vasculature, resulting in a hypoxic environment and a low pH, tumors are inefficient in counteracting an increase in temperature, which disrupts the cell machinery at the molecular level [9-11]. Thus tumors are prone to hyperthermia induced cell death as reported in the literature using laser-heated AuNPs [2-5, 7, 23].

Our results demonstrate that the hyperthermic cell killing ability of AuNPs is a function of their size and amount associated with the cells, which is analogous to previously published reports [7, 24]. In addition, as reported previously, while Ad vectors can be used to deliver AuNPs to tumors, we discovered that current technological limitations restrict our ability to deliver the required amount of AuNPs to tumors to induce hyperthermic cell death.

The observed inefficiency of AuNP-labeled Ad vectors can theoretically be countered by improvements in the AuNP payload capacity of the Ad vector, the number of Ad vectors bound to the tumor cell, the physical characteristics of the AuNPs themselves, or utilizing a different laser irradiation regime. With regards to Ad vectors, increasing the number of AuNPs coupled to Ad vectors would increase the number of AuNPs delivered to target cells. However, with the coupling strategies reported by our group, it is currently not possible to attach more NPs to Ad vectors. For example, with the non-specific coupling of AuNPs to amine groups on Ad capsid, a decrease in Ad infectivity was observed with increasing amounts of AuNPs bound to Ad vectors [17]. With specific coupling of Ni-NTA-AuNPs to Ad vectors expressing a 6-histidine (6-His) tag at different capsid locations, it is worthwhile to note that we observed AuNP coupling only to hexon, which is the most abundant protein in the Ad capsid, and not to any other surface exposed and/or abundant capsid protein like fiber or pIX [18]. In addition, in the

current study, instead of Ni-NTA and 6-His, we used the affinity of streptavidin-biotin, which is among the highest non-covalent affinity reported in the literature, to couple AuNPs to Ad vectors [25]. Thus, there is only a minor possibility for improvement in these non-specific and specific coupling strategies. However, a possible way to circumvent this problem could be the use of branched polymers with multiple binding sites for AuNPs, and subsequently attaching these AuNP branches to Ad vectors. However, it has been reported that coupling polymers to Ad vectors is detrimental to Ad vector infection *in vitro* and may be a limiting factor for using polymers for attaching more AuNPs to Ad vectors [26]. Nonetheless, coupling polymer seems to have less of an effect on infectivity *in vivo*, thus opening up the possibility of exploring this strategy to couple more AuNPs to Ad vectors [27]. In addition to investing in improved coupling strategies, it would be beneficial to improve Ad association with tumor cells. But, in this particular experimental setup we utilized a MOI of 5000 vp/cell, which cannot easily be increased without inducing viral vector-based toxicity [28]. Though, strategies to overcome viral vector-related toxicities and immunological complications are under development, such as physical masking of the antigenic viral surface to avoid triggering innate immune system, genetic exchange of capsid components among different serotypes to avoid detection by antibodies, and generation of gutless vectors to prevent the induction of an adaptive immune response [12].

Besides manipulating Ad vectors, the properties of AuNPs could be changed to improve hyperthermia induction ability. One approach could be to change the shape and size of AuNPs. For example, Jain et al. compared gold nanospheres, nanoshells, and nanorods, and observed that nanorods, which absorb near 800 nm, may be better than

other shapes for biomedical applications such as imaging and photothermal therapy. They also estimated that gold nanorods with efficient radius r_{eff}=11.43 nm are 14 times more effective absorbers at the resonance wavelength comparing to 20 nm nanospheres [29]. Moreover, it has been reported that AuNPs that absorb in the near-infrared (NIR) region would be optimal for hyperthermia because normal body cells lack the chromophores to absorb this wavelength [30]. Thus, laser irradiation at NIR wavelengths will not have any adverse thermal effects on healthy cells that did not accumulate AuNPs.

In addition to modifying the Ad vectors and AuNPs, utilization of different laser irradiation conditions can also be attempted to improve the hyperthermia capability of AuNP-labeled Ad vectors. For example, we used a nanosecond laser irradiation regime. However, picosecond lasers, capable of delivering much higher peak power, could be more efficient for hyperthermia induction with AuNP-labeled Ad vectors.

Lastly, our results demonstrate that AuNPs both outside and inside the cells contribute towards hyperthermia. Thus, utilizing a mixture of internalizing and non-internalizing Ad vectors may help in loading the inside as well the outside of tumor cells with AuNP-labeled Ad vectors, and may enhance the achieved hyperthermia induction. For example, RGD motifs in the Ad vector penton capsid protein interact with integrins on the cell surface, and thereby mediate the process of Ad internalization. Thus, a mutant Ad vector with deleted RGD motifs has a defective internalizing mechanism, but is capable of binding to cells via CAR, and could potentially be used to deliver AuNPs to the cell surface [31].

In summary, our previous work established the feasibility of utilizing Ad vectors for NP delivery to target cells. However, at this time, various technical roadblocks,

investigated in the current study, limit our ability to use these AuNP-labeled Ad vectors for hyperthermia induction for tumor therapy. Upon overcoming these hurdles with future endeavors, it maybe possible to realize the therapeutic potential of this nanoscale multifunctional NP-labeled Ad vector system for a combination of nanotechnology and gene therapy-based treatment of cancer.

Acknowledgements

The authors would like to thank Enid F. Keyser, Flow Cytometry Core of the UAB Arthritis and Musculoskeletal Center, University of Alabama at Birmingham (supported by NIH P30 grant AR48311), for help with flow cytometry to determine cell viability. This work was supported by following grants: ECS-0424310, EPS-0447675, BES-0521036 National Science Foundation Grants (Sergey B. Mirov), W81XWH-06-1-0630, UAB Center for Women's Reproductive Health Pilot and Feasibility grant, and NCI CA13148-35 UAB CCC Junior Faculty Development Grant Program (Maaike Everts).

References

1. Han G, Ghosh P, Rotello VM. Multi-functional gold nanoparticles for drug delivery. Adv Exp Med Biol 2007;620:48-56.
2. Kim J, Park S, Lee JE, et al. Designed Fabrication of Multifunctional Magnetic Gold Nanoshells and Their Application to Magnetic Resonance Imaging and Photothermal Therapy. Angew Chem Int Ed Engl 2006.
3. Huang X, El-Sayed IH, Qian W, El-Sayed MA. Cancer cell imaging and

photothermal therapy in the near-infrared region by using gold nanorods. J Am Chem Soc 2006;128(6):2115-20.

4. O'Neal DP, Hirsch LR, Halas NJ, Payne JD, West JL. Photo-thermal tumor ablation in mice using near infrared-absorbing nanoparticles. Cancer Lett 2004;209(2):171-6.

5. Hirsch LR, Stafford RJ, Bankson JA, et al. Nanoshell-mediated near-infrared thermal therapy of tumors under magnetic resonance guidance. Proc Natl Acad Sci U S A 2003;100(23):13549-54.

6. Bhattacharya R, Mukherjee P. Biological properties of "naked" metal nanoparticles. Adv Drug Deliv Rev 2008.

7. Zharov VP, Letfullin RR, Galitovskaya E. Microbubbles-overlapping mode for laser killing of cancer cells with absorbing nanoparticle clusters. . J Physics D: Appl Phys 2005;38 2571-81.

8. Javier DJ, Nitin N, Levy M, Ellington A, Richards-Kortum R. Aptamer-Targeted Gold Nanoparticles As Molecular-Specific Contrast Agents for Reflectance Imaging. Bioconjug Chem 2008.

9. Edwards MJ, Mulley R, Ring S, Wanner RA. Mitotic cell death and delay of mitotic activity in guinea-pig embryos following brief maternal hyperthermia. J Embryol Exp Morphol 1974;32(3):593-602.

10. Kampinga HH. Cell biological effects of hyperthermia alone or combined with radiation or drugs: a short introduction to newcomers in the field. Int J Hyperthermia 2006;22(3):191-6.

11. Maldonado-Codina G, Llamazares S, Glover DM. Heat shock results in cell cycle

delay and synchronisation of mitotic domains in cellularised Drosophila melanogaster embryos. J Cell Sci 1993;105 (Pt 3):711-20.

12. Saini V, Roth JC, Pereboeva L, Everts M. Importance of viruses and cells in cancer gene therapy. Adv Gene Mol and Cell Therapy 2007;1(1):30-43.

13. Szatmari T, Huszty G, Desaknai S, et al. Adenoviral vector transduction of the human deoxycytidine kinase gene enhances the cytotoxic and radiosensitizing effect of gemcitabine on experimental gliomas. Cancer Gene Ther 2008;15(3):154-64.

14. Lamont JP, Nemunaitis J, Kuhn JA, Landers SA, McCarty TM. A prospective phase II trial of ONYX-015 adenovirus and chemotherapy in recurrent squamous cell carcinoma of the head and neck (the Baylor experience). Ann Surg Oncol 2000;7(8):588-92.

15. Tagawa M, Kawamura K, Ueyama T, et al. Cancer therapy with local oncolysis and topical cytokine secretion. Front Biosci 2008;13:2578-87.

16. Saini V, Zharov VP, Brazel CS, Nikles DE, Johnson DT, Everts M. Combination of viral biology and nanotechnology: new applications in nanomedicine. Nanomedicine 2006;2(3):200-6.

17. Everts M, Saini V, Leddon JL, et al. Covalently linked Au nanoparticles to a viral vector: potential for combined photothermal and gene cancer therapy. Nano Lett 2006;6(4):587-91.

18. Saini V, Martyshkin DV, Mirov SB, et al. An adenoviral platform for selective self-assembly and targeted delivery of nanoparticles. Small 2008;4(2):262-9.

19. Maizel JV, Jr., White DO, Scharff MD. The polypeptides of adenovirus. I.

Evidence for multiple protein components in the virion and a comparison of types 2, 7A, and 12. Virology 1968;36(1):115-25.

20. Zharov VP, Galitovsky V, Mark V. Photothermal detection of local thermal effects during selective nanophotothermolysis. Appl Phys Lett 2003;83:4897-9.

21. Martin-Fernandez M, Longshaw SV, Kirby I, et al. Adenovirus type-5 entry and disassembly followed in living cells by FRET, fluorescence anisotropy, and FLIM. Biophys J 2004;87(2):1316-27.

22. Rux JJ, Burnett RM. Adenovirus structure. Hum Gene Ther 2004;15(12):1167-76.

23. Everts M. Thermal scalpel to target cancer. Expert Rev Med Devices 2007;4(2):131-6.

24. El-Sayed IH, Huang X, El-Sayed MA. Selective laser photo-thermal therapy of epithelial carcinoma using anti-EGFR antibody conjugated gold nanoparticles. Cancer Lett 2006;239(1):129-35.

25. Chilkoti A, Tan PH, Stayton PS. Site-directed mutagenesis studies of the high-affinity streptavidin-biotin complex: contributions of tryptophan residues 79, 108, and 120. Proc Natl Acad Sci U S A 1995;92(5):1754-8.

26. Mok H, Palmer DJ, Ng P, Barry MA. Evaluation of polyethylene glycol modification of first-generation and helper-dependent adenoviral vectors to reduce innate immune responses. Mol Ther 2005;11(1):66-79.

27. Hofherr SE, Shashkova EV, Weaver EA, Khare R, Barry MA. Modification of Adenoviral Vectors With Polyethylene Glycol Modulates In Vivo Tissue Tropism and Gene Expression. Mol Ther 2008.

28. Brunetti-Pierri N, Ng P. Progress and prospects: gene therapy for genetic diseases

with helper-dependent adenoviral vectors. Gene Ther 2008;15(8):553-60.

29. Jain PK, Lee KS, El-Sayed IH, El-Sayed MA. Calculated absorption and scattering properties of gold nanoparticles of different size, shape, and composition: applications in biological imaging and biomedicine. J Phys Chem B 2006;110(14):7238-48.

30. Weissleder R. A clearer vision for in vivo imaging. Nat Biotechnol 2001;19(4):316-7.

31. Shayakhmetov DM, Eberly AM, Li ZY, Lieber A. Deletion of penton RGD motifs affects the efficiency of both the internalization and the endosome escape of viral particles containing adenovirus serotype 5 or 35 fiber knobs. J Virol 2005;79(2):1053-61.

Figure Legends

Figure 1. Absorption coefficients of different sized AuNPs: 1.8 nm (yellow line), 5 nm (black line), and 20 nm (blue line).

Figure 2. AuNPs of 1.8 nm diameter are unable to induce hyperthermic tumor cell ablation upon laser irradiation. Non-irrradiated (white bars) and irradiated (black bars, 532 nm, 600 pulses, 1 minute, 5.2 W). * indicate $p < 0.05$.

Figure 3. AuNPs of 20 nm diameter can kill tumor cells via laser-induced hyperthermia. Non-irrradiated (white bars) and Irradiated (black bars, 532 nm, 600 pulses, 1 minute, 4.2 W). * indicate $p < 0.05$.

Figure 4. AuNPs on the surface and inside the cell contribute to laser-induced hyperthermic cell killing. Non-irrradiated (white bars) and Irradiated (black bars, 532 nm, 600 pulses, 1 minute, 4.5 W). * indicate $p < 0.05$.

Figure 5. Cellular binding of Adenovirus and AuNPs is temperature dependent.

Figure 6. AuNP-labeled Ad5 vectors unable to induce laser-mediated hyperthermic tumor cell ablation. Irradiated (black bars, 532 nm, 600 pulses, 1 minute, 4.5 W). * indicate $p < 0.05$.

Figure 1

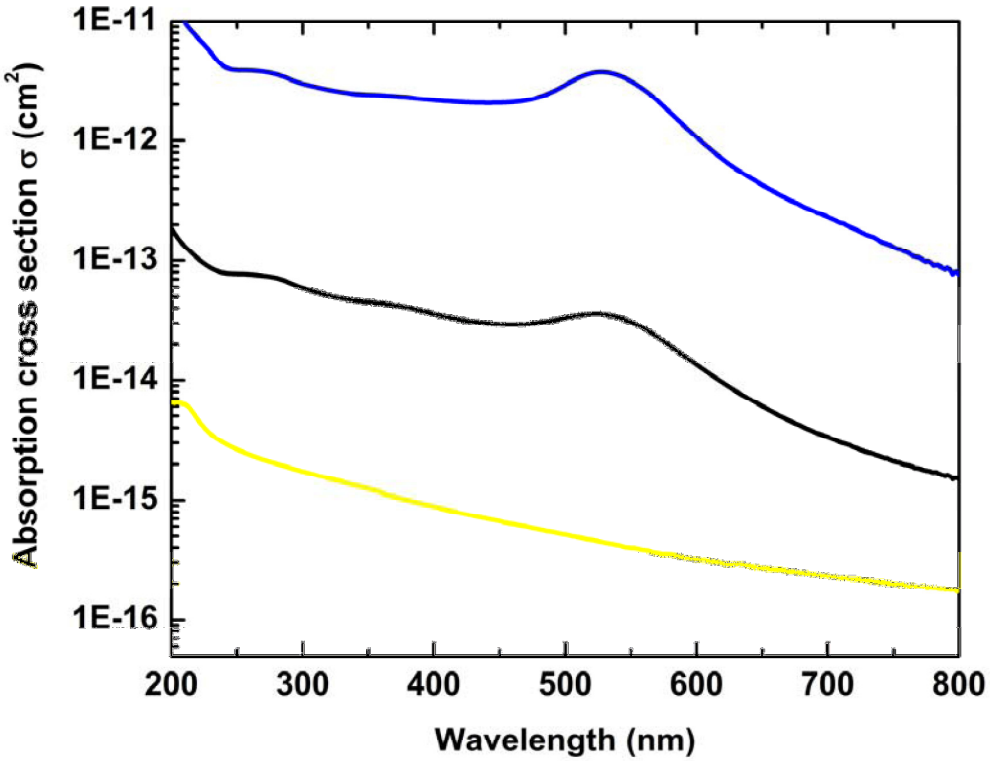
Absorption cross section σ (cm²)
1E-11
1E-12
1E-13
1E-14
1E-15
1E-16
200
300
400
500
600
700
800
Wavelength (nm)

Figure 2

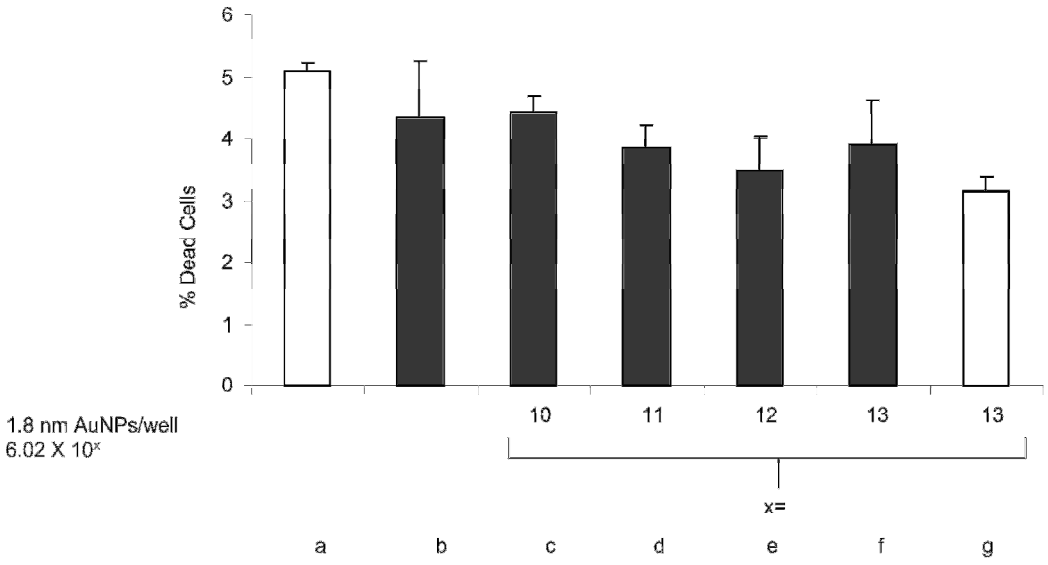
6
5
4
3
2
1
0
% Deac Cells
1.8 nm AuNPs/well
6.02 X 10^x
10
11
12
13
13
x=
a
b
c
d
e
f
g

Figure 3

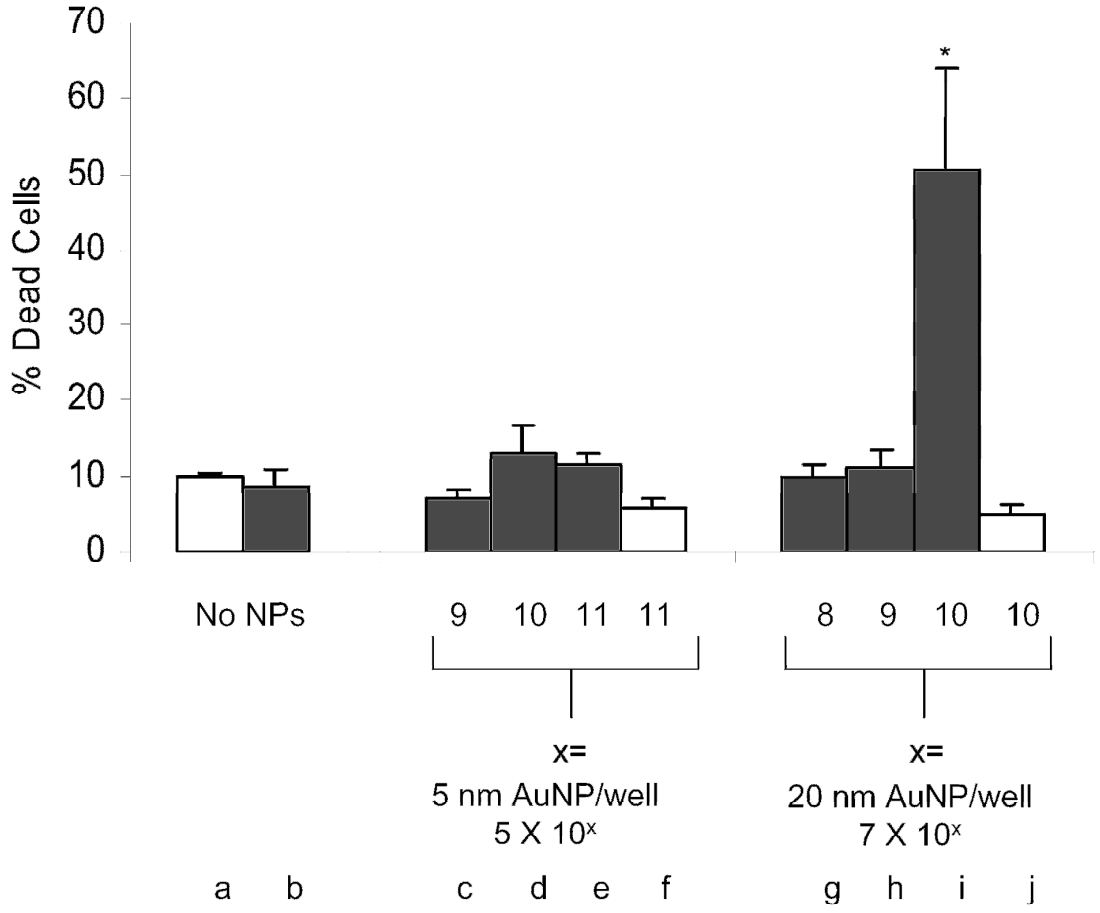
70
60
50
40
30
20
10
0
% Dead Cells
*
No NPs
9 10 11 11
8 9 10 10
x=
5 nm AuNP/well
5 X 10x
x=
20 nm AuNP/well
7 X 10x
a b c d e f g h i j

Figure 4

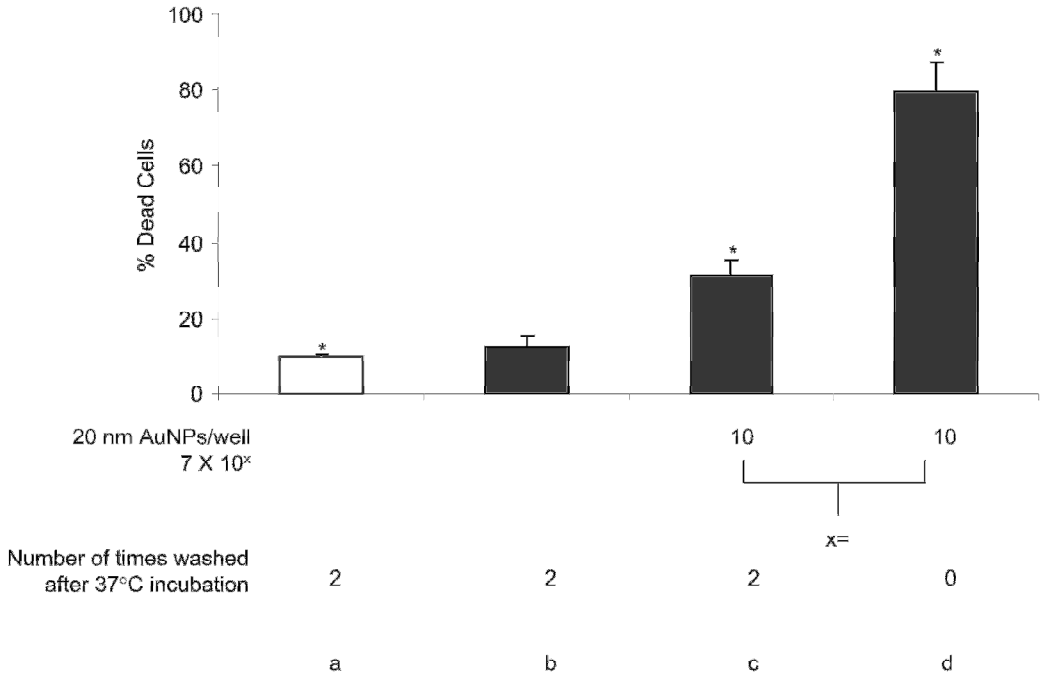
100
80
60
40
20
0
% Dead Cells
*
*
*
20 nm AuNPs/well
7 X 10^x
10
10
x=
Number of times washed
after 37°C incubation
2
2
2
0
a
b
c
d

Figure 5

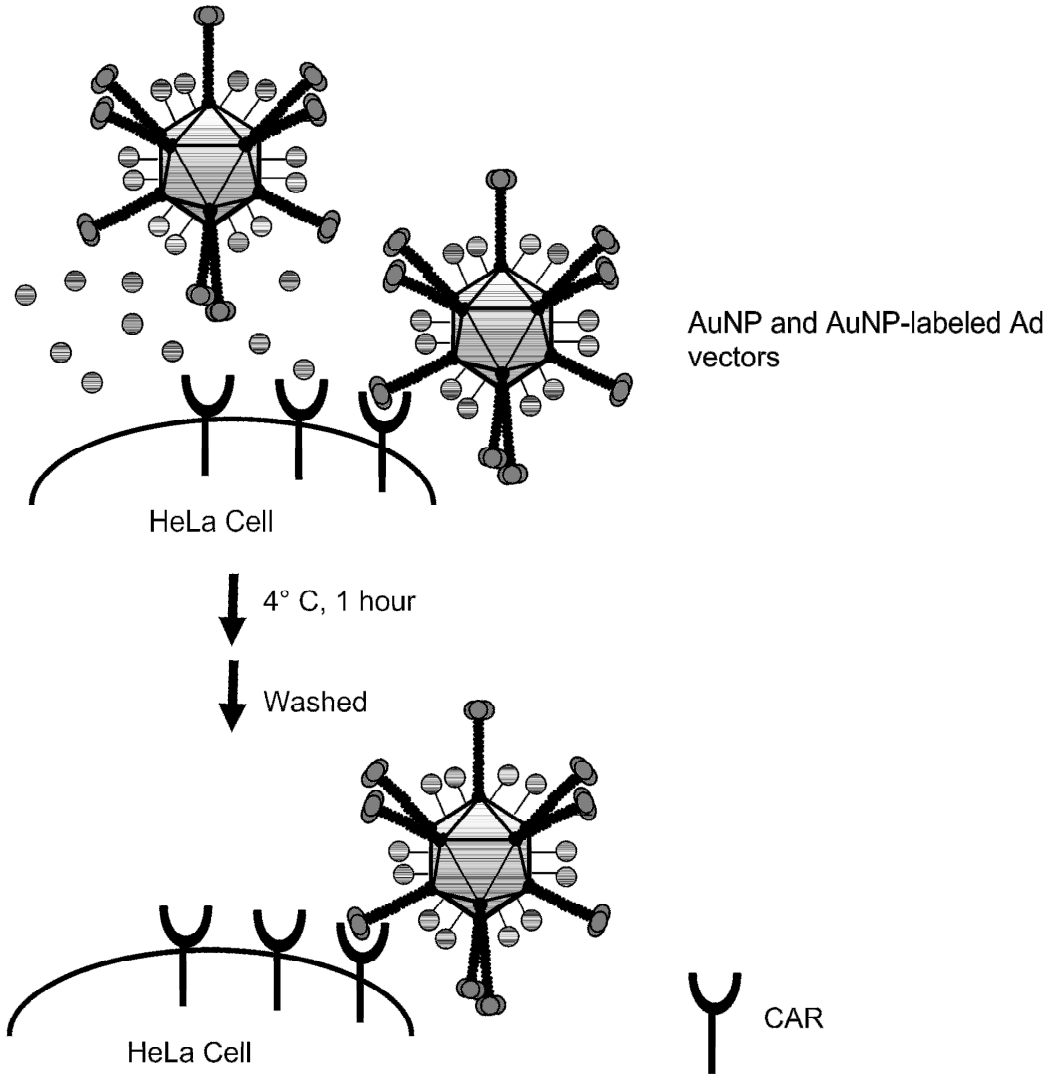
AuNP and AuNP-labeled Ad vectors
HeLa Cell
4° C, 1 hour
Washed
HeLa Cell
CAR

Figure 6

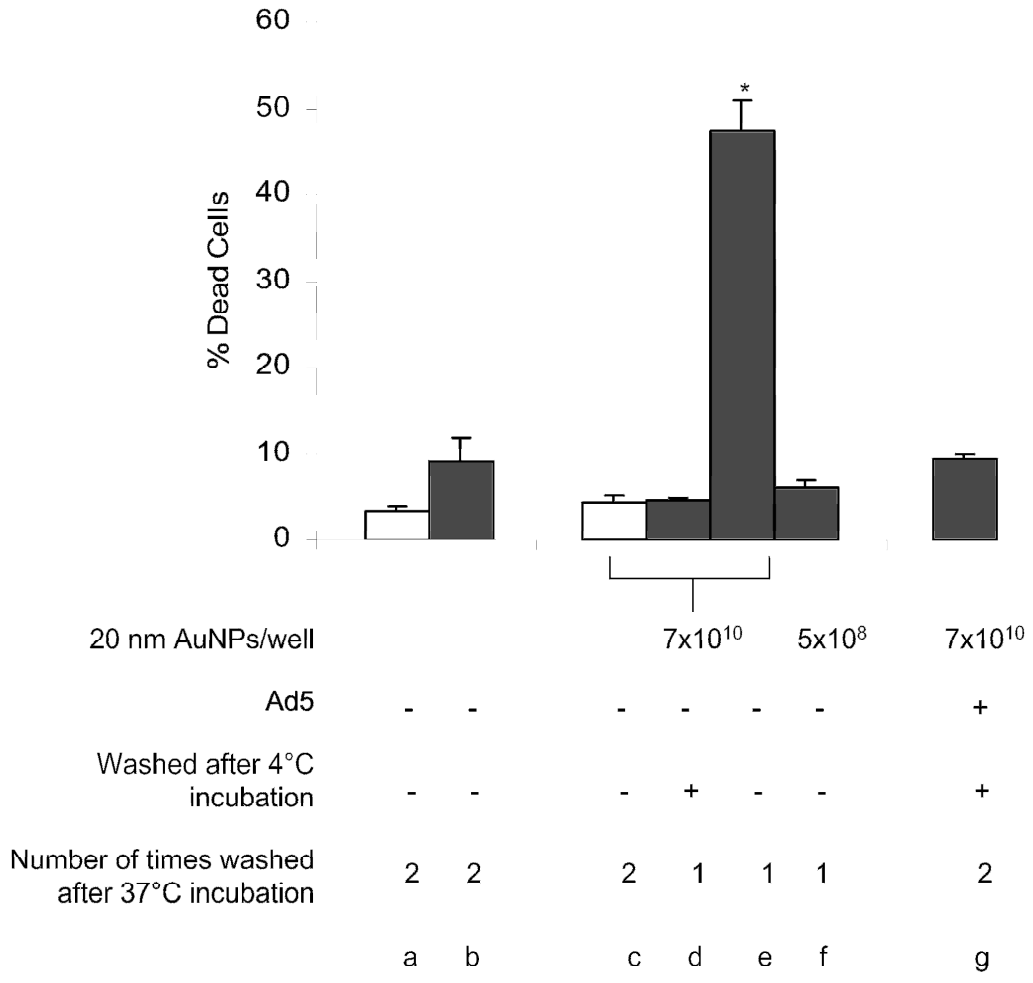
60
50
40
30
20
10
0
% Dead Cells
*
20 nm AuNPs/well
7x10^10
5x10^8
7x10^10
Ad5
- - - - - - +
Washed after 4°C incubation
- - - + - - +
Number of times washed after 37°C incubation
2 2 2 1 1 1 2
a b c d e f g

GENERAL DISCUSSION

Novel therapeutic systems are necessary for improving the efficacy of cancer therapy. In this regard, gene therapy and nanotechnology can provide novel treatment opportunities that have been much explored in recent years. For example, a variety of viral vectors have been utilized for treatment of tumors. In particular, great progress has been made in the development and clinical testing of multifunctional Ad vectors for targeting, imaging, and gene therapy of tumors as reviewed in *Introduction, Part One: Importance of Viruses and Cells in Cancer Gene Therapy.* Similarly, nanotechnology holds the potential for vastly expanding the range of available cancer therapy options. In particular, multifunctional metal NPs have been shown to be useful for targeting, imaging, and hyperthermia therapy of tumors. Therefore, a combination of nanoscale viral vectors and NPs has been envisioned for the development of a multifunctional nano-dimensional system that could potentially be used for simultaneous gene therapy and nanotechnology based cancer therapy, as reviewed in *Introduction, Part Two: Combination of Viral Biology and Nanotechnology: New Applications in Nanomedicine.*

To combine nanotechnology and Ad vector based gene therapy, novel strategies are needed for binding NPs to Ad vectors. To this end, we have developed two methods for coupling NPs non-specifically and specifically to Ad vectors. The non-specific coupling method has been described in S*tudy One: Covalently Linked Au Nanoparticles to a Viral Vector: Potential for Combined Photothermal and Gene Cancer Therapy.* Herein, we established the proof-of-principle that AuNPs can be coupled to Ad vectors,

that AuNP-labeled Ad vectors can infect HeLa cells, which express native Ad receptor-CAR, and that AuNP-labeled Ad vectors can be targeted to tumor cells. However, increasing AuNP:Ad input ratios in the reaction mixture progressively decreased Ad infectivity in HeLa cells and abrogated Ad targeting to tumor cells. We speculated that this negative effect might be a consequence of the non-specific coupling method, which might have resulted in unregulated AuNP binding to Ad capsid proteins, such as fiber knob, that are necessary for Ad infectivity and targeting.

To circumvent the problem of reduced Ad infectivity and targeting upon non-specific AuNP coupling, we explored an alternate method for specific coupling of AuNPs to Ad vectors, as described in *Study Two: An Adenoviral Platform for Selective Self-Assembly and Targeted Delivery of Nanoparticles.* Herein, we demonstrated that NP coupling to Ad capsid can be controlled, that specific NP coupling to Ad capsid proteins depends on both the number and accessibility of the protein on the Ad surface, that hexon is the optimal Ad capsid location for specific AuNP coupling, that specific coupling reduced the negative effects on Ad infectivity in HeLa cells between 1 and 2 orders of magnitude as compared to non-specific coupling, and, most notably, that specific coupling completely removed the negative effects on the tumor targeting ability of AuNP-labeled Ad vectors as compared to non-specific coupling. Thus we developed a specifically AuNP-labeled Ad vector that could be tested for its ability for laser-induced hyperthermic tumor cell ablation.

Hyperthermia has been proposed as a treatment for cancer for many decades. This strategy is based on the premise that rapidly proliferating cells are more susceptible to heat shock than non-proliferating cells through a variety of mechanisms, including

protein denaturation and aggregation, mitotic delay, cell cycle arrest, plasma membrane damage and apoptosis [1-3]. Contributing to this effect is the fact that tumors have a limited blood supply resulting in hypoxic environment with a low pH, where excess heat can not be readily dissipated. Hyperthermia has previously been shown to have synergistic or additive effects for tumor cell killing in combination with radiotherapy or chemotherapy [1]. More recently, hyperthermia combined with dendritic cell mediated immunotherapy has demonstrated antitumor effects [4]. Also, in a clinical study conducted in China, Ad-based gene therapy along with microwave induced hyperthermia has been shown to reduce the tumor burden [5]. Our results analyzing the utility of AuNP-labeled Ad vectors for hyperthermia therapy are described in *Study Three: Limitations of Adenoviral Vector-Mediated Delivery of Gold Nanoparticles to Tumors for Hyperthermia Induction.* Herein, we determined that 20 nm diameter AuNP has the optimal size for hyperthermia induction in our laser-irradiation system, that AuNPs on the surface and inside the cell contribute differentially towards hyperthermia induction, and that due to the technical limitation of delivery of required amounts of AuNPs by Ad vectors, at present it is not possible to utilize AuNP-labeled Ad vectors for hyperthermic tumor cell killing.

The NP coupling methods developed herein have universal applications in the filed of gene therapy and nanotechnology. For example, currently projects are underway in our laboratory where we are specifically coupling a variety of NPs, such as QDs, magnetic NPs, and radioactive NPs to Ad vectors. These NPs can be utilized for imaging, magnetic hyperthermia, and radiotherapy of a multitude of diseases including cancer and heart diseases (Figure 1). Besides Ad vectors, other viral vectors, such as adeno-

associated virus (AAV), herpes simplex virus (HSV), and measles virus among others, can be genetically modified for coupling NPs.

From a clinical perspective, the immune response against the NP-labeled Ad vectors needs to be considered before these vectors can be utilized in a translational setting. The immune response clears the Ad vectors as well as the cells infected with Ad vectors, resulting in diminished therapeutic efficacy. To achieve immune evasion, Ad vectors can be coated with polyethylene glycol (PEG) molecules [6], which is a well-studied strategy to protect a variety of nanoparticles such as quantum dots (QDs) and liposomes from the immune response [7, 8]. In this regard, Ad vectors have been coated with PEG molecules non-specifically by other groups and these PEG coated vectors have been shown to be shielded from the immune system. However, non-specific coupling resulted in almost complete abrogation of viral infectivity *in vitro*. To avoid this loss of infectivity while maintaining immune system evasion, based on the specific coupling strategy described in *Study three,* we are currently specifically coupling PEG molecules to the hexon protein, which is a major determinant of immune response against the Ad vector. These specifically polymer coated Ad vectors could potentially shield the vector from the patient's immune system and may become useful in reducing the therapeutic dosage of Ad vectors, which would result in a reduced risk of viral vector based toxicity, and also increase the efficacy of the therapy.

In addition to the immune response, the biodistribution and toxicity of the NP-labeled Ad vector system needs to be studied as well. In this regard, a recent study showed that size and charge are important determinants of nanoparticle biodistribution and excretion *in vivo* [9]. Moreover, it has been reported that the toxicity of AuNPs is

dependent on their interaction with the cell membrane, which can be modulated based on the coating of the nanoparticles [10]. Detailed future studies for the resolution of these issues will be critical for the clinical translation of the NP-labeled Ad vectors.

Though, as yet, nanotechnology is in its infancy, we expect to develop sophisticated, previously unimaginable biomedical therapies based on it in the future. For example, an unfulfilled aim of human want is to achieve longevity. Within the bounds of nature, scientific endeavor has been expended to achieve increased life expectancy. Towards this end, it has been proposed to replace aging organs with the new ones. Our proposed combinatorial multifunctional nanotechnology and viral vector based system could potentially be developed to achieve this envisioned organ-replacement based longevity. In this regard, skin is the largest organ and displays early signs of aging with depleted collagen and reduced elasticity contributing to the development of wrinkles. To counter skin aging, Ad vector targeted NPs could be loaded with molecules, such as inhibitors of elastase, an enzyme that beaks elastin fibers and reduces the skin elasticity. In addition, these NPs can serve as fillers to smooth out the wrinkles. Moreover, NPs can either be rendered biodegradable or shed off with the keratinocytes. At the molecular level, the temporary NP-derived beautiful skin could be supplemented with induction of new collagen formation by Ad vector-mediated gene delivery, thereby enhancing the ability of the skin to counter wrinkle formation.

A combination of nanotechnology and viral vector mediated gene therapy could also be beneficial for wound healing. NPs have been utilized in the past for tissue welding, which can be defined as the suturing of incisions. To achieve this, gold nanoshells were added in a solder of albumin and laser heat was used to set the solder in

and around the incision [11]. In the future, nanoshell or nanorod mediated wound healing can be enhanced by Ad vector mediated delivery of molecules, such as fibromodulin, that promote the process of wound healing [12].

A role for combined hyperthermia and gene therapy can also be envisioned for cystic fibrosis treatment. The lungs of cystic fibrosis patients are filled with thickened mucus that aids opportunistic infections and depletes the efficacy of viral vector mediated gene delivery of the cystic fibrosis transmembrane conductance regulator. AuNP mediated hyperthermia generation could be utilized to melt the mucus, thereby rendering it easy to dispose off the thickened layers and rescue the breathing process and enhance viral vector mediated delivery of the correct gene. Thus, our multifunctional nanotechnology and viral vector-based nanotherapy system has the potential to yield novel therapies for a multitude of biomedical conditions endangering human health. With the development of new technologies and a better understanding of the molecular pathways that underlie complex processes such as aging and wound healing, the envisioned applications could soon become a reality. However, due to lack of a treatment that can completely eliminate cancer, it is critical to develop and test novel therapies such as our proposed multifunctional nanoagent to achieve cancer eradication.

In the aggregate, we have developed two methods with broad applicability for coupling NPs to viral vectors. We also analyzed the utility of AuNP-labeled Ad vectors for hyperthermia therapy. Due to various technical obstacles we were unable to utilize AuNP-labeled Ad vectors for hyperthermic tumor cell ablation, but with future advancements it may become possible to realize this therapeutic option. Despite this current limitation, the coupling strategies described herein have paved the way for testing

other types of NP and viral vector combinations for simultaneous targeting, imaging, and nanotechnology and viral vector based gene therapy for successful treatment of tumors.

GENERAL REFERENCES

1. Kampinga HH. Cell biological effects of hyperthermia alone or combined with radiation or drugs: a short introduction to newcomers in the field. Int J Hyperthermia 2006;22(3):191-6.
2. Maldonado-Codina G, Llamazares S, Glover DM. Heat shock results in cell cycle delay and synchronisation of mitotic domains in cellularised Drosophila melanogaster embryos. J Cell Sci 1993;105 (Pt 3):711-20.
3. Edwards MJ, Mulley R, Ring S, Wanner RA. Mitotic cell death and delay of mitotic activity in guinea-pig embryos following brief maternal hyperthermia. J Embryol Exp Morphol 1974;32(3):593-602.
4. Guo J, Zhu J, Sheng X, et al. Intratumoral injection of dendritic cells in combination with local hyperthermia induces systemic antitumor effect in patients with advanced melanoma. Int J Cancer 2007.
5. Zhang S, Xu G, Liu C, et al. Clinical study of recombinant adenovirus-p53 (Adp53) combined with hyperthermia in advanced cancer (a report of 15 cases). Int J Hyperthermia 2005;21(7):631-6.
6. Mok H, Palmer DJ, Ng P, Barry MA. Evaluation of polyethylene glycol modification of first-generation and helper-dependent adenoviral vectors to reduce innate immune responses. Mol Ther 2005;11(1):66-79.

7. Ryman-Rasmussen JP, Riviere JE, Monteiro-Riviere NA. Surface coatings determine cytotoxicity and irritation potential of quantum dot nanoparticles in epidermal keratinocytes. J Invest Dermatol 2007;127(1):143-53.

8. Li WM, Mayer LD, Bally MB. Prevention of antibody-mediated elimination of ligand-targeted liposomes by using poly(ethylene glycol)-modified lipids. J Pharmacol Exp Ther 2002;300(3):976-83.

9. Balogh L, Nigavekar SS, Nair BM, et al. Significant effect of size on the in vivo biodistribution of gold composite nanodevices in mouse tumor models. Nanomedicine 2007;3(4):281-96.

10. Goodman CM, McCusker CD, Yilmaz T, Rotello VM. Toxicity of gold nanoparticles functionalized with cationic and anionic side chains. Bioconjug Chem 2004;15(4):897-900.

11. Gobin AM, O'Neal DP, Watkins DM, Halas NJ, Drezek RA, West JL. Near infrared laser-tissue welding using nanoshells as an exogenous absorber. Lasers Surg Med 2005;37(2):123-9.

12. Stoff A, Rivera AA, Mathis JM, et al. Effect of adenoviral mediated overexpression of fibromodulin on human dermal fibroblasts and scar formation in full-thickness incisional wounds. J Mol Med 2007;85(5):481-96.

Figure Legends

Figure 1. Multifunctional NP-labeled Ad vector model.

Figure 1

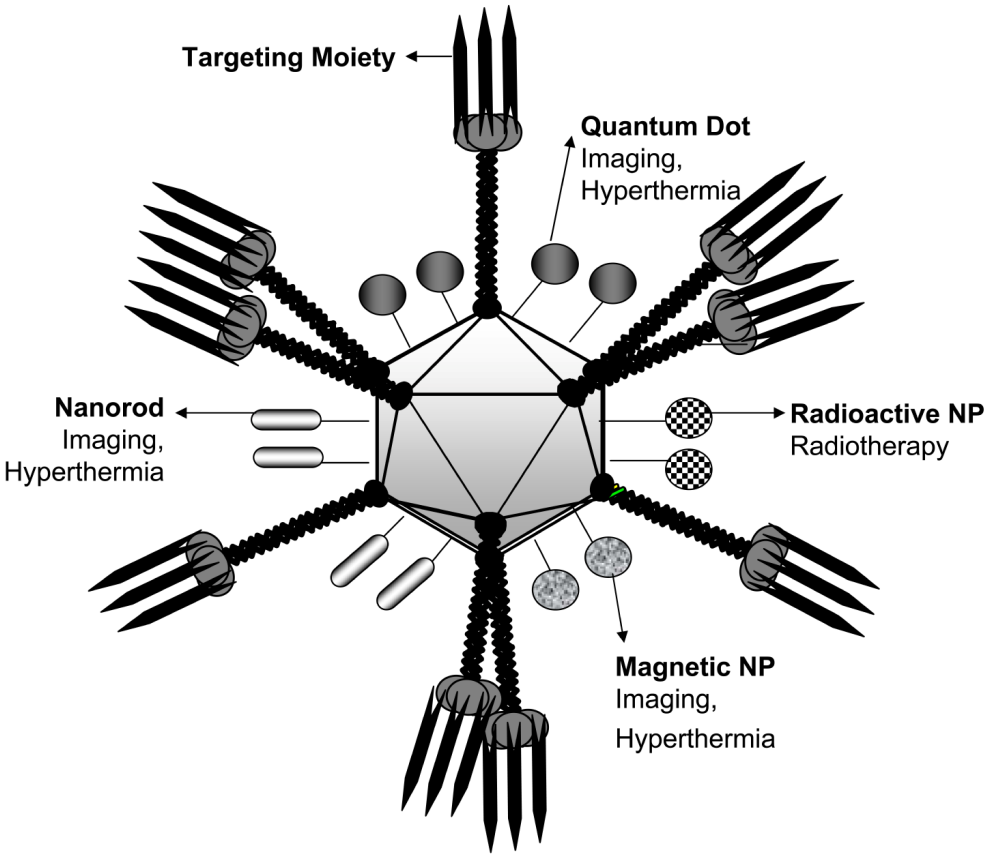
Targeting Moiety
Quantum Dot
Imaging,
Hyperthermia
Nanorod
Imaging,
Hyperthermia
Radioactive NP
Radiotherapy
Magnetic NP
Imaging,
Hyperthermia